ALLOSTERIC MODULATION OF METABOTROPIC GLUTAMATE RECEPTORS

By

Shen Yin

Dissertation

Submitted to the Faculty of the

Graduate School of Vanderbilt University

in partial fulfillment of the requirements

for the degree of

DOCTOR OF PHILOSOPHY

In

Pharmacology

December, 2013

Nashville, Tennessee

Approved:

Vsevolod V. Gurevich, Ph.D.

Richard M. Breyer, Ph.D.

Roger J. Colbran, Ph.D.

Danny G. Winder, Ph.D.

P. Jeffrey Conn, Ph.D.

Colleen M. Niswender, Ph.D.

ACKNOWLEGEMENTS

I would like to express my deep appreciation and gratitude to my advisor, Dr. Jeff Conn and Dr. Colleen Niswender, for having me take part in their research and for the patient guidance and mentorship that they have granted me. Together, they have helped me with every aspect of my Ph.D training and provided me with invaluable opportunities to explore the beauty of science. I would be proud to keep everything they have given me in heart and carry it on to my future career.

I would also like to thank my committee members, Dr. Vsevolod Gurevich, Dr. Roger Colbran, Dr. Danny Winder and Dr. Richard Breyer, four distinguished scientists for their thought-provoking suggestions both for my thesis research and for my career development. They have always been encouraging, inspiring and ready to help all the way along my Ph.D study. Hereby, I would like to express my sincere thank you to each of my committee members.

I will not be able to accomplish my study without the help of all the past and present members of Conn Lab and other labs at Vanderbilt Center for Neuroscience Discovery. As a more senior graduate student in the Conn Lab, Dr. Kari Johnson has shared her precious experience with me at each step of my Ph.D training. I want to thank her for her generosity and wish her all the best on her future career. Throughout my four years in the Conn Lab, Rocio Zamorano has always been a great teacher when I learn new techniques,

a helpful colleague to achieve success together and a good friend of mine to share the exciting moments. Drs. Meredith Noetzel, Kari Johnson, Nidhi Jalan-Sakrikar and Karen Gregory have kindly collaborated with me on my thesis project and have significantly contributed to the work. Dr. Douglas Sheffler and Dr. Hyekyung Cho Plumley have nicely trained me for experimental design and procedures and shared with me a number of experimental protocols. And all the rest of Conn Lab members have created a friendly, stimulating and enjoyable environment for me to work in and contributed to my work on some level.

In addition, the work presented in this dissertation would not have been possible without several funding sources. I deeply appreciate grants from the National Institutes of and the Vanderbilt International Scholar Program.

Finally, I would give my deepest appreciation to my parents and my boyfriend Jiang, who have always devoted themselves to share the happiness and support me in difficult situations. I also want to thank my dear friends in the Department of Pharmacology: Dr. Jing Jin, Craig Goodwin, Tu Mai, Jing Wu and many others, who have made my life at Vanderbilt so memorable.

TABLE OF CONTENTS

LIST OF TABLES

LIST OF FIGURES

LIST OF ABBREVIATIONS

6-OHDA	6-hydroxydopamine
7TMR/GPCR	Seven Transmembrane Spanning/G Protein Coupled Receptor
ADX88178	5-methyl-N-(4-methylpyrimidin-2-yl)-4-(1H-pyrazol-4-yl)thiazol-2-amine
AMPA	α-amino-3-hydroxy-5-methyl-4-isoxazolepropionic acid
AMN082	N1,N2-dibenzhydrylethane-1,2-diamine
ASK	apoptosis signal-regulating kinase
BINA	biphenyl-indanone A
cAMP	cyclic adenosine monophosphate
CBiPES	N-[4'-cyano-biphenyl-3-yl]-N-(3-pyridinylmethyl)-ethanesulfonamide hydrochloride
CDPPB	3-cyano-N-(1,3-diphenyl-1H-pyrazol-5-yl)benzamide
CNS	central nervous system
CPCCOEt	7-(hydroxyimino)cyclopropa[b]chromen-1a-carboxylate ethyl ester
CRD	cysteine-rich domain
CPPHA	N-[4-chloro-2-[(1,3-dioxo-1,3-dihydro-2H-isoindol-2-yl)methyl]phenyl]-2-hydroxybenzamide

DCG-IV	(2S,1'R,2'R,3'R)-2-(2,3-dicarboxycyclopropyl)glycine
DFB	[(3-fluorophenyl)methylene]hydrazone-3-fluorobenzaldehyde
ERK	extracellular signal-regulated kinase
GABA	γ-aminobutyric acid
GIRK	G protein coupled inwardly rectifying potassium channel
JNK	c-Jun N-terminal kinases
L-AP4	L-(+)-2-Amino-4-phosphonobutyric acid
L-DOPA	L-3,4-dihydroxyphenylalanine (levodopa)
LSP1-2111	((2S)-2-amino-4-[hydroxy[hydroxy(4-hydroxy-3-methoxy-5-nitro-phenyl)methyl] phosphoryl]butanoic acid)
LSP4-2022	(2S)-2-amino-4-(((4-(carboxymethoxy)phenyl)(hydroxy)methyl)(hydroxy)phosphoryl)butanoic acid
Lu AF21934	(1S,2S)-N1-(3,4-dichlorophenyl)cyclohexane-1,2-dicarboxamide
LY379268	(1R,4R,5S,6R)-4-Amino-2-oxabicyclo[3.1.0]hexane-4,6-dicarboxylic acid
LY487379	2,2,2-trifluoro-N-[4-(2-methoxyphenoxy) phenyl]-N-(3-pyridinylmethyl)ethanesulfonamide
MAPK	mitogen activated protein kinase

mGlu	metabotropic glutamate receptor
MMPIP	6-(4-methoxyphenyl)-5-methyl-3-(4-pyridinyl)-isoxazolo [4,5-c]pyridine-4(5H)-one hydrochloride
mTOR	mammalian target of rapamycin
NAM	negative allosteric modulator
NMDA	N-methyl-D-aspartate
PAM	positive allosteric modulator
PD	Parkinson's disease
PHCCC	N-phenyl-7-(hydroxylimino)cyclopropa[b]chromen-1a-carboxamide
PI3K	phosphatidylinositol 3-kinase
PIKE-L	phosphatidylinositol 3-kinase enhancer-long
SAM	silent allosteric modulator
VFD	Venus flytrap domain
VU0155041	(±)-cis-2-(3,5-Dicholorphenylcarbamoyl)cyclohexanecarboxylic acid
VU0364770	N-(3-chlorophenyl)picolinamide

CHAPTER 1

GENERAL INTRODUCTION

Metabotropic glutamate receptors

Glutamate is not only one of the 22 proteinogenic amino acids, but also the major excitatory neurotransmitter in the central nervous system (CNS). The glutamate receptors can be divided into two classes: the ionotropic glutamate receptors and the metabotropic glutamate receptors. While the ionotropic glutamate receptors (AMPA receptors, NMDA receptors and kainate receptors) mediate fast responses elicited by glutamate, the metabotropic glutamate (mGlu) receptors provide a mechanism by which glutamate can transduce environmental cues and modulate synaptic transmission via second messenger signaling pathways with slower time course. Because of their widespread distribution especially in the CNS, pharmacological manipulation of mGlus may represent ideal therapeutic interventions for a wide range of neurological and psychiatric disorders (Reviewed in (Gregory et al., 2013; Niswender and Conn, 2010)).

Classification of mGlus

The Seven Transmembrane Spanning/G Protein Coupled Receptors (7TMR/GPCR) account for 4% of the entire protein-coding genome (Bjarnadottir et al., 2006) and represent the targets of approximately 40-50% of medicinal drugs on the market (Thomsen et al., 2005). The core function of GPCRs is to serve as a transducer of signals from the extracellular environment to the intracellular machinery that aggregates to govern organismal responses. The GPCR superfamily can be classified into several classes: the Class A GPCRs (or Rhodopsin-like receptors) account for almost 85% of the GPCR genes, the Class B GPCRs (or secretin-like receptors) include 15 receptors and are regulated by peptide hormones, and the Class C GPCRs, which are characterized by a

large extracellular N-terminal domain and contain 22 distinct receptors. The Adhesion, Frizzled, Taste type-2 and other unclassified receptors comprise the rest of the superfamily (Bjarnadottir et al., 2006).

The mGlus belong to the Family C GPCRs, which also encompasses calcium sensing receptors, the $GABA_B$ receptor, taste receptors and other orphan Class C receptors. Since the cloning of rat $mGlu_1$ in 1991, 8 mGlu subtypes have been cloned thus far, named $mGlu_1$ through $mGlu_8$. Within the family, the eight mGlu subtypes can be further classified into three groups (Table 1.1), with an intragroup sequence homology of about 70% and an intergroup sequence homology of about 45% (reviewed in (Conn and Pin, 1997)). The group I mGlus include $mGlu_1$ and $mGlu_5$, group II includes $mGlu_2$ and $mGlu_3$, whereas $mGlu_{4,\ 6,\ 7\ and\ 8}$ comprise the group III mGlus. Such classification is further confirmed by the G-protein coupling and pharmacological profile of the three groups. While the group I mGluRs are coupled to G_q, the group II and group III are coupled to $G_{i/o}$ G proteins.

In addition to the G protein-coupling specificity, the three groups of mGlus also differ in their expression patterns. With the exception of $mGlu_6$ which is expressed exclusively in ON-bipolar cells in the retina, all mGlus are widely expressed in many locations within the brain. Group I mGlus are primarily expressed postsynaptically to modulate neuronal excitability, whereas group III mGlus are typically located presynaptically. Both pre- and postsynaptic expression has been detected for group II mGlus. In addition, $mGlu_3$ and $mGlu_5$ are also expressed in astrocytes. Expression of each mGlu subtypes has been mapped using immunohistochemistry. Specifically, high $mGlu_1$ expression was detected in the olfactory bulb, CA1 hippocampus, globus pallidus, thalamus and cerebellum (Petralia et al., 1997). Expression of $mGlu_5$ was found in the olfactory bulb, olfactory tubercle, cerebral cortex, hippocampus, striatum and nucleus accumbens (Shigemoto et al., 1993). For $mGlu_2$ and $mGlu_3$, significant staining was found in the cerebral cortex, hippocampus, thalamus and caudate-putamen (Petralia et al., 1996). $mGlu_4$ is highly enrich in the molecular layer of cerebellum, but is also expressed in globus pallidus substantia nigra and moderately in neocortex, hippocampus, striatum and thalamus

Classification	G protein coupling	Receptor Subtypes	Splice Variants	Selective Ligands
Group I	$G_{q/11}$	$mGlu_1$	$mGlu_{1a\text{-}h,}$ $mGlu_{1g393}$ $mGlu_{1g620}$ Taste $mGlu_1$	LY367385 (orthosteric agonist) Bay 36–7620 (NAM) Ro 67–7476 (PAM) Ro 67–4853 (PAM) VU71 (PAM)
		$mGlu_5$	$mGlu_{5a,b}$	CHPG (orthosteric agonist) MPEP (NAM) MTEP (NAM) CDPPB (PAM) CPPHA (PAM) VU0365396 (SAM)
Group II	$G_{i/o}$	$mGlu_2$	$mGlu_2$	LY487379 (PAM) BINA (PAM)
		$mGlu_3$	GRM3Δ2 GRM3Δ4 GRM3Δ2Δ3	ML337 (NAM)
Group III	$G_{i/o}$	$mGlu_4$	$mGlu_{4a,b}$ Taste $mGlu_4$	LSP1-2111 (orthosteric agonist) LSP4-2022 (orthosteric agonist) PHCCC (PAM) VU0155041(PAM) VU0364770 (PAM) ADX88178 (PAM)
		$mGlu_6$	$mGlu_{6a\text{-}c}$	
		$mGlu_7$	$mGlu_{7a\text{-}e}$	AMN 082 (allosteric agonist) MMPIP (NAM) ADX71743 (NAM)
		$mGlu_8$	$mGlu_{8a\text{-}c}$	(S)-3,4-DCPG (orthosteric agonist) AZ12216052 (PAM)

Table 1.1. Classification, G protein coupling, splice variants and selective ligands for mGlu subtypes.

(Bradley et al., 1999). $mGlu_7$ is abundantly expressed in striatum, globus pallidus, and substantia nigra pars reticulata (Kosinski et al., 1999), whereas $mGlu_8$ is expressed primarily in hippocampus and piriform cortex (Ferraguti et al., 2005; Kinoshita et al., 1996). mGlu receptors also expressed in peripheral tissues and play important roles in pathological conditions including congenital stationary night blindness (Mathiesen et al., 2005; Zeitz et al., 2007) and malignant transformation, such as melanoma (Choi et al., 2011; Pollock et al., 2003).

Different mGlu subtypes have been suggested to colocalize at various synapses. Previous immunohistochemistry and in situ hybridization studies suggest that $mGlu_2$ and $mGlu_4$ are co-localized in several brain regions (Bradley et al., 1999; Neki et al., 1996; Ohishi et al., 1995; Ohishi et al., 1993) and $mGlu_2$ is also functionally expressed at corticostriatal synapses (Johnson et al., 2005).

All mGlu subtypes have been discovered to undergo alternative splicing, primarily at the C-terminus, and some of the better characterized splice variants are described below. In humans, 8 different splice variants of mGlu1 exist, named $mGlu_{1a, 1b, 1c, 1d, 1e, 1g, 1g\text{-}393, 1g\text{-}620 \text{ and } 1h}$. Two newly identified exons in human *GRM1* express a novel splice variant of metabotropic glutamate 1 receptor. $mGlu_{1a}$ is the longest variant and the others result from differential splice site usage, generating distinct isoforms with differing C-termini (reviewed in (Hermans and Challiss, 2001)). The splice variant containing only the VFD has been shown to act as a dominant negative, preventing full length $mGlu_1$ isoforms from signaling (Beqollari and Kammermeier, 2010). Also within the group I mGlus, $mGlu_{5a}$ and $mGlu_{5b}$ are two splice variants for $mGlu_5$ with similar pharmacological profiles (Joly et al., 1995; Minakami et al., 1994). Three splice variants of $mGlu_3$ exist in human brain due to exon skipping events: GRM3Δ2 (lacking exon 2), GRM3Δ4 (lacking exon 4), and GRM3Δ2Δ3 (lacking exons 2 and 3). Among the three variants, GRM3Δ4 is most abundantly expressed and represents an $mGlu_3$ receptor without a seven-transmembrane domain, which may have unique functions and relate to non-coding single nucleotide polymorphisms (SNPs) in patients with cognitive dysfunction (Sartorius et al., 2006). As to the group III mGlus, the $mGlu_4$ gene was described as undergoing

alternative splicing to generate $mGlu_{4a}$ and $mGlu_{4b}$ (Thomsen et al., 1997); however, this result has not been replicated by other groups (Corti et al., 2002). Three $mGlu_6$ splice variants exists in human retina, with $mGlu_{6b}$ lacking 97 nucleotides from exon 6 and $mGlu_{6c}$ including 5 nucleotides from intron 5 (Valerio et al., 2001). Both $mGlu_7$ and $mGlu_8$ can undergo alternative splicing at the C-terminus, resulting in at least 5 splice variants for $mGlu_7$ and 2 variants for $mGlu_8$ (Corti et al., 1998; Schulz et al., 2002). In addition, another splice variant, $mGlu_{8c}$, contains a 74 nucleotide insertion, resulting in a frame shift and termination of the polypeptide before the seven transmembrane domains (Malherbe et al., 1999). As the C-terminal intracellular domain plays important roles in protein-protein interactions and signal transduction, different splice variants may possess distinct profiles with regards to receptor activation, receptor modification and receptor internalization (Enz, 2012). With the advances in sequencing technology, the diversity of mGlu splice variants is increasing rapidly. For example, 7 splice variants have been predicted for $mGlu_4$ according to Ensembl genome database, although their existence still needs to be validated experimentally.

Several isoforms of mGlus also exist due to alterations at the N-terminus; for example, Taste $mGlu_1$ and Taste $mGlu_4$ (Chaudhari et al., 2000), which play roles in detecting the taste of umami. These receptor variants, with approximately 50% of the N-terminus truncated, are expressed in taste buds. Compared to full-length receptors, these N-truncated variants lack much of the glutamate binding domain and thus exhibit lower potency when activated by glutamate (Chaudhari et al., 2000).

The structure of mGlus

General structural features of mGlus

As members of the Family C 7TMRs, the mGlus are characterized by a large N-terminal domain, commonly referred to as the Venus Flytrap Domain (VFD). Studies of the crystal structures of the $mGlu_{1, 3 \text{ and } 7}$ VFDs reveal that each VFD contains two lobes, which together form a clam shell-like structure, with the

glutamate binding site found between the two lobes (Acher and Bertrand, 2005; Kunishima et al., 2000; Muto et al., 2007; Tsuchiya et al., 2002). Besides glutamate, the VFDs of some mGlus also bind other endogenous agonists of mGlus, such as cinnabarinic acid (Fazio et al., 2012) and L-serine-O-phosphate (Klunk et al., 1991) (Hampson et al., 1999), as well as magnesium and calcium, which can modulate receptor activity (Francesconi and Duvoisin, 2004; Kubo et al., 1998; Kunishima et al., 2000). Both structural (Kunishima et al., 2000; Muto et al., 2007; Tsuchiya et al., 2002) and biochemical data (Romano et al., 1996) suggest that the VFDs from two distinct mGlu receptors sit back to back and dimerize together. Upon ligand binding, large conformational changes lead to closure of the two lobes. Closure of one or both VFDs within each mGlu dimer initiates receptor activation (Kniazeff et al., 2004).

Connecting the VFD and the seven transmembrane spanning domain (7TMD) is the cysteine-rich domain (CRD). Based on structural studies with $mGlu_2$, the CRD contains 9 cysteine residues; 8 of them form internal disulfide bonds to stabilize the structure of this domain. In addition, the ninth cysteine forms a disulfide bond linked to the VFD (Muto et al., 2007), such that the CRD senses the conformational changes induced by ligand binding and transmits it to the 7TMD. The 7TMD and intracellular loops play important roles in receptor-G protein coupling and receptor modulation. It has been shown that a single mutation in the 7TMD that disrupts the hydrogen-bonding network in TM6 and TM7 induces high constitutive activity of $mGlu_8$ (Yanagawa et al., 2013), suggesting that TM6 and TM7 constrain the receptor in an inactive conformation and that rearrangement between these two helixes is critical for receptor activation. The 7TMD also provides an opportunity to modulate receptor activity at a site other than the traditional agonist-binding VFD. All mGlu small molecule allosteric modulators discovered to date are believed to bind to receptor 7TMDs. Classification, action and therapeutic implications of such allosteric modulators will be discussed in the following sections. The intracellular loops of mGlus are involved in G protein coupling and receptor phosphorylation. Specifically, the second intracellular loop is implicated in G protein coupling

specificity of the mGlus (Gomeza et al., 1996; Havlickova et al., 2003; Pin et al., 1994), which is usually the function of the third intracellular loop for Class A, rhodopsin-like receptors.

The C-terminal domain of the mGlus is within close proximity to the inner leaflet of the lipid bilayer. Although recent structural studies of the purified intracellular C-terminal domains from $mGlu_{6,\ 7\ and\ 8}$ suggest that the C-termini of unliganded mGlus are mediated by linear motifs rather than secondary/tertiary structures (Seebahn et al., 2011), these intracellular tails of mGlus interact with various intracellular proteins, and are subject to alternative splicing (see section 3.1 and 3.2.2), phosphorylation, and SUMOylation (reviewed in (Enz, 2012)).

The dimeric complex of mGlus

As mentioned above, mGlus form stable, covalently linked dimers. Data suggesting constitutive formation of mGlu homodimers emerged as early as 1996 (Romano et al., 1996), and was further supported by data obtained from mGlu VFD/CRD crystal structures (Kunishima et al., 2000). Evidence from biochemical studies reveals that that one or more cysteine residues on the N-terminal extracellular domain mediate the covalent and non-covalent interactions between two mGlu protomers (Ray and Hauschild, 2000; Romano et al., 2001). In addition, several studies have shown that mGlus do not appear to form higher-order oligomers (Brock et al., 2007; Doumazane et al., 2011b), although this is the case for some other Class C 7TMRs, such as the $GABA_B$ receptor (Comps-Agrar et al., 2012).

The activation machinery of mGlu homodimers has been studied in depth, particularly by Jean Philippe Pin's group, using a quality control system adapted from the $GABA_B$ receptor to generate mGlu dimers bearing specific mutations within one of the protomers. These data suggest that closure of one VFD per dimer is sufficient to activate the receptor, although closure of both VFDs is required to achieve full activity (Kniazeff et al., 2004). When one or both VFDs are occupied,

the 7TM domain of either protomer can be activated through intersubunit rearrangement (Brock et al., 2007). These findings are consistent with the hypothesis that only a single 7TM domain is turned on upon activation of each homodimeric receptor (Goudet et al., 2005; Hlavackova et al., 2005; Hlavackova et al., 2012).

Besides forming homodimers, the VFD of $mGlu_1$ can heterodimerize with full length $mGlu_5$ and vice versa (Beqollari and Kammermeier, 2010). In addition, a splice variant of $mGlu_1$ that contains only the VFD functions as a dominant negative to potently block the signaling of full length $mGlu_1$ or $mGlu_5$ (Beqollari and Kammermeier, 2010). Unfortunately, there is a paucity of evidence demonstrating the extent to which heterodimers exist *in vivo*. The discovery of heteromers in native systems would dramatically shift our understanding of the functional roles of this important family of 7TMRs and would suggest that mGlus exhibit greater diversity in signaling and function than has previously been appreciated. In addition, mGlu receptor heteromerization could also explain discordant pharmacological findings observed in native brain tissue (Ayala et al., 2008; Niswender et al., 2010).

Evidence for full length mGlu heterodimers initially emerged in *in vitro* expression systems (Doumazane et al., 2011a; Kammermeier, 2012). By using a time-resolved FRET assay, Doumazane et al. demonstrated that group I mGlus can interact with each other, but do not associate with group II and group III mGlu subtypes; in contrast, group II and III mGlu receptors can co-assemble within and outside of the two groups. In addition, Kammermeier's study utilizing injected superior cervical ganglion cells suggests that heterodimerization may alter the pharmacology of mGlus and their modulators. Together, these findings indicate that the functions and signaling of mGlus could be much more diverse and complex than previous estimated, although the existence and pharmacology of mGlu heterodimers still needs to be established using native tissue. However, examples already exist for heterodimers of mGlus and Class A 7TMRs in the CNS. Gonzalez-Maeso et al. reported that $mGlu_2$ receptors interact with 5-HT_{2A} receptors through transmembrane helix domains and form functional complexes in brain cortex (Gonzalez-Maeso et al.,

2008). Subsequent mutagenesis studies revealed that three residues within transmembrane domain 4 of $mGlu_2$ are necessary to form the 5-HT_{2A}-$mGlu_2$ receptor heterocomplex (Moreno et al., 2012). Furthermore, hallucinogenic 5-HT_{2A} agonists elicit unique responses at 5-HT_{2A}/$mGlu_2$ complexes, which is implicated in the pathogenesis of psychosis (Gonzalez-Maeso et al., 2008). However, it should be noted that, although the formation of $mGlu_2$/$5HT_{2A}$ heterocomplexes has been validated by other groups, (Delille et al., 2012) the unique signal transduction pathways mediated by the hetereodimeric complex was not replicated. In addition, it was also shown that $mGlu_2$ can interact with 5-HT_{2B}, indicating that complex formation is not specific to the 5-HT_{2A}-$mGlu_2$ pair and challenging the biological relevance of the 5-HT_{2A}-$mGlu_2$ complex.

Signaling of mGlus

As shown in Figure 1.1, mGlu receptors signal to intracellular machinery through both G protein-dependent and independent pathways.

G protein-dependent signaling

Classically, group I mGlus are generally coupled to $G_{q/11}$ and activate phospholipase Cβ, which hydrolyses phosphotinositides into inositol 1,4,5-trisphosphate (IP3) and diacylglycerol, a pathway leading to calcium mobilization and activation of protein kinase C (PKC). Other effectors downstream of G_q include phospholipase D, ion channels, c-Jun N-terminal kinase (JNK), mitogen-activated protein kinase/extracellular receptor kinase (MAPK/ERK), and the mammalian target of rapamycin (mTOR) pathway (Li et al., 2007; Page et al., 2006; Sayer, 1998; Servitja et al., 1999) (Figure 1.1). In addition, evidence has emerged that group I mGlus can also activate G_s and $G_{i/o}$ and their downstream pathways, and that distinct regions on the receptor are responsible for coupling of different G proteins (Francesconi and Duvoisin, 1998; McCool et al., 1998).

Group I mGlu

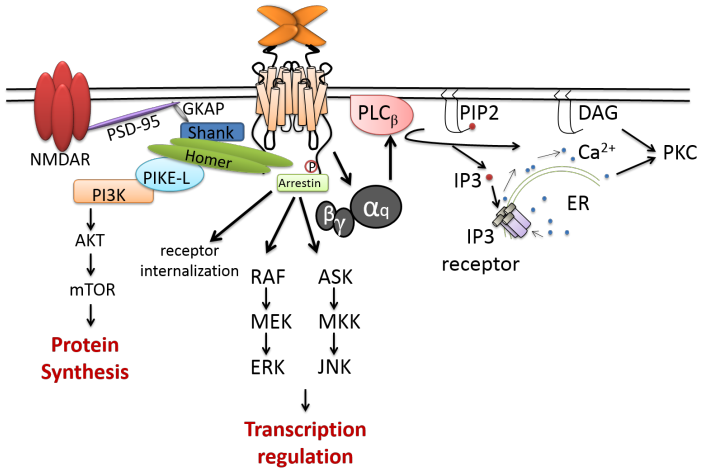

Group II and

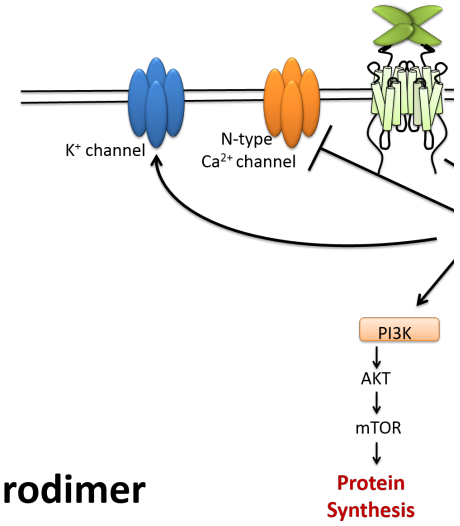

mGlu Heterodimer

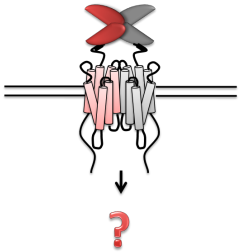

Figure 1.1. Signaling pathways of mGlu receptors. The group I, II and III mGlu receptors induce signal transduction through both G protein-dependent and independent pathways, while the signaling profile of heterodimeric mGlu receptor remains unexplored. GKAP, guanylate kinase-associated protein; PSD-95, postsynaptic density protein 95; NMDAR, N-methyl-D-aspartate receptor; PI3K, phosphatidylinositol 3-kinase; PIKE-L, phosphatidylinositol 3-kinase enhancer-long; mTOR, mammalian target of rapamycin; ERK, extracellular signal-regulated kinase; ASK, apoptosis signal-regulating kinase; JNK, c-Jun N-terminal kinases; PIP2, Phosphatidylinositol 4,5-bisphosphate; DAG, diacyl-glycerol; IP3, inositol 1,4,5-trisphosphate; ER, endoplasmic reticulum; PKC, protein kinase C; AC, adenylate cyclase**;** PKA, protein kinase A.

As stated previously, the group II and group III mGlu receptors are coupled to $G_{i/o}$ proteins and negatively regulate the activity of adenylyl cyclase. In addition, many ion channels have also been reported to be regulated by $G_{\alpha i}$ and the liberated $G_{\beta\gamma}$ subunit (Guo and Ikeda, 2005; Kammermeier, 2012; Niswender et al., 2008a). $G_{i/o}$-mediated activation of MAPK and phosphatidyl inositol 3-kinase (PI3 kinase) pathways, as supported by the inhibitory effect of pertussis toxin (Iacovelli et al., 2002), add another level of complexity to the G protein-mediated signaling of group II and III mGlus.

G protein-independent signaling

While 7TMRs transduce signals through various cellular pathways, their responsiveness may also be regulated by receptor desensitization. When a receptor is stimulated, activated G protein-coupled receptor kinase (GRK) then initiates a combination of events including receptor phosphorylation, arrestin binding, and receptor internalization (reviewed in (Krupnick and Benovic, 1998)), providing a feedback mechanism that prevents receptor over-stimulation. For mGlus, such regulation is more thoroughly studied for group I mGlus than the other two groups. For example, internalization of $mGlu_1$ has been shown to depend on GRK4 and β arrestin-1 (Dale et al., 2001; Iacovelli et al., 2003). Desensitization of $mGlu_5$, however, seems to be dependent on GRK2 activity, suggesting different mGlu subtypes are regulated by distinct mechanisms (Sorensen and Conn, 2003).

Besides regulating receptor desensitization, recruited β-arrestins are also well-known as scaffolding protein for signaling molecules. Reports have shown that active Src is recruited to activated 7TMRs by interaction with β-arrestin, which then results in phosphorylation of downstream molecules and consequently activation of the MAPK cascade (Luttrell et al., 1999). In addition, arrestins also directly facilitate the subcellular localization and activation of two MAPK cascades (the RAF→MEK→extracellular signal-regulated kinases (RAF-MEK-ERK) cascade and

the apoptosis signal-regulating kinase→MKK→c-Jun N-terminal kinases (ASK-MKK-JNK cascade)) (Pierce and Lefkowitz, 2001), further expanding the dimension and complexity of signal transduction upon GPCR activation. This role of arrestins in meditating signal transduction events has been demonstrated for mGlus as well. For example, activation of $mGlu_7$ significantly reduces N-methyl D-aspartate receptor (NMDAR)-mediated currents in prefrontal cortex pyramidal neurons in a β-arrestin/ERK signaling pathway-dependent manner (Gu et al., 2012).

In addition, mGlu receptors also demonstrate the ability to activate signaling cascades through protein-protein interactions. For instance, the C-terminal domains of $mGlu_1$ and $mGlu_5$ interact with Homer proteins, a group of scaffolding proteins for multiprotein complexes. Besides interacting with the receptor, Homer proteins demonstrate binding ability with inositol-1,4,5-triphosphate (IP3) receptors, ryanodine receptors, transient receptor channel-1 and 4 (TRPC1, TRPC4), P/Q-type Ca^{2+} channels, Shank, the phosphoinositide 3-kinase (PI3K)enhancer-long (PIKE-L) etc., coupling receptor activation to other signaling components within the cell (Bockaert et al., 2004; Fagni et al., 2004; Rong et al., 2003). $mGlu_5$ has been found to interact with the NMDA receptor via Homer and other scaffolding proteins and potentiate receptor activity (Attucci et al., 2001; Pisani et al., 2001; Tu et al., 1999). In addition, it has been shown that disruption of $mGlu_5$–Homer interactions selectively blocks mGlu activation of the PI3K-Akt-mTOR pathway (Ronesi and Huber, 2008) and contribute to phenotypes of Fmr1 knockout mice, an animal model for Fragile X syndrome (Ronesi et al., 2012). Interestingly, Homer proteins include long Homer isoforms and short isoforms (Homer1a and Ania), which act as endogenous dominant-negatives and disrupt protein complexes containing the long Homer variant. The ratio of Homer 1a/long Homer bound to $mGlu_5$ may associate with cognitive aging (Menard and Quirion, 2012) and has been shown to be altered in Fmr1 knockout mice (Ronesi et al., 2012). In addition, genetic deletion of Homer1a rescues several phenotypes in Fmr1 knockout mice, suggesting the importance of Homer proteins in the mechanism of Fragile X syndrome and potential therapeutic intervention for this disease (Ronesi et al., 2012). Besides the

PI3K-Akt-mTOR pathway, Homer also links $mGlu_5$ to PIKE-L, which prevents cell apoptosis upon $mGlu_5$ activation (Rong et al., 2003). Interestingly, it has been shown that the disruption of Homer-$mGlu_5$ interaction reduces astrocyte apoptosis (Paquet et al., 2013), suggesting opposite functions of Homer in regulation of cell apoptosis in neurons and astrocytes. Besides the CNS, a point mutation of $mGlu_1$ within the Homer binding region that has been discovered in the somatic cells of lung cancer patients (Esseltine et al., 2013), indicating important roles of Homer in the periphery.

Another well-studied protein-protein interaction is the $mGlu_7$-protein interacting with C kinase 1 (PICK1) interaction. PICK1 was discovered as a peripheral membrane protein that interacts with protein kinase Cα (PKCα) (Staudinger et al., 1995). Besides PICK1, the C-terminus of $mGlu_7$ also interacts with Ca^{2+}-calmodulin, G protein βγ subunits to modulate the activity of voltage-gated Ca^{2+} channel and negatively regulate neurotransmitter release (Dev et al., 2001). Interestingly, phosphorylation of the receptor by PKC increases receptor binding to PICK1, which is required for stable surface expression of $mGlu_7$ (Suh et al., 2013; Suh et al., 2008), but, at the same time, inhibits the binding of $G_{\beta\gamma}$ subunits and Ca^{2+}-calmodulin, providing a delicate regulatory machinery. Disruption of the $mGlu_7$-PICK1 interaction has been performed by genetic knock-in of an $mGlu_7$ mutant that does not bind PICK1. The resulting animals exhibited significant defects in hippocampus-dependent spatial working memory and high susceptibility to convulsant drugs (Zhang et al., 2008). Additionally, injection of a competing peptide to rodents also resulted in behavioral symptoms and EEG discharges that are characteristic of absence epilepsy (Bertaso et al., 2008). These data indicate that the $mGlu_7$-PICK1 interaction is important for regulating $mGlu_7$ signaling and may underlie certain disease mechanisms, including cognitive disorders and epilepsy.

Therapeutic indications of $mGlu_4$

Pharmaceutical manipulation of mGlus represent ideal therapeutic interventions for a wide range of neurological and psychiatric, as well as peripheral disorders, but this section will primarily focus on the therapeutic indication of $mGlu_4$ for Parkinson's disease (PD). PD is a debilitating neurodegenerative disorder characterized by movement symptoms including tremor, rigidity, bradykinesia and postural instability, as well as disturbances in sleep, depression and cognition (Jankovic, 2008; Johnson et al., 2009). The pathology of PD stems from severe degeneration of dopaminergic neurons in the substantia nigra pars compacta (SNc), a brain structure that plays important roles in the basal ganglia to control motor function (Surmeier and Sulzer, 2013). Within the basal ganglia, dopamine released from SNc neurons delicately controls the balance of output between the "direct pathway" and the "indirect pathway", which oppose each other in controlling motor output in the basal ganglia. In PD patients, however, the loss of dopaminergic neurons leads to an overall increase of activity in the indirect pathway, which ultimately inhibits motor function in PD patients (reviewed in (Johnson et al., 2009)). Thus, according to this model, a rebalancing of the basal ganglia circuitry is predicted to alleviate disease symptoms.

The current gold standard treatment for PD is dopamine replacement therapy using L-DOPA, the precursor of dopamine. However, long-term treatment with L-DOPA results in "wearing-off" of efficacy and development of side effects, such as dyskinesias and psychiatric complications (Chen and Swope, 2007). In addition, no treatment is available to delay the progression of the disease. The $mGlu_4$ receptor is highly expressed presynaptically at the first synapse in the indirect pathway (the GABAergic striatopallidal synapse) (Bradley et al., 1999) and receives glutamate input from subthalamic nucleus, providing an exciting alternative approach to rebalance the basal ganglia circuitry for PD treatment. Administration of the group III mGlu agonists L-AP4 or L-SOP, and recently

the more $mGlu_4$-selective agonists LSP1-2111 and LSP4-2022, has been shown to reduce GABAergic transmission at the striatopallidal synapse and demonstrate efficacy in several rodent PD models, including haloperidol-induced catalepsy and 6-OHDA-induced motor deficits (Beurrier et al., 2009; Goudet et al., 2012; Macinnes and Duty, 2008; MacInnes et al., 2004; Matsui and Kita, 2003; Valenti et al., 2003; Wittmann et al., 2001). Recently, numerous highly selective $mGlu_4$ PAMs have been developed from different chemical series and exhibit robust efficacy in preclinical rodent models. Administration of either PHCCC or VU0155041, two $mGlu_4$ PAMs that bind to distinct binding sites on the receptor, reversed parkinsonian behavior in PD animal models, such as reserpine-induced akinesia as well as haloperidol-induced catalepsy (Marino et al., 2003; Niswender et al., 2008b). In another example, VU0364770, a systemically active $mGlu_4$ PAM, produced a reversal of forelimb asymmetry induced by unilateral 6-hydroxydopamine (6-OHDA) lesion of the median forebrain bundle either alone or in combination with L-DOPA (Jones et al., 2012). In contrast, Lu AF21934 alone exhibited no effect in the akinesia induced by unilateral 6-OHDA lesion of the SNc unless a sub-threshold dose of L-DOPA was co-administered. Similarly, ADX88178 alone had no impact on forelimb akinesia induced by a bilateral 6-OHDA lesion. However, coadministration of ADX88178 with a low dose of L-DOPA enabled a robust reversal of the forelimb akinesia deficit. The difference between PAMs in 6-OHDA lesion models could result from distinctions in the lesion protocols used by the different research groups. It is also possible that the discrepancy is mediated by different pharmacological profiles of $mGlu_4$ PAMs. Detailed studies of PAMs using the same lesion procedure will be required to elucidate the mechanism for these differences.

Besides a symptom-alleviating effect, $mGlu_4$ PAMs also possess other potential benefits, such as potential disease-modifying efficacy and a lack of L-DOPA-mediated side effects, such as dyskinesia. PHCCC and VU0155041 has been shown to reduce dopaminergic cell death (Battaglia et al., 2006; Betts et al., 2012), possibly due to reduced excessive excitatory drive onto dopamine neurons, and provide the potential to slow disease progression. In addition, LuAF21934, a selective $mGlu_4$ PAM related to the VU0155041

series, has been shown to decrease the incidence of L-DOPA-induced dyskinesia (Bennouar et al., 2013), further making $mGlu_4$ an attractive target for PD treatment.

Mechanism of allosteric modulation

Through years of research, orthosteric ligands useful in determining the physiological roles of mGlus have been developed which display group-selectivity. However, as all orthosteric ligands bind to the N-terminal VFD of mGlus, which is evolutionarily designed to bind glutamate, it is difficult to achieve subtype selectivity since the glutamate binding site is highly conserved across all eight subtypes. In addition, brain penetration and pharmacokinetics of these orthosteric ligands can be limited by their amino acid-like properties. Many of these hurdles have been overcome by targeting allosteric binding sites on the receptors. As indicated by the name, allosteric modulators bind to a site other than the endogenous agonist binding site, and provide modulatory effects on the affinity/efficacy of the orthosteric agonist, termed cooperativity. Indeed, the complex structure of mGlus offers a number of possibilities to develop novel allosteric modulators. Because of the greater sequence divergence demonstrated at allosteric sites, a series of subtype-selective allosteric agonists and positive, negative or silent allosteric modulators (PAM, NAM or SAMs) of mGlus have been identified through high through-put screening campaigns ((Kinney et al., 2005; Mitsukawa et al., 2005; Niswender et al., 2008b; Varney et al., 1999) and many others), which have greatly advanced studies on mGlu functions and accelerated the development of mGlu reagents as disease therapeutics.

The mechanism of action of allosteric modulators is exemplified by the dataset shown in Figure 1.2, PAMs potentiate the response to orthosteric agonists by shifting the concentration-response curve of an orthosteric agonist to the left (with or without increasing the maxium response), indicating that the agonist response is being pharmacologically amplified. NAMs are molecules that antagonize the activity of agonists in a noncompetitive fashion through negative cooperativity. SAMs are neutral allosteric modulators that exhibit no apparent effect on agonist reponses on their own;

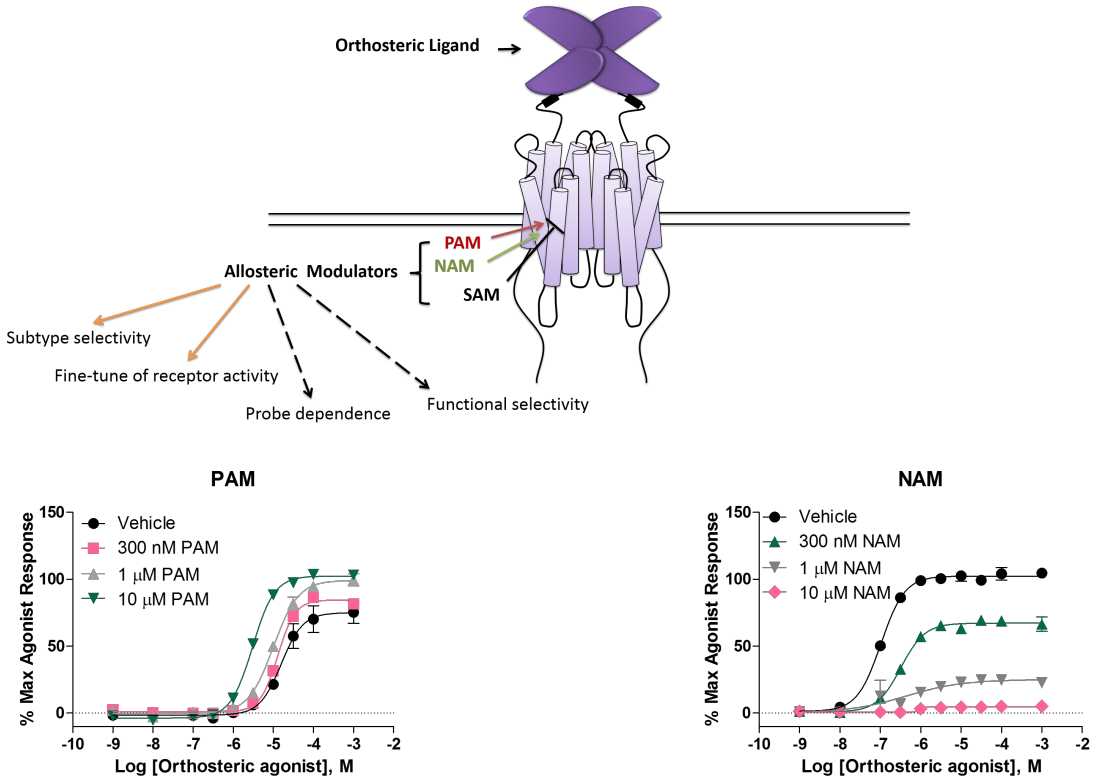

Figure 1.2. Mechanism of action of allosteric modulators. Instead of binding to the glutamate binding site on the N-terminal VFD, mGlu PAMs and NAMs bind to the 7TMD on the receptor and induce selective modulating effects, which can be blocked by SAMs. PAMs potentiate the response to orthosteric agonists by shifting the dose response curve of an orthosteric agonist to the left, whereas NAMs progressively antagonize the activity of agonists through negative cooperativity in a noncompetitive fashion.

however, such compounds can block the binding and subsequent receptor modulation induced by PAMs or NAMs.

Besides improved selectivity, PAMs and NAMs also provide some other advantages when compared to their orthosteric counterparts. First, the biological effects of PAMs and NAMs are dependent on the presence of the endogenous agonist; thus, they have the potential to preserve the spatial and temporal aspects of endogenous signaling. As PAMs which lack allosteric agonist activity will not constantly activate the receptor, they may also reduce the liability of receptor desensitization compared to the direct activation by orthosteric, or even allosteric, agonists. Allosteric modulators also bring a further advantage in that their modulating effect is saturable, thus providing a larger therapeutic window and potentially decreasing the risk of overdose. In addition, these allosteric molecules often possess drug-like properties and better pharmacokinetics and brain penetration compared to orthosteric ligands, an important feature considering the therapeutic indication of mGlus in CNS disorders.

Thusfar, the majority of identified mGlu allosteric modulators bind to the 7TMD region of the receptor. Results from mutagenesis studies indicate that the mGlu allosteric binding site likely corresponds to the orthosteric binding site in Class A 7TMRs (Chen et al., 2008; Gregory et al., 2013; Litschig et al., 1999; Malherbe et al., 2003; Pagano et al., 2000; Schaffhauser et al., 2003). Interestingly, PAMs can directly activate an N-terminal truncated mGlu (El Moustaine et al., 2012; Goudet et al., 2004), suggesting that VFD-CRD region prevents PAMs from activating the receptor until glutamate is bound. The modulating effects induced by allosteric modulators can be quantified using operational models of allosterism (Gregory et al., 2012; Leach et al., 2007):

$$y = basal + \frac{(E_m - basal)(\tau_A[A](K_B + \alpha\beta[B]) + \tau_B[B]K_A)^n}{(\tau_A[A](K_B + \alpha\beta[B]) + \tau_B[B]K_A)^n + ([A]K_B + K_AK_B + K_A[B] + \alpha[A][B])^n}$$

where *A* and *B* are the molar concentration of the orthosteric agonist and the allosteric modulator, respectively; K_A and K_B are the equilibrium dissociation constant of the orthosteric agonist and the allosteric modulator, respectively; τ_A and τ_B quantify the efficacy of the orthosteric agonist and the allosteric modulator, respectively. *Basal,* E_m and *n* represent the basal system response, maximal possible system response and the transducer function that links occupancy to response. Importantly, these models have introduced two parameters, α and β, to describe cooperativity of an allosteric ligand on the affinity and efficacy of orthosteric agonist. The operational models of allosterism not only allow quantitative estimation of modulator affinity and cooperativity values, which can be used to guide compound optimization processes, but can be used to derive reliable estimates of modulator affinities when radioligand is not available (Gregory et al., 2012).

Based on molecular pharmacology data, it has been hypothesized that binding of one PAM per mGlu dimer is sufficient to potentiate receptor activity (Goudet et al., 2005). In contrast, binding of NAMs to both protomers appears to be necessary to inhibit receptor activation (Hlavackova et al., 2005).

Allosteric modulators for $mGlu_2$ and $mGlu_4$

As allosteric modulators have been discovered for each individual mGlu subtype, selective modulators for $mGlu_2$ and $mGlu_4$ will be discussed here in detail.

BINA, LY487379 (along with CBiPES) and THIIC represent three chemical scaffolds of highly selective $mGlu_2$ PAMs that lacks activity at $mGlu_3$ (Fell et al., 2011; Galici et al., 2006; Johnson et al., 2005). Several NAMs from the dihydrobenzo[1,4]diazepin-2-one series, as exemplified by MNI-137, have been reported to antagonized both $mGlu_2$ and $mGlu_3$ in a non-competitive fashion (Hemstapat et al., 2007; Woltering et al., 2008a; Woltering et al., 2008b). Additionally, a group of $mGlu_2$ SAMs have been identified through FRET-based binding assays and slight modification of these SAMs yields three $mGlu_2$ NAMs with $mGlu_3$ PAM activity, indicating that identification of SAMs is a useful approach to discover novel mGlu allosteric modulators (Schann et al., 2010).

Mutagenesis studies have revealed that amino acids that are essential for $mGlu_2$ PAM activity are dispensible for NAMs, and the converse has also been reported (Lundstrom et al., 2011; Rowe et al., 2008; Schaffhauser et al., 2003). These data suggest that $mGlu_2$ PAMs and NAMs may bind to different allosteric pockets, although binding studies using appropriate allosteric radioligands are required to validate this hypothesis.

Allosteric modulation has also been demonstrated to be a successful approach to selectively modulate $mGlu_{4, 7 \text{ and } 8}$. An $mGlu_1$ partial antagonist, PHCCC, was the first identified PAM for $mGlu_4$ with no activity on 6 of the other mGlu subtypes except for $mGlu_6$ (Beqollari and Kammermeier, 2008; Maj et al., 2003; Marino et al., 2003). In the in vitro $mGlu_4$ assays in which is has been examined, PHCCC exhibits no agonist activity by itself but increases the potency of glutamate at $mGlu_4$ and acts as a proof-of-concept compound for targeting $mGlu_4$ as a potential therapeutic strategy for disorders such as Parkinson's disease (Marino et al., 2003). Further optimization of the PHCCC scaffold has been challenging (Niswender et al., 2008, Williams et al 2010); however, a high-throughput screening campaign led to the identification of VU0155041 and VU0080421 as examples of non-PHCCC scaffold $mGlu_4$ PAMs (Niswender et al., 2008b; Niswender et al., 2008c). Recently, many other $mGlu_4$ PAMs, including 4PAM-2, VU0364770, ADX88178, LuAF21934 and others (Bennouar et al., 2013; Drolet et al., 2011b; Jones et al., 2012; Le Poul et al., 2012), have emerged with significant improvements in potency, selectivity and pharmacokinetic profile compared to PHCCC. Particularly, VU0364770, ADX88178 and LuAF21934 exhibit high potency with good pharmacokinetic profiles for use as tool compounds; each of these ligands shows *in vivo* efficacy in animal models of PD and other disorders. Interestingly, VU0155041 also exhibits allosteric agonist activity at $mGlu_4$ when tested *in vitro* (Niswender et al., 2008b), suggesting an alternative mechanism of action compared to PHCCC. Indeed, data obtained from radioligand binding assays has demonstrated that VU0155041 binds to a unique allosteric site on $mGlu_4$ which is different from the binding site of PHCCC and 4PAM-2 (Drolet et al., 2011b).

Advantages and complications of allosteric modulation

In addition to the improved selectivity, PAMs and NAMs also provide some other advantages comparing to orthosteric counterparts. First, the biological effects of PAMs and NAMs are dependent on the presence of the endogenous agonist, thus they have the potential to preserve the spatial and temporal aspects of endogenous signaling. As PAMs themselves will not continuously activate the receptor, they may also reduce the liability of receptor desensitization comparing to the direct activation by orthosteric, or even allosteric, agonists. Allosteric modulators also bring a further advantage in that their modulating effect is saturable, thus providing a larger therapeutic window and potentially decreasing the risk of overdose. In addition, these allosteric molecules often possess drug-like properties and better permeability at the blood-brain barrier, an important feature considering the therapeutic indication of mGlus in CNS disorders.

Despite all the advantages mentioned above, many allosteric modulators are lipophilic, which diminishes their solubility, can affect their pharmacokinetic profile, and potentially increases off-target binding. The shallow structure-activity relationship among classes of allosteric ligands also represents a significant hurdle in the development of allosteric modulators. Additionally, because of the substantial activity alteration generated by minor structural changes, a number of mGlu allosteric modulator classes are susceptible to subtle "molecular switches" (Wood et al., 2011), by which compounds within a series can switch from NAM to PAM, PAM to NAM, or exhibit altered selectivity (Lamb et al., 2011; Sharma et al., 2009; Sheffler et al., 2012; Zhou et al., 2010).

Allosteric compounds have also complicated our understanding of receptor pharmacology. As allosteric modulators potentiate/inhibit the receptor through cooperativity with the orthosteric ligand being used, it is not surprising that "probe dependence" has been reported in some cases, in that modulators have differential effects depending upon the orthosteric ligand that is present (Suratman et al., 2011; Valant et al., 2012). Although examples still have yet to be discovered for mGlu receptors, caution

should be taken to choose the orthosteric ligand for *in vitro* studies. In addition, similar to what has been described with some orthosteric ligands (Urban et al., 2007), many allosteric ligands have been found to differentially stimulate multiple signaling cascades downstream of a receptor (Kenakin, 2005), a phenomenon often termed "functional selectivity" "biased signaling", or "ligand directed trafficking" (Marlo et al., 2009; Zhang et al., 2005). Indeed, 7TMRs may adopt multiple structural conformations, and allosteric modulators may stabilize any of them, which can translate into the regulation of some signaling pathways but not others.

The first aim of this dissertation is to study the signaling bias of $mGlu_4$ PAMs induced by concommitant activation of a G_q-coupled receptor. The second part of this dissertation is to study the heterodimerization of $mGlu_{2/4}$ and the differentially regulated pharmacology of allosteric modulators by the formation of mGlu heterodimers. Although these findings highly complicate the application of allosteric modulators as disease therapeutics, it is conceivable that it could be utilized to enhance the therapeutic outcome or avoid adverse effects.

CHAPTER II

FUNCTIONAL SELECTIVITY INDUCED BY MGLU4 RECEPTOR ALLOSTERIC MODULATORS DURING CONCOMITANT ACTIVATION OF Gq COUPLED RECEPTORS

Introduction

Seven Transmembrane Spanning/G-Protein-Coupled Receptors (7TMRs/GPCRs) represent the majority of drug targets currently used in clinical practice. Much interest has recently been placed on the discovery and characterization of allosteric modulators for these receptors due to several potential advantages over traditional orthosteric ligands in terms of drug development (reviewed in (Keov et al., 2011)). For example, many natural endogenous ligands are peptides or small amino acids which possess limitations in pharmacokinetic properties, preventing their development as drug candidates. Additionally, the orthosteric agonist binding sites of many 7TMRs are highly conserved across family members, making selectivity for a particular receptor within one group difficult to achieve. Due to their interaction with the receptor at a site distinct from the orthosteric site, allosteric ligands often possess very high receptor selectivity. Allosteric modulators also have the ability to provide a more subtle and physiologically-relevant approach to increasing or decreasing target activity because receptor regulation will occur only in the presence of the endogenous ligand (Bridges and Lindsley, 2008; Conn et al., 2009). Furthermore, allosteric potentiators, or positive allosteric modulators (PAMs), may, in some cases, avoid receptor desensitization and/or down-regulation that can occur after chronic administration of an orthosteric agonist (Bridges and Lindsley, 2008; Conn et al., 2009). As allosteric modulators function by exerting either positive (PAMs) or negative (NAMs) cooperativity with the orthosteric ligand, mechanistically they will

exhibit a “ceiling” effect (i.e., maximal receptor occupancy may not translate to maximal effect on receptor activation), which may avoid target/mechanism-mediated side effects that could arise from accidental overdose.

While allosteric modulators of 7TMRs provide potential advantages/distinctions over orthosteric ligands, these compounds also greatly complicate our understanding of receptor pharmacology. In recent years, there has been a growing appreciation of the ability of a single 7TMR to simultaneously regulate multiple signaling cascades (Kenakin, 2005), some of which are G protein-independent, such as β arrestin-regulated pathways. This phenomenon, now well established for orthosteric ligands, has been termed “functional selectivity”, “biased signaling”, or “ligand directed trafficking” (Keov et al., 2011; Urban et al., 2007); we will refer to this phenomenon as functional selectivity. There are now also clear examples of 7TMR allosteric modulator-mediated functional selectivity (Marlo et al., 2009; Mathiesen et al., 2005). While this behavior introduces complexity into ligand development, it is anticipated that capitalizing on functionally selective effects will provide exciting opportunities to tailor new drug therapy to specifically regulate coupling of 7TMRs to beneficial signaling pathways but not others, potentially reducing adverse effects.

There are numerous mechanisms by which functionally selective pharmacology can be induced by allosteric ligands. For example, 7TMRs have the ability to adopt multiple structural conformations, any of which might be stabilized by an allosteric modulator. This can translate into the ability of a modulator to preferentially regulate some pathways and not others based on the particular conformation they stabilize. Receptor activity is also regulated by other cellular proteins, such as G-proteins, arrestins, or scaffolding proteins, which also act in an allosteric fashion to affect receptor conformations. In this case, compound pharmacology can be altered depending on the context in which a receptor is expressed (e.g., (Niswender et al., 2010)), presumably due to the different proteins or cellular components interacting with the receptor in various cell types.

An alternate possibility that may affect the outcome of functional selectivity would be convergent signaling pathways that are activated (or inhibited, or simply absent) in a certain temporal or spatial context. It has previously been demonstrated that activation of the $G_{i/o}$-coupled $GABA_B$ receptor, in conjunction with the G_q- coupled metabotropic glutamate 1 ($mGlu_1$) receptor, produces a signaling convergence at the level of phospholipase C β3 ($PLC_{\beta3}$) to induce potentiated calcium mobilization (Pin et al., 2009; Rives et al., 2009). In these studies, this phenomenon was not due to heterodimerization/oligomerization of the receptors, was generalizable to other receptor pairs, and was demonstrated to exhibit functional relevance in cerebellar Purkinje cells and cultured cortical neurons where these two receptors are co-expressed (Rives et al., 2009). In the current study, we extend these findings to explore potentially functionally selective effects induced by this type of signaling convergence. We describe that, as for the $GABA_B$ and $mGlu_1$ receptor combination, activation of a G_q coupled histamine receptor, the H_1 receptor, dramatically potentiates the ability of the $G_{i/o}$-coupled metabotropic glutamate 4 ($mGlu_4$) receptor to induce intracellular calcium mobilization. However, histamine does not potentiate the ability of $mGlu_4$ activation to modulate other "common" $G_{i/o}$-regulated signaling cascades, such as cAMP inhibition. These results suggest that H_1 co-activation biases $mGlu_4$-mediated signaling events toward certain signaling pathways. Furthermore, when small molecule PAMs of $mGlu_4$, are included in these assays, the potentiated signaling of $mGlu_4$ is further biased by histamine toward calcium-dependent pathways. Our results suggest that convergence of these signaling pathways may result in substantial, and potentially unexpected, increases in calcium responses downstream of $mGlu_4$ activation, particularly when receptor activity is potentiated using positive allosteric modulators.

Methods

Cell line establishment and cell culture

Establishment and culture of the human $mGlu_4$ ($hmGlu_4$)/G_{qi5}/CHO-DHFR(-) has been described in (Niswender et al., 2008b). All cell culture reagents were purchased from Invitrogen (Carlsbad, CA) unless otherwise noted.

Guinea pig H_1 (gp H_1)/CHO-K1 cells were obtained by stable transfection of CHO-K1 cells with guinea pig H_1 receptor in pcDNA3.1 vector (a generous gift of Mike Zhu, Ohio State University). Single G418-resistant clones were isolated and screened for H_1-mediated calcium mobilization as described below. Monoclonal gpH_1/CHO-K1 cells were cultured in 90% Dulbecco's modified Eagle's medium (DMEM), 10% dialyzed fetal bovine serum (FBS), 100 U/ml penicillin/streptomycin, 20 mM HEPES, 1 mM sodium pyruvate, 2 mM L-glutamine, 20 μg/ml proline (Sigma-Aldrich, Inc., St. Louis, MO) and 400 μg/ml G418 sulfate (Mediatech, Inc., Herndon, VA).

Rat $mGlu_4$/CHO-K1 cells, rat $mGlu_2$/CHO-K1 cells, rat $mGlu_4/H_1$/CHO-K1 cells, and rat $mGlu_2/H_1$/CHO-K1 cells were obtained by stable transfection of either CHO-K1 cells or gpH_1/CHO-K1 cells with rat $mGlu_4$ or $mGlu_2$ receptor in a pIRESpuro3 vector (Invitrogen). Polyclonal cells were cultured in 90% DMEM, 10% dialyzed FBS, 100 U/ml penicillin/streptomycin, 20 mM HEPES, 1 mM sodium pyruvate, 2 mM L-glutamine, 20 μg/ml proline (Sigma-Aldrich, Inc., St. Louis, MO), 20 μg/ml puromycin (Sigma-Aldrich, Inc., St. Louis, MO) without or with 400 μg/ml G418 sulfate (for H_1 expressing cell lines, Mediatech, Inc., Herndon, VA).

Rat $mGlu_4/M_1$/CHO-K1 cells were generated by stable transfection of rat $mGlu_4$/CHO-K1 cells with rat M_1 muscarinic receptor DNA in pcDNA3.1 vector. Polyclonal cells were cultured in 90% DMEM, 10% dialyzed FBS, 100 U/ml penicillin/streptomycin, 20

mM HEPES, 1 mM sodium pyruvate, 2 mM L-glutamine, 20 μg/ml proline (Sigma-Aldrich, Inc., St. Louis, MO), 400 μg/ml G418 sulfate (Mediatech, Inc., Herndon, VA) and 20 μg/ml puromycin (Sigma-Aldrich, Inc., St. Louis, MO).

Calcium mobilization assays

For assays performed using the Flexstation (Molecular Devices, Sunnyvale, CA), cells were seeded at a density of 60,000 cells/100 μl/well in Costar 96-well tissue culture-treated plates. For assays performed using the Hamamatsu FDSS 6000 or 7000 (Hamamatsu, Japan), cells were seeded at 30,000 cells/20 μl/well in Greiner 384-well clear-bottomed, tissue culture–treated plates. Cells were incubated in assay medium (90% DMEM, 10% dialyzed FBS, 20 mM HEPES and 1 mM sodium pyruvate) overnight at 37°C/5% CO_2 and assayed the following day.

Fluo-4/acetoxymethyl ester (Invitrogen) was dissolved as a 2.3 mM stock in DMSO and mixed in a 1:1 ratio with 10% (w/v) Pluronic acid F-127 and diluted in assay buffer (Hanks' balanced salt solution, 20 mM HEPES, and 2.5 mM probenecid; Sigma-Aldrich) to a final concentration of 2 μM. Cells were dye-loaded for 45 min at 37°C; dye was then removed and replaced by appropriate volume of assay buffer. For single-add experiments, a series of different concentrations of glutamate or histamine were diluted into assay buffer as 2× stock. For histamine fold-shift and potency experiments, histamine was diluted as 2× stock and added at the first add. After 150 sec, the appropriate volume of a 5× glutamate stock was added in a second addition. For experiments using antagonists or PAMs, compounds were added at a 2× final concentration in the first addition followed by the desired concentration of agonist in the second addition.

Total RNA isolation, reverse transcription and polymerase chain reaction (RT–PCR)

CHO-K1 cells, $mGlu_4$/CHO-DHFR(-) cells, $mGlu_4/G_{qi5}$/CHO-DHFR(-) cells, and $mGlu_4$/HEK/GIRK cells were seeded in 10 cm cell culture dishes one day before the experiment. On the second day, cells were harvested and total mRNA from each cell line was extracted using an RNeasy Mini Kit (Qiagen, Valencia, CA). Total RNA was quantified by Nanodrop and 0.5 ug was reversely transcribed into cDNA by iScript cDNA Synthesis Kit (Bio-Rad, Philadelphia PA) according to the manufacturer's protocol. Reactions were carried out both in the presence and in the absence of reverse transcriptase (as negative controls). One tenth of each yielded cDNA sample was used to perform polymerase chain reaction (PCR) using primers for histamine H_2, H_3 and H_4 receptors. The primers were designed to match the conserved sequence for human, rat and mouse histamine receptors:

H_2 Forward: AGCTTTGGCCAGGTCTTCTGCA

H_2 Reverse: GGCTGCCAGTGTCACGGTGG

H_3 Forward: GCTGTGGCTGGTGGTAGACT

H_3 Reverse: AGGAGCTTGGTGAAGGCTCTGCGG

H_4 Forward: TGATAGGCAATGCTGTGGTC

H_4 Reverse: GCCAGTGACCTGGCTAGCTTCCT

Water was used as a negative control for PCR reactions for H_2-H_4 receptors. 1 ng of rat brain cDNA was used as the positive control for H_2 and H_3 receptor and pcDNA3.1-H_4 plasmid was used as positive controls for H_4 receptor. The amplification protocol for H_2 and H_3 was 95 °C for 2 min, 30 cycles of 95 °C for 30 s, 58 °C for 30 s, and 72 °C for 1.5 min. For H_4, the annealing temperature was set at 52°C. The final extension step was at 72 °C for 5 min. The PCR products were then electrophoresed on a 1% agarose gel containing ethidium bromide in parallel with 1 Kb Plus DNA Ladder (Invitrogen).

Phosphoinositide hydrolysis assays

$mGlu_2/H_1$/CHO-K1 cells were plated in 24-well plates at a density of 100,000 cells/well/0.5 mL in growth medium two days before the assay. On the following day, growth media was removed and replace with 0.5 ml/well assay media containing 0.5 μCi/ml [^{3}H]-inositol. Cell plates were incubated at 37°C/5% CO_2 overnight and assayed on the third day. For stimulation of phosphoinositide hydrolysis, the [^{3}H]-inositol-containing assay medium was first aspirated from wells and replaced with 200 μl of assay buffer (HBSS supplemented with 20 mM HEPES and 30 mM LiCl). Cells were then treated with 250 μl of assay buffer or histamine (2×, 1 μM final concentration, diluted in assay buffer) and 50 μl of serial dilutions of glutamate (10×, diluted in assay buffer). After drug addition, the assay plates were incubated at 37°C/5% CO2 for 1 h, and then 1 ml of stop solution (10 mM formic acid) was added into each well to terminate the reaction. Cells were incubated in stop solution for 1 h at room temperature then the cell extracts were transferred to anion exchange columns (AG 1-X8 Resin, 100-200 mesh, formate form; Bio-Rad Laboratories, Hercules, CA) for separation of [^{3}H]inositol-containing compounds. After loading of cell extracts, each column was washed sequentially with 9 ml of water, 9 ml of 5 mM inositol, and 9 ml of water. Finally, the [^{3}H]inositol-containing compounds that bound to columns were eluted with 9 ml of PI Eluent (200mM ammonium formate and 100 mM formic acid) into scintillation vials and measured by liquid scintillation counting. Baseline response was removed from both histamine-treated and control group respectively and data were fit with GraphPad Prism (La Jolla, CA) to a 4-parameter logistic equation.

Adenylate cyclase assays

Adenylate cyclase assays were performed according to the methods described in (Sheffler and Conn, 2008; Watts and Neve, 1996). Cells were plated at 60,000 cells/well in Assay Media in 96 well plates 24 h prior to assay. The next day, media was removed from the cells and replaced with 100 μL of serum free DMEM containing 20 mM HEPES. After 1

h incubation at 37 °C, the media was replaced with 50 µL 37 °C stimulation buffer (DMEM, 15 mM HEPES, pH 7.4, 0.025% ascorbic acid). After a 10 min incubation at room temperature, the stimulation buffer was removed and the cells were placed on ice. For dose response curves of glutamate in rat $mGlu_4$/CHO-K1 cells and rat $mGlu_4/H_1$/CHO-K1 cells, 20 µL of the phosphodiesterase inhibitor 3-isobutyl-1-methylxanthine (IBMX) (4×, 500 µM final concentration, diluted in stimulation buffer) was first added to all wells to prevent cAMP breakdown. 20 µL of stimulation buffer was then added, followed by 20 µL of forskolin (4×, 10 µM final concentration, diluted in stimulation buffer) or DMSO-matched vehicle control. Finally, serial dilutions of glutamate (20 µL, 4×, diluted in stimulation buffer) were added to the wells. For histamine fold-shift experiments in $mGlu_4/G_{qi5}$/CHO-DHFR(-) cell line, cells were treated with 20 µL IBMX (4×, 500 µM final concentration, diluted in stimulation Buffer), 20 µL stimulation buffer or histamine (4×, 10 µM final concentration, diluted in stimulation buffer), 20 µL of forskolin (4×, 20 µM final concentration) or vehicle and 20 µL of serial dilutions of glutamate. For histamine fold-shift experiments in $mGlu_4/H_1$/CHO-K1 cells, serial dilutions of $mGlu_4$ PAMs were diluted as 4× stock in stimulation buffer containing 4 µM glutamate (1 µM final concentration). Cells were treated with 20 µL IBMX (4×, 500 µM final concentration, diluted in timulation Buffer), 20 µL of forskolin (4×, 20 µM final concentration) or vehicle, 20 µL stimulation buffer or histamine (4×, 300 nM final concentration, diluted in stimulation buffer) and 20 µL of serial dilutions of $mGlu_4$ PAMs.

After 20 min incubation in water bath at 37 °C, drugs were then removed from the wells and the reaction was terminated by addition of 40 µL ice-cold 3% trichloroacetic acid (TCA). Cell lysates were chilled at 4 °C for at least 2 h. Accumulated cAMP was quantified using a competitive binding assay adapted from (Nordstedt and Fredholm, 1990) with minor modifications. Briefly, TCA extracts (15 µL) from assay plates were added to a deep well 96 well plate (Axygen Scientific) in triplicates. [^{3}H]-cAMP (PerkinElmer) (1 nM final concentration) was diluted in cAMP Assay Buffer (100 mM Tris–HCl, pH 7.4, 100 mM NaCl, 5 mM EDTA) and added to each well (25 µL/well). Lastly, 500 µL of cAMP-binding proteins (approximately 100 µg of crude extract from

bovine adrenal cortex) was added to each well. The deep-well plates were incubated on ice for 2 h and harvested with a Brandel cell harvester (Gaithersburg, MD) onto Whatman GF/B filters. Radioactivity bound to filters was quantified by liquid scintillation counting using a PerkinElmer Top Count. The concentration of cAMP in each well was calculated according to a cAMP standard curve ranging from 0.01 to 1000 pM.

Positive allosteric modulators of $mGlu_4$

Glutamate, histamine and *N*-Phenyl-7-(hydroxyimino)cyclopropa [*b*]chromen-1a-carboxamide (PHCCC) were purchased from Tocris Biosciences (Ellisville, Missouri). Acetylcholine was purchased from Sigma-Aldrich Incorporated (St. Louis, MO). *cis*-2-[[(3,5-Dichlorophenyl)amino]carbonyl]cyclohexanecarboxylic acid (VU0155041), *N*-(4-(*N*-(2-chlorophenyl)sulfamoyl)phenyl)picolinamide (4PAM-2), and 5-methyl-*N*-(4-methylpyrimidin-2-yl)-4-(1*H*-pyrazol-4-yl)thiazol-2-amine (ADX88178) were synthesized in-house according to methods in (Celanire et al., 2011; Engers et al., 2010; Niswender et al., 2008b; Reynolds, 2008).

Astrocyte culture

Rat cortical astrocytes were prepared using neocortices from 2-4 day old Sprague Dawley rats. Neocortics from pups were dissected and dissociated in DMEM by trituration and the cells were centrifuged and resuspended in growth media (DMEM supplemented with 10 % FBS, 1 mM sodium pyruvate, 2 mM L-glutamine and antibiotics) in poly-D-lysine-coated tissue culture dishes. Cells were maintained at 37 °C in an atmosphere of 95 % air/ 5 % CO_2 until ready for assay.

Phosphoinositide hydrolysis assays using hippocampal slices

Hippocampal slices were prepared according to the procedures described in (Ayala et al., 2009). Following tissue recovery, the tissue was combined, washed with warm Krebs

buffer (108 mM NaCl, 4.7 mM KCl, 1.2 mM $MgSO_4$, 1.2 mM KH2PO_4, 2.5 mM $CaCl_2$, 25 mM $NaHCO_3$ and 10 mM glucose), and 25 ml of gravity packed slices were incubated with 175 ml Krebs buffer containing 0.5 mCi [^{3}H]myo-inositol in 37ºC water bath for 45 min. 10 mM LiCl was added to slices and incubated for an additional 15 min. Histamine and/or L-AP4 were then added, followed by 15 min incubation. Carbachol was used as positive control and Krebs buffer was used as negative control. The reaction was terminated and phosphoinositide was extracted, purified and quantified using liquid scintillation counting as previously described in (Ayala et al., 2009).

Results

Activation of histamine H_1 receptor biases the signaling of $mGlu_4$ toward calcium mobilization

We have long been interested in the identification and characterization of small molecule positive allosteric modulators (PAMs) of $mGlu_4$ for the symptomatic and disease modifying treatment of Parkinson's disease. To characterize compounds, we employ a cell line in which the normally $G_{i/o}$-coupled $mGlu_4$ is co-expressed with the chimeric G protein G_{qi5} to permit induction of a calcium response downstream of $mGlu_4$ activation, a technique that is commonly employed in high throughput screening campaigns for various 7TMRs as it is an easy and cost-effective method to measure compound activity. In addition to identifying small molecule allosteric modulators, we had designed parallel studies to explore the impact of endogenous neurotransmitters and ligands on the modulation of $mGlu_4$ function. In the course of these studies, we discovered that application of the autacoid histamine to $mGlu_4$-expressing cells, prior to application of a concentration of glutamate designed to induce a 20% maximal response, resulted in a strong potentiation of the calcium mobilization signal normally induced by glutamate in $mGlu_4$/G_{qi5}-expressing cells. In these studies, the potentiation effect of histamine highly resembled the effects of synthetic PAMs of $mGlu_4$, such as the prototype PAM *N*-Phenyl-

7-(hydroxyimino)cyclopropa[*b*]chromen-1a-carboxamide (PHCCC), with one important difference. While both histamine and PHCCC were able to potentiate the effects of an EC_{20} concentration of glutamate (Figure 2.1A and B, "Glutamate Add"), unlike PHCCC, histamine induced a weak response when added alone to $mGlu_4/G_{qi5}$ cells (Figure 2.1B, "Compound Add"). In our experience using this $mGlu_4/G_{qi5}$ assay, response of compound alone is not common. In Figures 2.1C and D, concentration-response curves are shown for the compound response in the absence and presence of an EC_{20} concentration of glutamate. The control PAM PHCCC was inactive when added alone but exhibited a potency of 5.1±0.3 μM when potentiating the response to a low concentration of glutamate. In contrast, histamine generated a concentration-dependent response alone with a potency of 8.3±1.4 μM; in addition, histamine also potentiated the EC_{20} glutamate response (EC_{50}=1.2±0.1 μM).

Small molecule PAMs of $mGlu_4$ have been shown to potentiate multiple responses downstream of $mGlu_4$ activation (Jones et al., 2011; Niswender et al., 2008b). Therefore, if histamine directly binds to the $mGlu_4$ protein and acts as a prototypical $mGlu_4$ PAM, it would be expected to modulate additional, $G_{i/o}$-dependent pathways downstream of $mGlu_4$ activation, such as cAMP inhibition. In contrast to our studies with calcium mobilization (Figure 2.1B, 2.1D and 2.2A), histamine did not potentiate the ability of $mGlu_4$ activation to inhibit cAMP levels (Figure 2.2B). These results suggested that histamine induced biased signaling downstream of $mGlu_4$ activation. It also indicated that the mechanism of histamine's potentiation might differ from previously identified small molecule PAMs.

While our previous results did not rule out the possibility that histamine directly interacted with $mGlu_4$, the distinct signaling profile induced by histamine suggested that the mechanism of histamine's potentiation might be due to activity at a site distinct from $mGlu_4$, such as a histamine receptor. To determine if low levels of endogenous histamine receptors were involved in mediating the potentiation response, we performed RT-PCR experiments from our $mGlu_4$-expressing cells and determined that they expressed low

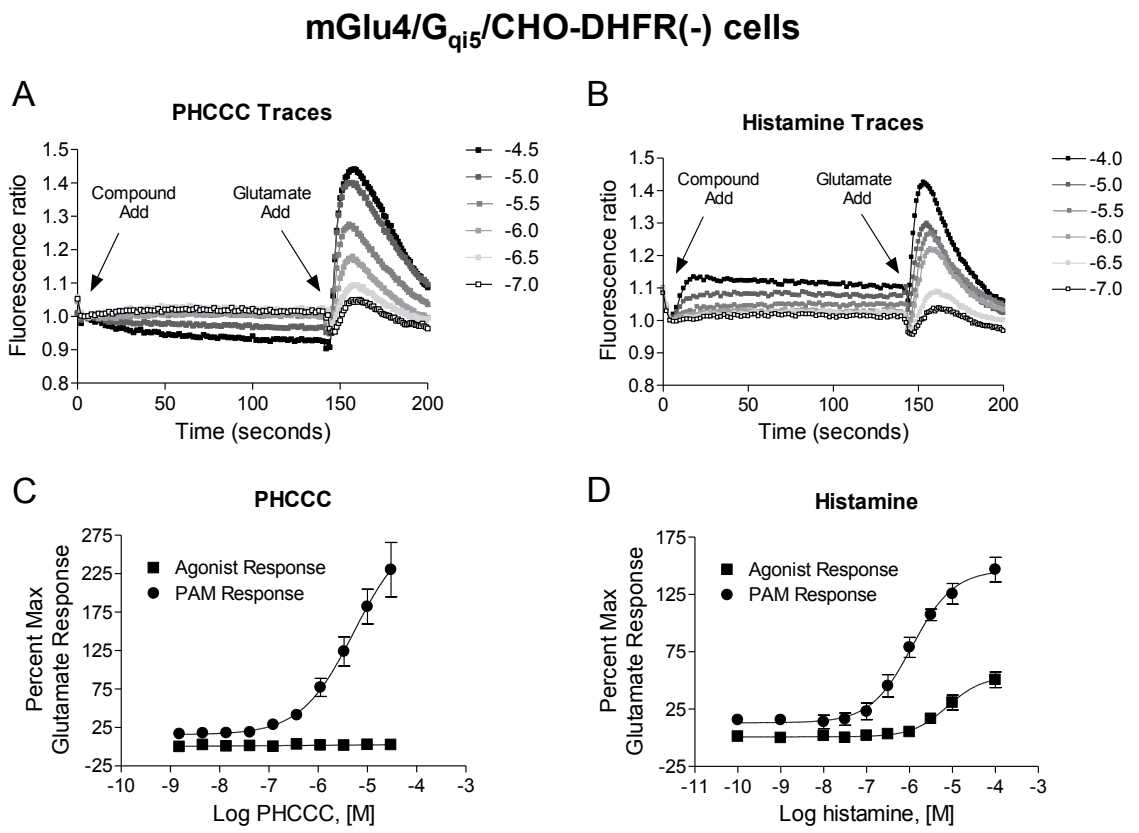

Figure 2.1. Histamine differs from the small molecule $mGlu_4$ PAM, PHCCC, in its potentiation effect. A and B, fluorescence traces of PHCCC and histamine in calcium mobilization assays measured in CHO-DHFR(-) cells co-expressing $mGlu_4$ and the chimeric G protein G_{qi5} in cells. PHCCC (A, ranging from 100 nM to 30 μM) or histamine (B, ranging from 100 nM to 100 μM) was added in the "Compound Add", while an EC_{20} concentration of glutamate (2.5 μM final) was added after 150 sec in the "Glutamate Add". C and D, Compound activity alone (Agonist Response) and PAM activity (PAM Response) in the presence of an EC_{20} concentration of glutamate (2.5 μM final) from traces represented in A and B are shown for PHCCC and histamine, respectively. For both responses, the increase in fluorescence units is normalized to the maximum response elicited by 1 mM glutamate in this cell line. PHCCC elicited no agonist response and possessed a potency of 5.1±0.3 μM for the PAM response. The potency of histamine for the PAM response was 1.2±0.4 μM and for the agonist response was and 8.3±1.4 μM. Data shown were performed in triplicate; Mean ± SEM.

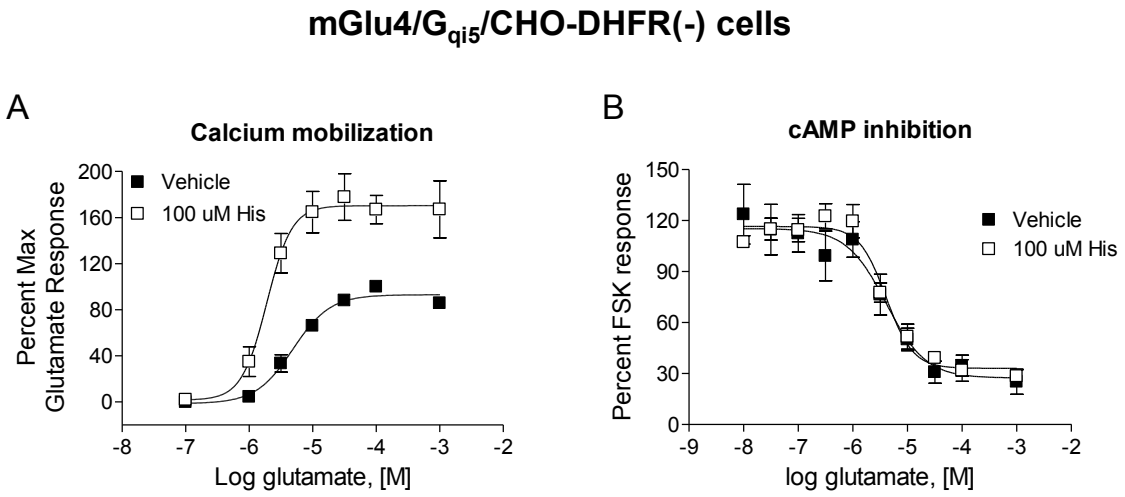

Figure 2.2. Histamine potentiates calcium responses downstream of $mGlu_4$ without impacting glutamate-dependent cAMP inhibition. A, Glutamate-induced calcium mobilization was measured in the presence of vehicle control (■) or 100 μM histamine (□). The responses are normalized to maximum effect of glutamate in the same cell line. Potencies in the absence or presence of 100 μM histamine were 5.1±0.9 μM vs. 2.0±0.3 μM (*p=0.029; unpaired t-test). Maximal responses in the absence or presence of 100 μM histamine were: 100.0±1.0% vs. 179.1±20.0% (*p=0.017; unpaired t-test). B, Glutamate-dependent intracellular cAMP concentration was quantified in the absence (■) or presence (□) of 100 μM histamine using a competitive binding assay as described in *2.5. Adenylate cyclase assays*. Data were normalized to the 20 μM forskolin-induced response. Potencies in the absence or presence of 100 μM histamine were 4.1±0.3μM vs. 4.3±0.8μM (p=0.76; unpaired t-test). Maximal inhibition values in the absence or presence of 100 μM histamine were: 88.1±8.3% vs. 83.9±2.3% (p=0.65; unpaired t-test). Data shown were performed in triplicate; Mean ± SEM. Statistical analysis was performed using GraphPad Prism (La Jolla, CA).

levels of H_1 histamine receptor mRNA (Figure 2.3A). PCR with primers against H_2, H_3 and H_4 receptor did not yield any specific bands to support the existence of other histamine receptors (Figure 2.4). To address the potential contribution of functional activity of G_q-coupled H_1 receptors, we co-applied the H_1 receptor antagonist mepyramine and 100 μM histamine to $mGlu_4$-expressing cells in the first addition and then added an EC_{20} concentration of glutamate in the second addition. These studies revealed that mepyramine blocked the response induced by histamine application alone to a baseline level (Figure 2.3B), consistent with full blockade of H_1. While mepyramine was also able to block the response induced by the glutamate EC_{20} addition, the blockade saturated at the level of the EC_{20} glutamate response (Figure 2.3B).

These findings suggested that the potentiation effect was likely mediated by low levels of endogenous H_1 protein present in our $mGlu_4$ cell line. However, they did not completely rule out the possibility of direct histamine binding to $mGlu_4$, since mepyramine might have exerted its effect by displacing binding of histamine from the $mGlu_4$ receptor. Additionally, our original cell line contained the chimeric G protein G_{qi5} to induce $mGlu_4$-mediated calcium mobilization, which would not be reflective of $mGlu_4$ signaling in native tissues. In order to test the hypothesis that the potentiation effect was definitively mediated by H_1 activity versus direct histamine interaction with $mGlu_4$ and occurred in presence of native cellular G proteins, we screened a panel of cell lines to identify a line that did not express H_1 mRNA. We found that CHO-K1 cells, in contrast to the CHO-DHFR(-) cell background used for the initial screening, did not express H_1 mRNA (Figure 2.3A). By utilizing the CHO-K1 cells as the parental cell line, we generated two new cell lines that contained either the $mGlu_4$ receptor alone, or $mGlu_4$ co-expressed with the H_1 receptor; neither of these cell lines contained G_{qi5}. As shown in Figure 2.5A, $mGlu_4$ was functional and coupled to glutamate-induced cAMP inhibition in cells expressing either $mGlu_4$ alone or the $mGlu_4$+H_1 combination. We then performed studies in which we attempted to potentiate glutamate-induced calcium mobilization using increasing concentrations of histamine in cells without (Figure 2.5B) and with (Figure

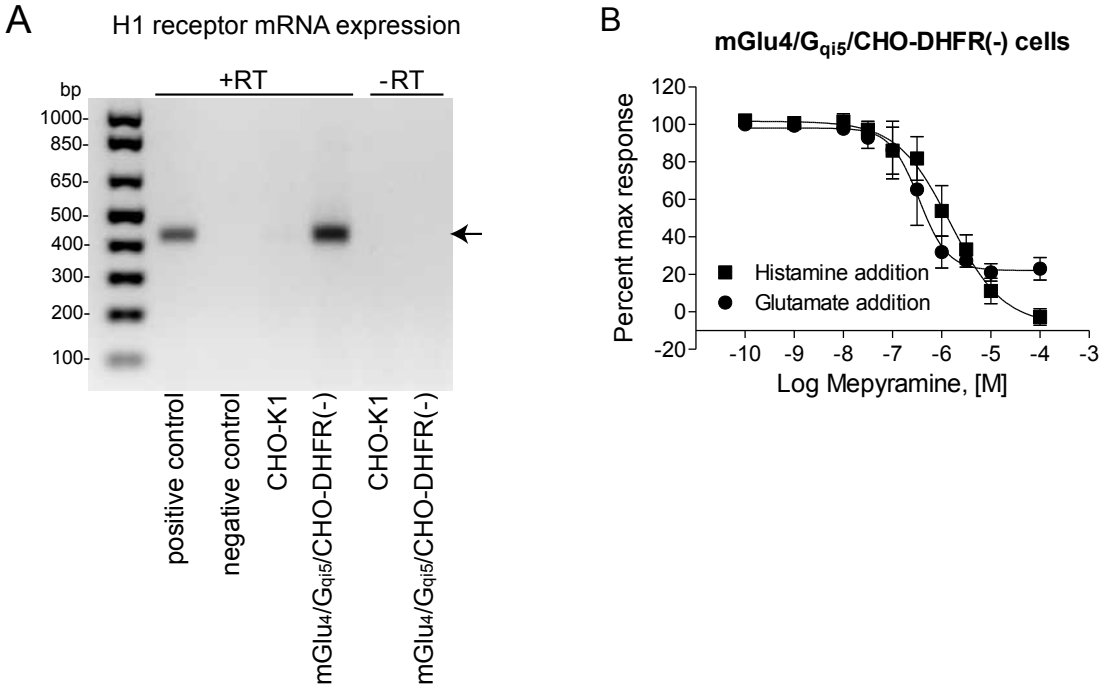

Figure 2.3. The histamine H_1 receptor may be involved in the potentiation effect of histamine. A, mRNA expression of histamine H_1 receptor in different cell lines. mRNA was extracted from CHO-K1 cell line and $mGlu_4/G_{qi5}$/CHO-DHFR(-) cell line and RT-PCR was performed as described under Materials and Methods. "+RT" indicates presence of reverse transcriptase during the reaction of reverse transcription, whereas "–RT" represents absence of reverse transcriptase as negative controls. Predicted size of the PCR product for the H_1 receptor was 423 bp, as shown with arrow. B, Mepyramine abolishes the agonist response and potentiation effect of histamine. Increasing concentrations of mepyramine were added to $mGlu_4/G_{qi5}$/CHO-DHFR(-) cells with 100 μM histamine prior to addition of an EC_{20} concentration of glutamate (2.5 μM glutamate final). Calcium mobilization induced by the histamine addition and the subsequent glutamate addition was measured as described. Potencies of mepyramine in the histamine add or the glutamate add were: 1.55±0.5 μM vs. 393±154 nM (p=0.10; unpaired t-test). Data shown were performed in triplicate; Mean ± SEM. Statistical analysis was performed using GraphPad Prism (La Jolla, CA).

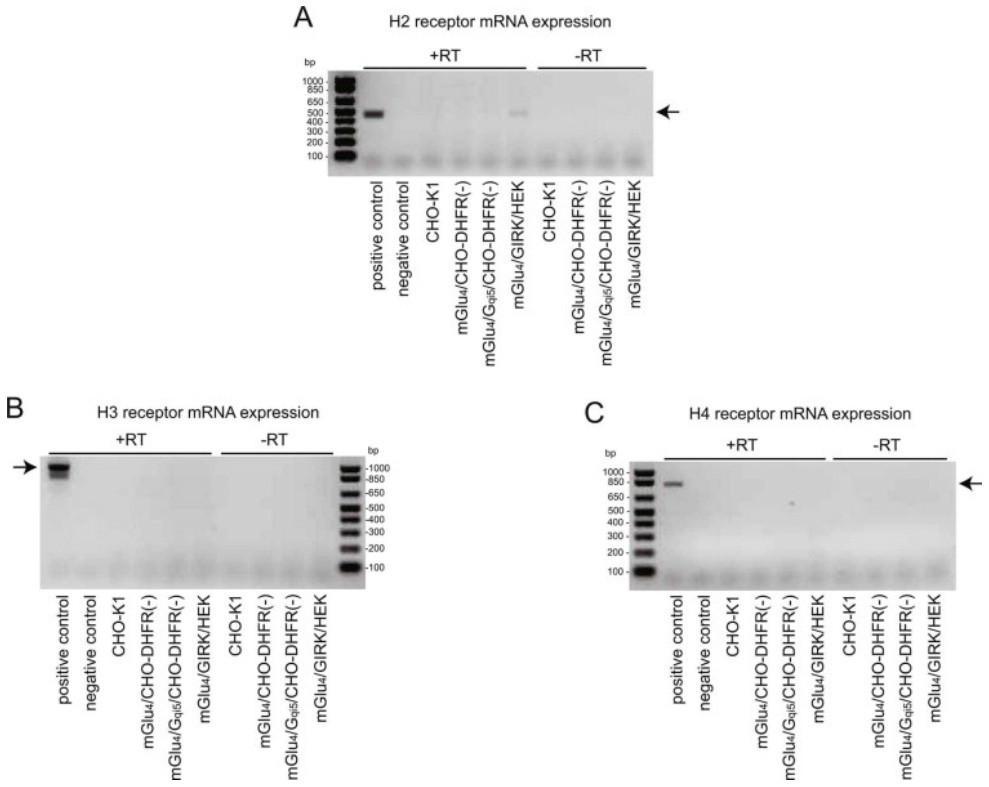

Figure 2.4. mRNA expression of histamine H_2, H_3 and H_4 receptor (A-C respectively) in different cell lines. mRNA was extracted from different cell lines as labeled and RT-PCR was performed as described under Supplemental Methods. "+RT" indicates presence of reverse transcriptase during the reaction of reverse transcription, whereas "–RT" represents absence of reverse transcriptase as negative controls. Predicted size of PCR products for H_2, H_3 and H_4 were 462 bp, 957 bp and 834 bp, respectively, as shown with arrows.

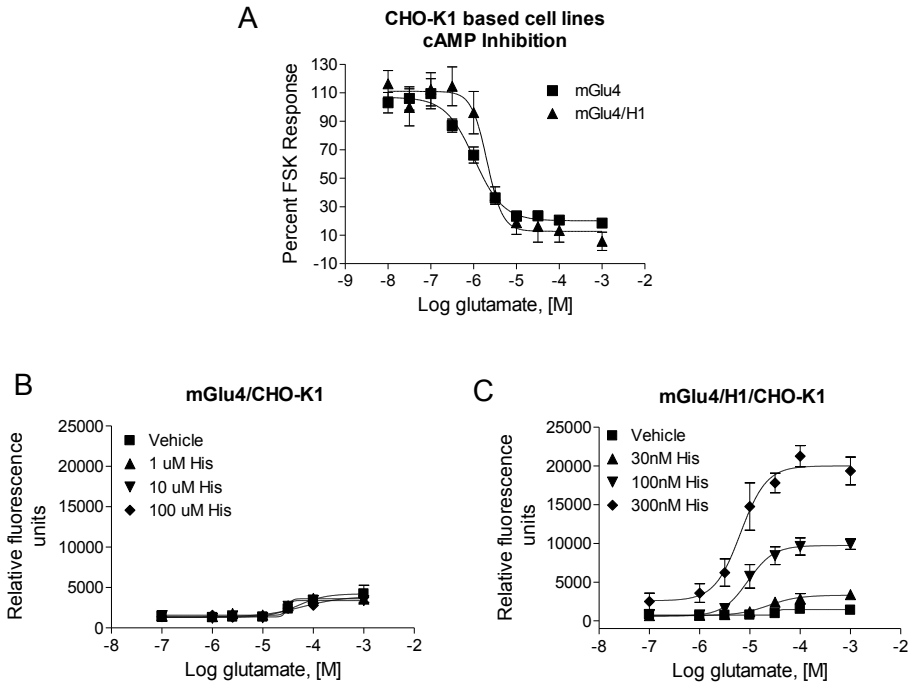

Figure 2.5. The histamine H_1 receptor is required for the potentiation effect of histamine. A, Glutamate exhibits potencies of 1.0±0.03 μM and 2.3±0.1 μM, respectively, in adenylate cyclase assays in $mGlu_4$/CHO-K1 cells and $mGlu_4/H_1$/CHO-K1 cells (*p=0.0048, unpaired t-test). Intracellular cAMP concentration was measured as described in *2.5. Adenylate cyclase assays* and responses were normalized to the 10 μM forskolin response in each cell line, respectively. B, The effect of 1 μM (▲), 10 μM (▼) and 100 μM (◆) histamine on glutamate-induced calcium mobilization in $mGlu_4$/CHO-K1 cells is shown. Maximal responses of vehicle, 1 μM, 10 μM or 100 μM histamine-treated cells were 3391±1033, 3254± 841, 3067± 527 and 3214± 643 relative fluorescence units, respectively (p=0.99; One-way ANOVA). C, The effect of 30 nM (▲), 100 nM (▼) and 300 nM (◆) histamine in potentiating calcium responses mediated by glutamate in $mGluR_4/H_1$/CHO-K1 cells is shown. Maximal responses in vehicle, 30 nM, 100 nM or 300 nM histamine-treated cells were 1548±230, 3390±636, 10099±819, 21261±1356 relative fluorescence units, respectively (*p<0.0001; One-way ANOVA). Data shown were performed in triplicate; Mean ± SEM. Statistical analysis was performed using GraphPad Prism (La Jolla, CA).

2.5C) H_1. These results clearly showed that the potentiation required the presence of H_1 receptors.

Concomitant activation of Gq coupled receptors pathway-selectively potentiate the calcium signaling of Gi-coupled receptors

According to our findings, the potentiated calcium response that we observed was mediated by concomitant activation of the G_q-coupled H_1 receptor and $G_{i/o}$-coupled $mGlu_4$ receptor. We speculated that, if this potentiation was due to a signaling convergence, the phenomenon would extend to other G_q and $G_{i/o}$ coupled receptor pairs. To test this hypothesis, we co-expressed $mGlu_4$ with the muscarinic acetylcholine M_1 receptor, another G_q-coupled receptor which is also extensively expressed in the CNS. We observed that activation of the M_1 receptor via acetylcholine in this $mGlu_4$-co-expressing cell line induced similar glutamate-dependent calcium mobilization compared to cells co-expressing H_1 and $mGlu_4$ (Figure 2.6A). We also hypothesized that such signaling crosstalk might be generalizable to other $G_{i/o}$-coupled mGlu receptors. As carried out for $mGlu_4$, we constructed two $mGlu_2$ cell lines in a CHO-K1 background, one of which expressed $mGlu_2$ alone and the other in combination with H_1 receptor. As shown in Figure 2.5B, cells expressing $mGlu_2$ alone did not respond to histamine; in contrast, cells co-expressing H_1 and $mGlu_2$ exhibited robust potentiation of calcium responses after co-application of histamine and glutamate (Figure 2.6C). As shown previously (Rives et al., 2009), signaling of $G_{i/o}$ and G_q receptors converges on the PLC_β pathway. To determine if this was also the mechanism of potentiated calcium responses for the receptors examined here, phosphoinositide hydrolysis assays were performed in cells co-expressing $mGlu_2$ and H_1 receptors. Consistent with our observations in calcium mobilization assays, histamine dramatically potentiated $mGlu_2$-induced phosphoinositide hydrolysis (Figure 2.6D).

Functionally selective effects of $mGlu_4$ positive allosteric modulators induced by co-activation of H_1 and $mGlu_4$

We are very interested in the development of small molecule positive allosteric modulators of $mGlu_4$ and were particularly intrigued with our initial studies (Figure 2.2) that suggested that histamine may induce functionally selective activation of signaling pathways downstream of $mGlu_4$. Furthermore, we hypothesized that co-application of histamine with $mGlu_4$ PAMs could further selectively potentiate calcium responses compared to signaling induced by other $G_{i/o}$-dependent pathways. To evaluate this hypothesis, we used our generated $mGlu_4/H_1$/CHO-K1 cell line which does not express G_{qi5}. For these studies, we chose PAMs from four distinct chemical scaffolds (Celanire et al., 2011; Niswender et al., 2008b; Reynolds, 2008) (Figure 2.7). These compounds were chosen based on differential *in vitro* potency and efficacy at $mGlu_4$; additionally, VU0155041 displays allosteric agonist activity in some assays (Niswender et al., 2008b) and has been proposed to bind to a different site on the $mGlu_4$ receptor compared to PHCCC and 4PAM-2 (Drolet et al., 2011a). In these experiments, we added increasing concentrations of each PAM either alone or in combination with histamine in the first addition. As shown in Figure 2.8, addition of each PAM alone (white traces, "Compound/Histamine Add") resulted in no calcium mobilization, even after glutamate addition ("Glutamate Add"). Addition of 300 nM histamine alone induced a relatively strong calcium response (dark gray traces); no potentiation of glutamate (second addition) was observed in this case due to the low concentration of glutamate added in these experiments. In contrast, addition of histamine + PHCCC, 4PAM-2, or ADX88178 (Figure 2.8A, B, and C) resulted in a prolonged calcium transient after the first addition and a very strong potentiation of the glutamate addition. Consistent with its potential to display allosteric agonist activity in some assays, VU0155041 behaved differently from the other PAMs, and substantial potentiation was observed in the first addition when this compound was added with histamine (Figure 2.8D); in contrast, no further potentiation was observed during the glutamate addition. In Figure 2.9, the concentration-response curves for these compounds, plus and minus 100 nM and 300 nM histamine, are plotted

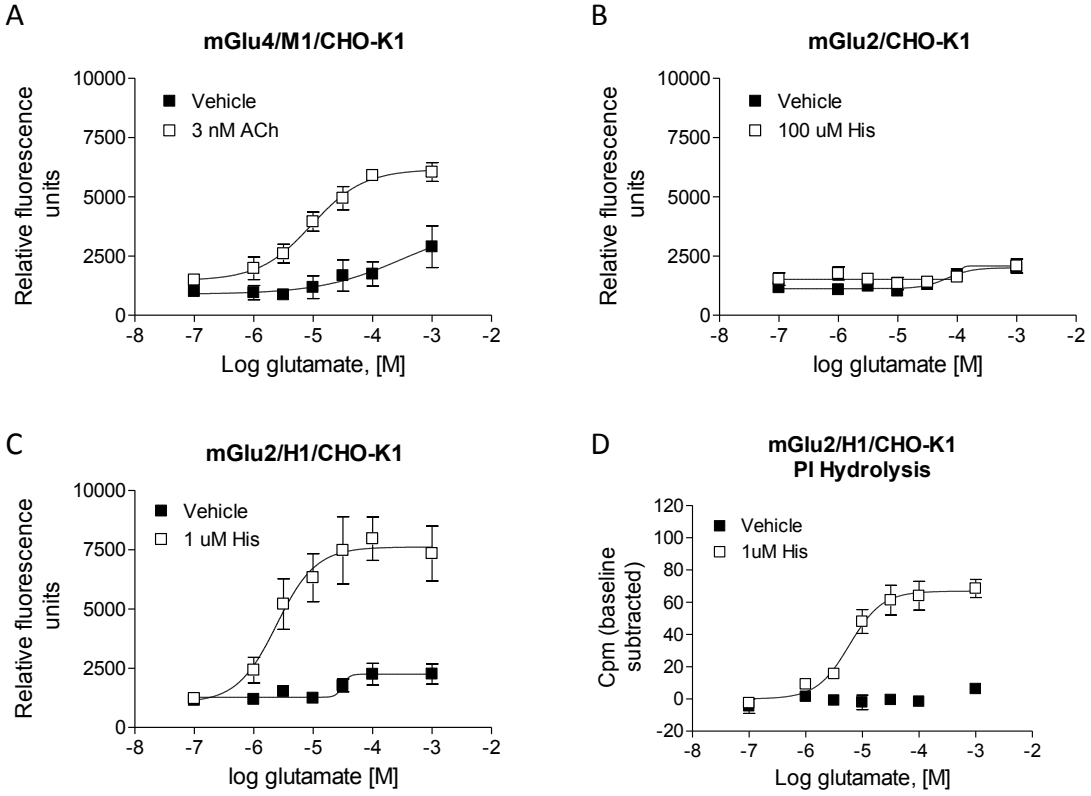

Figure 2.6. Phospholipase C pathway potentiation extends to additional G_q and $G_{i/o}$ pairs. A, Acetylcholine (Ach) potentiates calcium responses induced by $mGlu_4$ activation in $mGlu_4/M_1$/CHO-K1 cells. 3 nM Ach (□) or vehicle (■) control was added to cells in the first add, while increasing concentrations of glutamate were applied 150 sec later in the second add and calcium mobilization was measured. Maximal responses in the absence or presence of 3 nM Ach were: 2889±878 vs. 6175±280 relative fluorescence units (*p=0.024; unpaired t-test). Data shown were performed in triplicate; Mean ± SEM. B and C, histamine potentiates the calcium response of $mGlu_2$ in the presence of the histamine H_1 receptor in $mGlu_2/H_1$/CHO-K1 cells. In $mGlu_2$/CHO-K1 cells, maximal responses in the absence or presence of 100 μM histamine were: 2072±23.7 vs. 2122±272 relative fluorescence units (p=0.86; unpaired t-test). In $mGlu_2/H_1$/CHO-K1 cells, maximal responses in the absence or presence of 1 μM histamine were: 2796±285 vs. 8223±1128 relative fluorescence units (*p=0.010; unpaired t-test). Data shown were performed in triplicate; Mean ± SEM. D, Histamine potentiates $mGlu_2$ responses in

phosphoinositide hydrolysis assays in $mGlu_2/H_1$/CHO-K1 cells. Cells were treated with increasing concentrations of glutamate in the presence of 1 μM histamine (□) or vehicle control (■). After 1h incubation at 37℃, accumulated inositol phosphates were measured according to description in *2.4. Phosphoinositide hydrolysis assays*. Maximal responses in the absence or presence of 1 μM histamine were: 6.9±1.8 vs. 68.7±5.8 cpm (*p=0.0005; unpaired t-test). Data from triplicate experiments are shown (Mean ± SEM) with relative baseline responses subtracted from each group. All Statistical analysis was performed using GraphPad Prism (La Jolla, CA).

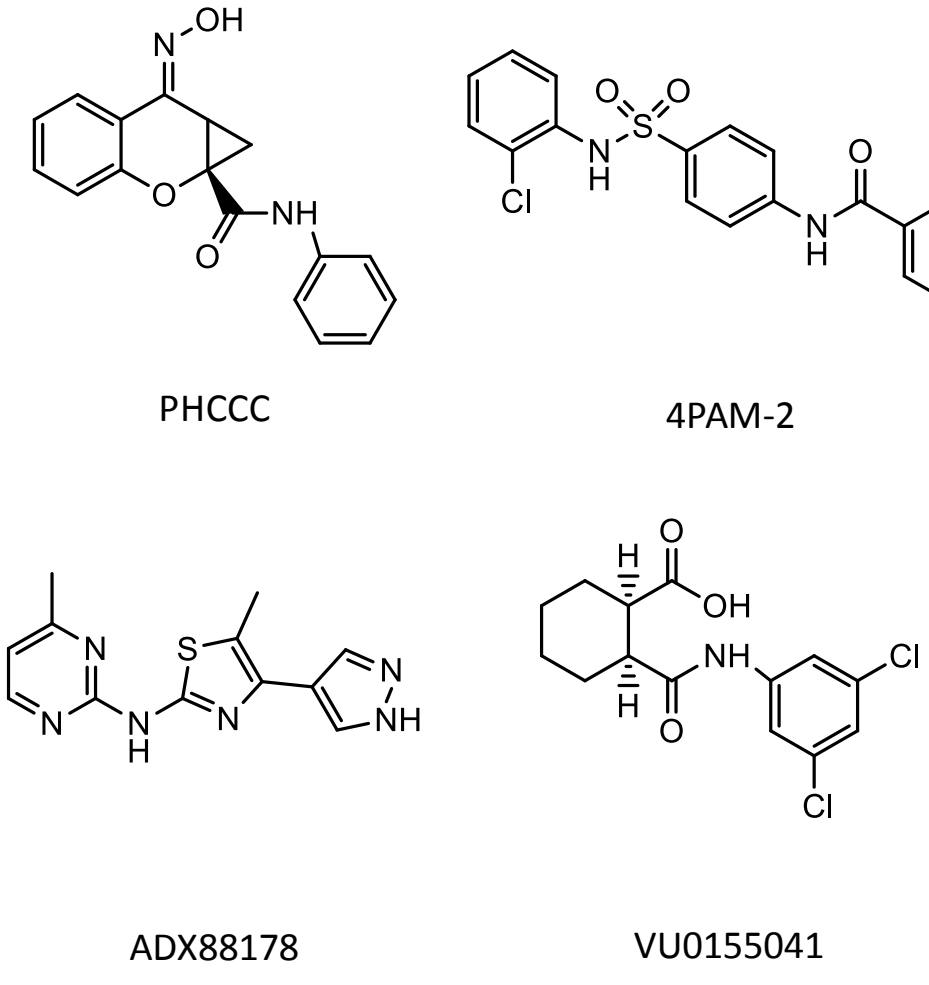

Figure 2.7. Chemical structures of $mGlu_4$ PAMs used in these studies: PHCCC, 4PAM-2, ADX88178 and VU0155041.

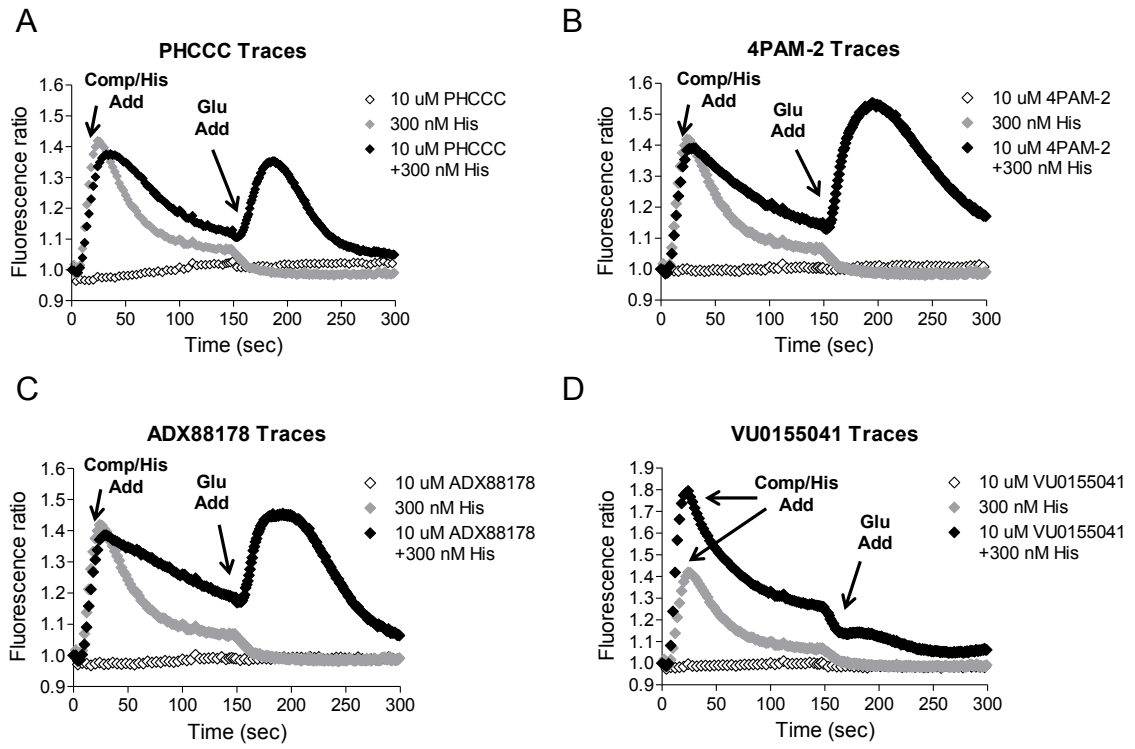

Figure 2.8. Histamine dramatically potentiates the effect of PAMs on $mGlu_4$-mediated calcium mobilization in cells co-expressing $mGlu_4$ and H_1 receptors. Traces of calcium transients showing the effects of $mGlu_4$ PAMs, histamine or the combination of both in potentiating the response of an EC_{20} concentration of glutamate (1 μM glutamate final) are shown. In these traces, a 10 μM concentration of each $mGlu_4$ PAM (PHCCC, 4PAM-2, ADX88178 or VU0155041, in A-D respectively; (◊)), 300nM histamine (♦) or combination of both (♦) were applied in the first add ("Compound/Histamine Add"). After 150 sec, 1 μM glutamate (concentration determined based on cAMP experiments shown in Figure 5A) was applied in the second add ("Glutamate Add"). Calcium responses were measured as the fluorescence ratio, which involves dividing all fluorescence data for each point in the kinetic trace by the fluorescence value obtained in the first baseline sample read, which corrects for differences in dye loading and cell plating.

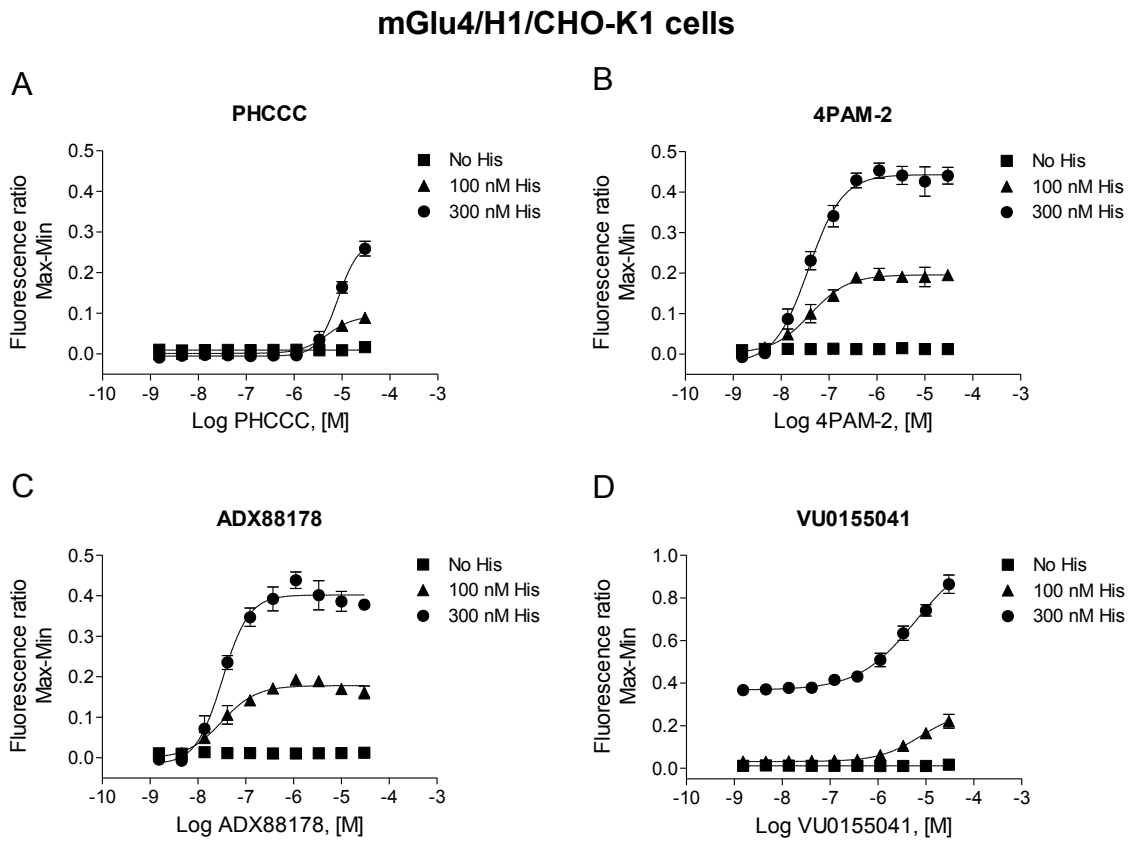

Figure 2.9. Histamine dose-dependently potentiates the efficacy of PAMs on $mGlu_4$-mediated calcium mobilization in cells co-expressing $mGlu_4$ and H_1 receptors. Results of traces in Figure 7 were plotted in concentration-response curve format. Increasing concentrations of the mGlu4 PAMs PHCCC, 4PAM-2, ADX88178 or VU0155041 (A-D, respectively) were applied either alone (■) or together with 100 nM (▲) or 300 nM (●) histamine in the first add. After 150 sec, a 1 μM glutamate concentration was applied in the second add. Calcium responses were measured as the fluorescence ratio, which involves dividing all fluorescence data for each point in the kinetic trace by the fluorescence value obtained in the first baseline sample read, which corrects for differences in dye loading and cell plating. Data were further normalized by taking the maximum calcium response minus the minimum response measured 3 seconds prior to either the first or second addition. For PHCCC (A), 4PAM-2 (B), and ADX88178 (C) responses, the effect on the second addition ("Glutamate Add") window is shown. For VU0155041 (D), the effect on the first addition ("Compound Add") is shown.

Potencies for the different conditions were: PHCCC alone, no fit, PHCCC+100 nM histamine, 8.2±5.1 μM, PHCCC+300 nM histamine, 7.6±1.4 μM; 4PAM-2 alone, no fit, 4PAM-2+100 nM histamine, 54.2±29.0 nM, 4PAM-2+300 nM histamine, 40.8±10.0 nM; ADX88178 alone, no fit, ADX88178+100 nM histamine, 37.2±15.1 nM, ADX88178+300 nM histamine, 30.0±5.2 nM; VU0155041 alone, no fit, VU0155041+100 nM histamine, 9.5±3.9 μM, VU0155041+300 nM histamine, 6.5±1.6 μM. Maximal responses in the absence or presence of 100 nM or 300 nM histamine were: for PHCCC, 0.016±0.003, 0.089±0.010, 0.259±0.018 (*$p<0.0001$; One-way ANOVA); for 4PAM-2, 0.017±0.002, 0.212±0.013, 0.460±0.022 (*$p<0.0001$; One-way ANOVA); for ADX88178, 0.016±0.002, 0.197±0.003, 0.438±0.020 (*$p<0.0001$; One-way ANOVA); and for VU0155041, 0.018±0.003, 0.221±0.032, 0.864±0.043 (*$p<0.0001$; One-way ANOVA). Data shown were performed in triplicate; Mean ± SEM. Statistical analysis was performed using GraphPad Prism (La Jolla, CA).

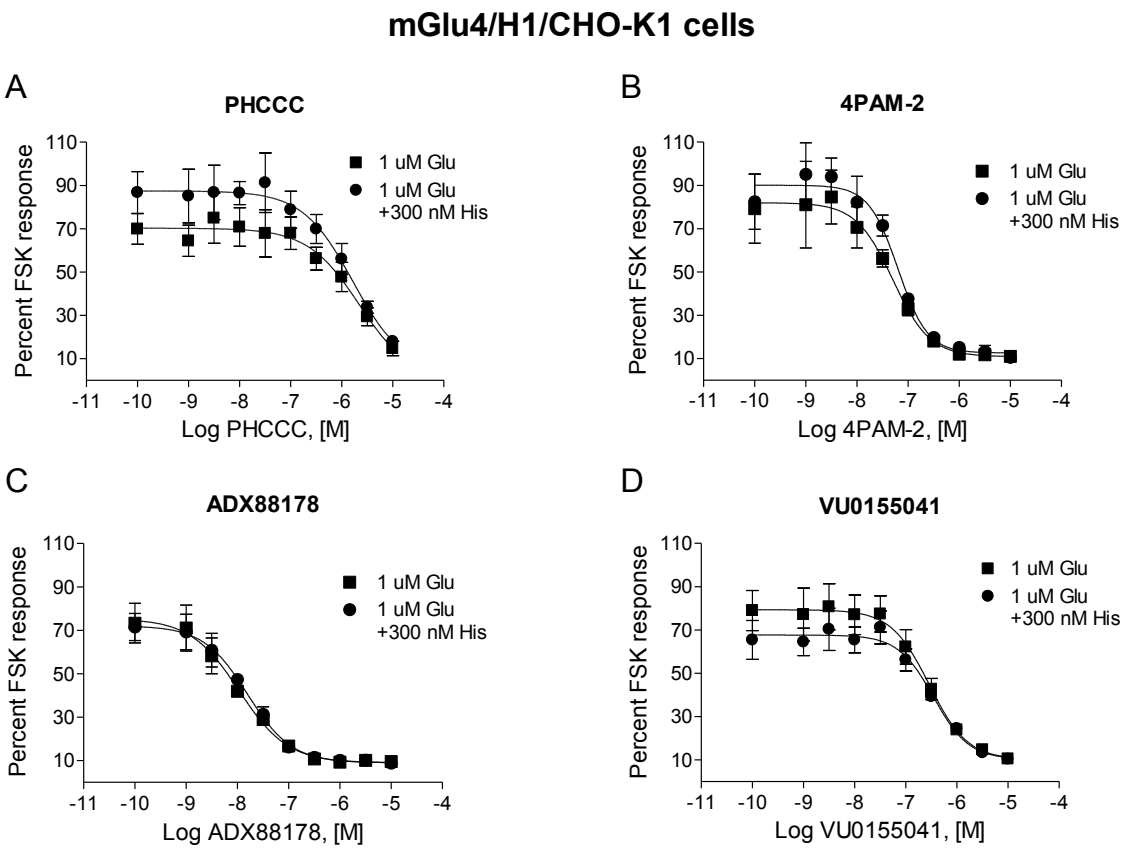

Figure 2.10. In contrast to effects on calcium mobilization, histamine has no effect on the activity of mGlu4 PAMs in adenylate cyclase assays in cells expressing both $mGlu_4$ and H_1 receptors. Increasing concentration of $mGlu_4$ PAMs (PHCCC, 4PAM-2, ADX88178 or VU0155041, A-D, respectively) were co-diluted with 1 μM glutamate and incubated with $mGlu_4/H_1$/CHO-K1 cells either alone or together with 300 nM histamine. Intracellular cAMP concentration was measured as described and then normalized to either 20 μM forskolin response or 20 μM forskolin+300nM histamine, respectively. Potencies in the absence or presence of 300 nM histamine were: PHCCC, 2.5±0.6 μM vs. 1.8±0.4 μM (p=0.40; unpaired t-test); 4PAM-2, 55.5±12.6 nM v.s 66.1±8.6 nM (p=0.53; unpaired t-test); ADX88178, 11.7±2.0 nM vs. 16.0±4.3 nM (p=0.42; unpaired t-test); and VU0155041, 287.3±23.1 nM vs. 360.0±38.8 nM (p=0.18; unpaired t-test). Maximal inhibition values in the absence or presence of 300 nM histamine were: PHCCC, 85.3±3.4% vs. 82.0±2.7% (p=0.49; unpaired t-test); 4PAM-2, 89.0±1.2 nM vs. 89.4±0.6% (p=0.77; unpaired t-test); ADX88178, 90.4±1.5% vs. 91.1±0.6% (p=0.70;

unpaired t-test); and VU0155041, 89.5±0.4% vs. 90.0±0.1% (p=0.85; unpaired t-test). Data shown were performed in triplicate; Mean ± SEM. Statistical analysis was performed using GraphPad Prism (La Jolla, CA).

for the PAM (Figure 2.9A, B, and C) and agonist (Figure 2.9D) windows of the experiments shown in Figure 2.8; the responses to histamine in this assay are clearly concentration-dependent and the potencies of the PAMs obtained are consistent with the potencies observed in other assays (Celanire et al., 2011; Engers et al., 2010; Niswender et al., 2008b).

In parallel experiments designed to test the potential for functional selectivity, we assessed the ability of histamine to affect cAMP inhibition responses induced by these PAMs in these same cells. For these studies, we performed concentration-response curves of these compounds, in the presence of an EC_{20} concentration of glutamate, with or without 300 nM histamine. Again, in contrast to calcium mobilization assays and as can be seen in Figure 2.10, histamine did not affect the cAMP responses to any of the PAMs tested. These results further suggest that co-activation/potentiation of the histamine H_1 receptor and $mGlu_4$ results in functionally selective effects, resulting in unexpected calcium mobilization induced by $mGlu_4$ PAMs.

Exploration of H_1-$mGlu_4$ signaling crosstalk in native tissues

Based on these interesting findings, we sought to explore the signaling crosstalk between H_1 and $mGlu_4$ using native tissues that coexpress the two receptors. It has been reported that the histamine H_1 receptor is functionally expressed in astrocytes (Lipnik-Stangelj and Carman-Krzan, 2004a, b). $mGlu_4$ levels have been reported to be very low in astrocytic cultures relative to $mGlu_5$ (Peavy and Conn, 1998, *J Neurochem*, 71(2):603-612 and Besong *et al*., 2002, *J Neurosci*, 2213, 5403-5411). However, a low level of $mGlu_4$ was detected in astrocytes by Besong et al, which was shown to be mediated astrocytic cytokine release (Besong et al., 2002). Therefore, primary rat cortical astrocyte cultures were prepared according to the method described in Besong et al (see Method for details) and evaluated in calcium assays. Consistent with previous studies, we performed immunoblot studies which revealed expression of $mGlu_4$ monomers in astrocytes, but not $mGlu_4$ dimers, the functional format of the receptor (Figure 2.11A). When tested in

calcium assays, we did not observe effects of $mGlu_4$ activation on calcium mobilization or crosstalk between H_1 and $mGlu_4$ receptors, although histamine was able to induce profound calcium responses in these astrocytes (Figure 2.11B). We further explored the possibility of signaling crosstalk in hippocampal slices, where both receptors are expressed. 100 μM carbachol (Cch), a muscarinic agonist as a positive control, induced significant hydrolysis of phosphoinositide (Figure 2.11C). While 100 μM histamine triggered modest responses when added alone, this effect was not potentiated by co-addition of 1 mM L-AP4 (Figure 2.11C), supporting an absence of signaling crosstalk in this brain region.

Discussion

In this chapter, we have explored the ability of convergent signaling to induce functionally selective effects downstream of allosteric modulation. These studies capitalized on initial reports, such as those of Rives et al. (Rives et al., 2009), showing that convergent signaling downstream of the $G_{i/o}$-coupled $GABA_B$ and G_q-coupled $mGlu_1$ receptors could result in potentiated calcium signaling. The effects reported in Rives et al. were apparent in transfected cells as well as in neurons, indicating that this potentiation can be observed in native tissues. We observed a similar interaction between $mGlu_4$ and H_1 histamine receptors in terms of calcium mobilization. In previous studies (Rives et al., 2009), the mechanism for potentiation was a convergence of signaling via G_q G proteins and the $G_{\beta\gamma}$ subunits of the $G_{i/o}$ G protein at the level of $PLC_{\beta3}$. To explore the generalizability of this phenomenon for different mGlus, in addition to our $mGlu_4$ and H_1 cells lines, we generated cells expressing $mGlu_4$ and the G_q coupled M_1 muscarinic receptor as well as cells co-expressing $mGlu_2$ and H_1. As shown in Figure 2.6, activation of the M_1 receptor via acetylcholine in $mGlu_4$-co-expressing cells induced similar glutamate-dependent calcium mobilization compared to cells co-expressing H_1 and $mGlu_4$. As shown for $mGlu_4$, CHO-K1 cells expressing $mGlu_2$ alone did not respond to

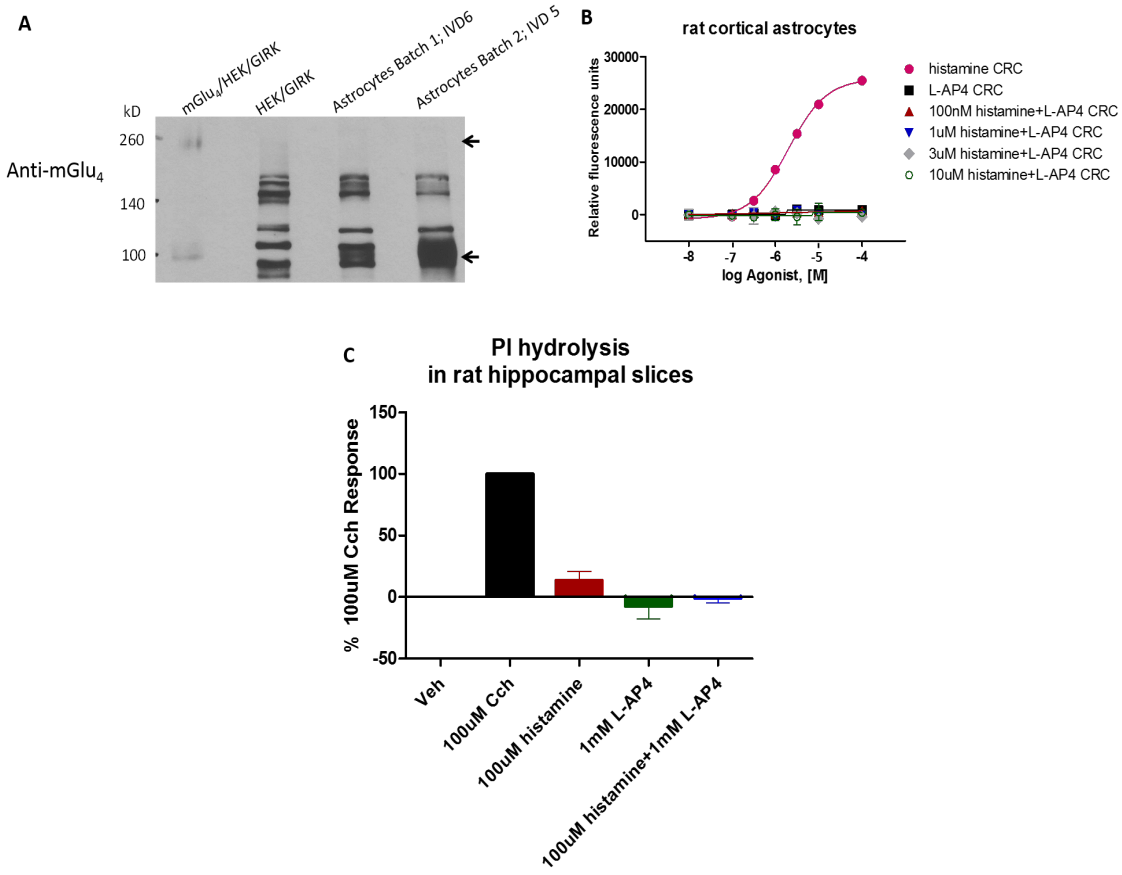

Figure 2.11. Interaction of H_1 receptor and $mGlu_4$ was not detected in rat cortical astrocytes or hippocampal slices. A. expression of $mGlu_4$ in rat cortical astrocytes were determined using Western blotting. Lanes from left to right: $mGlu_4$/HEK/GIRK (positive control); HEK/GIRK (negative control); astrocytes from batch 1, day 6 after in vitro culture; astrocytes from batch 2, day 5 after in vitro culture. B. Agonist-induced responses were measured using calcium mobilization assay as described above. Vehicle or 100 nM, 1 μM, 3 μM and 10 μM histamine was added in the first add and serial dilutions of L-AP4 were added in the second add. Serial dilutions of histamine were used as positive control. C. Agonist-induced phosphoinositide hydrolysis was measured as described and the measured scintillation values were normalized to vehicle response (as 0%), with 100 μM carbachol response as 100%.

histamine; in contrast, cells co-expressing H_1 and $mGlu_2$ exhibited robust potentiation of calcium responses when histamine and glutamate were co-applied. Finally, consistent with signaling that converges on the PLC_β pathway by co-activated $G_{i/o}$ and G_q receptors (Rives et al., 2009), histamine dramatically potentiated $mGlu_2$-induced phosphoinositide hydrolysis, suggesting that the potentiation mechanism we are observing here is similar. Since PLC_β can be activated by both $G_{\alpha q}$ and $G_{\beta\gamma}$ subunit from the G_i G-protein, we propose that occupation of both might have a synergistic effect on IP_3 production, inducing potentiated calcium mobilization. Indeed, mutagenesis studies of the $PLC_{\beta 2}$ protein have shown that distinct binding sites may exist for $G_{\alpha q}$ and $G_{\beta\gamma}$ on the enzyme (Lee et al., 1993).

The present studies extend previous observations by showing that the potentiation effect induced by G_q and $G_{i/o}$ convergent activation is signaling pathway specific and does not extend to other $G_{i/o}$-mediated signaling events, such as cAMP inhibition. These findings suggest that this cascade convergence effectively results in functional selectivity at a signaling level. During the course of our development of $mGlu_4$ PAMs, we have been interested in potential signaling bias or functionally selective effects induced by these compounds, particularly ligands belonging to different chemical scaffolds. In the assays we have examined, the majority of $mGlu_4$ PAMs will potentiate multiple signaling pathways downstream of $mGlu_4$ activation, including calcium mobilization induced using the chimeric G protein G_{qi5} and GIRK channel activation (Jones et al., 2011; Niswender et al., 2008b), in addition to potentiation of cAMP inhibition as shown in this chapter. Our studies here show that the signal bias induced by histamine can be greatly potentiated in the presence of small molecule PAMs, with PAMs and histamine inducing dramatic potentiation of calcium responses versus other $G_{i/o}$-dependent responses. More importantly, our studies now show that PAMs with no ability to potentiate glutamate-dependent calcium mobilization alone in the absence of chimeric G proteins (Figure 2.8, white traces) can induce substantial calcium signaling when the H_1 receptor, and presumably other G_q coupled receptors, are co-activated (Figure 2.8,black traces).

This unmasking of a substantial calcium response could be highly important in the physiological effects induced by PAMs *in vivo*. While the H_1 receptor and $mGlu_4$ do exhibit different expression patterns in neurons (for example, $mGlu_4$ is predominantly presynaptic and H_1 predominantly postsynaptic), which may account for the absence of crosstalk in hippocampal slices (Figure 2.11C), there are locations where their expression may overlap, such as dendritic cells of the immune system (Fallarino et al., 2010; Vanbervliet et al., 2011). Additionally, the observations that signaling convergence can extend to other receptor pairs suggests that it is highly likely that there are locations in which G_q and $G_{i/o}$ receptors may co-localize. In particular, $mGlu_2$ is expressed in many postsynaptic neurons (Neki et al., 1996; Petralia et al., 1996) and $mGlu_2$ PAMs are currently being developed for schizophrenia treatment, suggesting that a similar phenomenon may also impact $mGlu_2$ PAM signaling in postsynaptic neurons.

Another interesting point of speculation is that the strategy outlined here might provide a viable mechanism to potentiate the signaling of an intractable target. For example, there is substantial evidence indicating that activation of H_1 in neurons may have beneficial effects in terms of attention and wakefulness (reviewed in (Thakkar, 2011)). Due to the substantial expression of H_1 in various immune system cells, however, it would be difficult to pursue direct H_1 agonists or PAMs as drugs for attention without inducing substantial adverse effects. Exploiting the activity of a convergent signaling partner, however, might be an alternate mechanism by which to increase signaling of a G_q coupled 7TMR that is difficult to modulate directly. While $mGlu_4$ expression in dendritic cells of the immune system may preclude it as a strategy to potentiate H_1 signaling, restricted postsynaptic neuronal expression of other $G_{i/o}$-coupled receptors that are not expressed in immune cells could be an interesting strategy to explore.

In conclusion, we have shown that co-activation of $mGlu_4$ and the H_1 histamine receptor induces strong potentiation of calcium mobilization but not traditional $G_{i/o}$ signaling pathways, indicating functional selectivity in signal transduction. These functionally selective effects are observed in the absence of chimeric or promiscuous G proteins and are synergistically potentiated in the presence of small molecule PAMs. Finally, these

studies reveal that signaling events induced by PAMs may be “unmasked” in the presence of convergent signaling by G_q coupled receptors, which may lead to complex and unexpected pharmacology. The concept of functional selectivity may be the next frontier in the translation of novel therapeutics into patient populations, and it is anticipated that further exploration of compound pharmacology will certainly aid in the understanding of therapeutic efficacy and adverse effects.

CHAPTER III

HETERODIMERISATION OF MGLU2/4 DIFFERENTIALLY REGULATE EFFECT OF ALLOSTERIC MODULATORS

Introducton

The metabotropic glutamate (mGlu) receptors are members of the Family C Seven Transmembrane Spanning/G Protein Coupled Receptors (7TMRs/GPCRs) and are activated by the major excitatory neurotransmitter, glutamate. In their simplest context, Group I mGlus ($mGlu_1$ and $mGlu_5$) primarily modulate postsynaptic neuronal activity, whereas the Group II mGlus ($mGlu_2$ and $mGlu_3$) are found in both presynaptic and postsynaptic locations, and the Group III receptors ($mGlu_{4, 6, 7, \text{and } 8}$) are predominantly expressed presynaptically, where they act as auto- and heteroreceptors to regulate neurotransmitter release (reviewed in (Niswender and Conn, 2010)). The eight mGlu receptor subtypes have been historically thought to function as homodimers (Kunishima et al., 2000; Romano et al., 1996). However, recent *in vitro* studies suggest that mGlu receptors can also form heterodimers (Doumazane et al., 2011a; Kammermeier, 2012) with group I mGlus interacting with each other but not associating with other subtypes, and members of group II and III receptors co-assembling *in vitro*.

Among the group III mGlu receptors, $mGlu_4$ plays an important role in the basal ganglia, a primary site of pathology in movement disorders such as Parkinson's disease (PD).

Activation of $mGlu_4$ reduces transmission at synapses that project from the striatum to the globus pallidus (striatopallidal synapses) as well as synapses between the subthalamic nucleus and the substantia nigra pars compacta (STN-SNc synapses (Marino et al., 2003; Valenti et al., 2005; Valenti et al., 2003)), two synapses that are overactive in PD. At each of these synapses, the response to the general group III mGlu agonist L-AP4 is potentiated by PHCCC (Marino et al., 2003; Valenti et al., 2005), a positive allosteric modulator (PAM) that is selective for $mGlu_4$. In contrast to findings at the striatopallidal and STN-SNc synapses, we now report the surprising observation that PHCCC is without effect in regulating $mGlu_4$-modulated transmission at corticostriatal synapses.

Previous immunohistochemistry and in situ hybridization studies suggest that $mGlu_2$ and $mGlu_4$ are co-localized in several brain regions (Bradley et al., 1999; Neki et al., 1996; Ohishi et al., 1995; Ohishi et al., 1993) and $mGlu_2$ is also functionally expressed at corticostriatal synapses (Johnson et al., 2005). We tested the hypothesis that heterodimers of $mGlu_{2/4}$ may display a unique profile in response to selective $mGlu_4$ PAMs and that these mGlu subtypes would form hetero-complexes in the striatum. Through evaluation of $mGlu_4$ PAMs from different chemical scaffolds, we show here that hetero-interactions between $mGlu_2$ and $mGlu_4$ differentially impact responses to individual mGlu receptor PAMs and an $mGlu_2$ negative allosteric modulator (NAM). Furthermore, co-immunoprecipitation studies suggest that $mGlu_2$ and $mGlu_4$ receptors form hetero-complexes in the striatum and the unique pharmacological profile of effects of selected $mGlu_4$ receptor PAMs, as well as an $mGlu_2$ NAM, is recapitulated at the corticostriatal synapse. These studies directly impact our understanding of mGlu

receptors and regulation by allosteric modulators in the basal ganglia and provide critical insights into potential functions and pharmacological properties of mGlu receptors that are co-expressed in multiple other regions and cell populations.

Methods

Cell line establishment and cell culture

Cell culture reagents were purchased from Life Technologies (Carlsbad, CA) unless otherwise noted. Rat $mGlu_2$ or rat $mGlu_4$ were cloned into the pIRESpuro3 vector, transfected into HEK/GIRK cells and selected with puromycin. Polyclonal rat $mGlu_2$/HEK/GIRK and rat $mGlu_4$/HEK/GIRK cells were cultured in growth media as previously described in (Niswender et al., 2008a), supplemented with Non-Essential Amino Acids. Rat $mGlu_4$ was also subcloned into the pIREShyg3 vector and the resulting plasmid was transfected into rat $mGlu_2$/HEK/GIRK cells; cells were then selected with 200 μg/mL hygromycin B. Polyclonal cells were cultured in growth media supplemented with 100 μg/ml hygromycin B.

Western blot analysis

Cells were scraped into lysis buffer (50 mM Tris·HCl, pH 7.5, 150mM NaCl, 0.5% Nonidet P40 and 0.5% Deoxycholate) containing protease inhibitor cocktail (Roche, Indianapolis, IN) and incubated on ice for 20-30 min. The supernatant was separated from cell debris by centrifugation at 16,000×g for 10 min at 4°C. Protein concentrations

in cell lysates were quantified by Bio-Rad Protein Assay (Bio-Rad, Hercules, CA) or Bradford protein assay (Bio-Rad) and aliquots of lysate were heated in SDS sample buffer (containing 10% SDS and 9.3% DTT) at 65°C for 5 min. Samples were loaded to SDS–polyacrylamide gel for electrophoresis and transferred to nitrocellulose membranes (Bio-Rad). After transfer, membranes were blocked in TBST (25mM Tris, 150mM NaCl and 0.05% Tween-20) containing 5% non-fat milk at room temperature for 1 h. $mGlu_2$ antibodies (Advanced Targeting Systems, San Diego, CA, cat # AB-N32) and $mGlu_{4a}$ antibodies (Upstate, Billerica, MA, cat # 06-765) were diluted in blocking solution and incubated with the membranes at 4°C overnight. Membranes were then washed with TBST and incubated with horseradish peroxidase-conjugated goat anti-mouse IgG secondary antibody (Santa Cruz, Santa Cruz, CA, cat # sc-2060, 1:7,500 diluted in blocking buffer (Jackson ImmunoResearch, West Grove, PA, cat # 115-035-166, 1:10,000 diluted in blocking buffer) for $mGlu_2$ or horseradish peroxidase-conjugated goat anti-rabbit IgG secondary antibody (Santa Cruz, Santa Cruz, CA, cat # sc-2004, 1:7,500 diluted in blocking buffer or Jackson ImmunoResearch, West Grove, PA, cat # 111-035-144, 1:10,000 diluted in blocking buffer) for $mGlu_4$ at room temperature for 1 h. Membranes were washed again with TBST and an enhanced chemiluminescent assay (Thermo Scientific, Waltham, MA, cat # 32106 or 34075) was performed to detect immunoreactive proteins.

Co-immunoprecipitation

In cell line experiments, $mGlu_2$/HEK/GIRK, $mGlu_4$/HEK/GIRK and $mGlu_{2/4}$/HEK/GIRK cells were lysed with IP lysis buffer (50 mM Tris·HCl, pH 7.5, 150mM NaCl, 2mM

EDTA, 1% Nonidet P40 with Complete Mini protease inhibitor cocktail (Roche, Basel, Switzerland, cat # 04693159001)) for IP experiments using the $mGlu_4$ antibody; buffer was supplemented with 0.5% sodium deoxycholate for experiments using the $mGlu_2$ antibody. Cell lysates were passed through G27 needles and incubated on ice for 30 min. The supernatant was centrifuged and pre-cleared with protein A/G beads (Santa Cruz, sc-2003) at 4°C for 2-3 h. $mGlu_2$- (Advanced Targeting Systems, San Diego, CA, cat # AB-N32) or $mGlu_4$ (Upstate, Billerica, MA, cat # 06-765) antibodies were bound to protein A/G beads by rotating at 4°C for 2-3 h. Pre-cleared cell lysates were then added to antibody-bound protein A/G beads or to beads without antibody as a negative control. After overnight rotation at 4°C, the beads were washed 3 times with washing buffer (IP lysis buffer without EDTA or protease inhibitors) and pelleted by low-speed centrifugation. SDS sample buffer was added to elute bound proteins. Samples were heated at 65°C for 5 min and subjected to SDS-PAGE and western blot analysis.

For co-immunoprecipitation assays in rat or mouse brain samples, Sprague Dawley rats of mixed gender (Charles River, Wilmington, MA) and ICR(CD-1) or male mice (Harlan, Indianapolis, IN) 22-30 days old were anesthetized under isoflurane anesthesia, decapitated, and brains were rapidly removed and cut into 0.5-1 mm coronal slices using a brain matrix or a vibratome (Leica, Buffalo Grove, IL). Slices were transferred to a chilled metal surface and dorsal striatum and medial prefrontal cortex (prelimbic and infralimbic regions) were dissected using a scalpel blade and immediately frozen on dry ice. Samples were homogenized in buffer containing (in mM): 50 Tris HCl, pH 7.4, 50 NaCl, 10 EGTA, 5 EDTA, 2 NaF, 1 Na_3VO_4, 1 PMSF supplemented with 1× Complete

Mini protease inhibitor cocktail, phosphatase inhibitor cocktails 2 and 3 (Sigma-Aldrich, St. Louis, MO). Homogenized samples were centrifuged at 16,100×g for 15 min at 4 °C and pelleted membranes were stored at -80°C. Membrane pellets were resuspended in IP lysis buffer (same as IP lysis buffer for IP $mGlu_4$ in cell lines, supplemented with 1mM PMSF) and nutated at 4°C for 1 h. Supernatant was prepared by centrifugation at 16,100×g for 15 min and pre-cleared by protein A/G beads at 4°C for 2-3 h. $mGlu_4$ antibodies or normal rabbit IgG (Millipore, Billerica, MA, cat# 12-370) were bound to protein A/G beads by rotating at 4°C for 2-3 h. Pre-cleared cell lysates were then added to $mGlu_4$ antibody bound protein A/G beads or rabbit IgG-coupled beads as a negative control. After overnight rotation at 4°C, the beads were washed and samples were eluted and analyzed as described above.

Thallium flux assays

Thallium flux assays were performed according to methods described in (Niswender et al., 2008b) with minor modifications. For dye loading, media was exchanged with Assay Buffer (Hanks Balanced Salt Solution (HBSS) containing 20mM HEPES, pH 7.4) using an ELX405 microplate washer (BioTek), leaving 20 µL/well, followed by addition of 20 µL/well 2× FluoZin-2 AM (330 nM final) indicator dye (Life Technologies, prepared as a DMSO stock and mixed in a 1:1 ratio with pluronic acid F-127) in Assay Buffer. After a 1 h incubation at room temperature, dye was exchanged with Assay Buffer, leaving 20 µL/well. Thallium flux was measured at room temperature using a Functional Drug Screening System 7000 (FDSS 7000, Hamamatsu). Baseline readings were taken (2 images at 1 Hz; excitation, 470 ± 20 nm; emission, 540 ± 30 nm), and test compounds

(2×) were added in a 20 µL volume and incubated for 140s before the addition of 10 µL of Thallium Buffer with or without agonist (5×). Data were collected for an additional 2.5 min and analyzed using Excel (Microsoft Corp, Redmond, WA) as previously described (Niswender et al., 2008b), and the concentration-response curves were fitted to a four-parameter logistic equation to determine potency estimates using GraphPad Prism:

$$y = bottom + \frac{top - bottom}{1 + 10^{(LogEC50 - A)Hillslope}}$$

where *A* is the molar concentration of the compound; *bottom* and *top* denote the lower and upper plateaus of the concentration-response curve; HillSlope is the Hill coefficient that describes the steepness of the curve; and EC_{50} is the molar concentration of compound required to generate a response halfway between the *top* and *bottom*.

Operational modeling of allosterism

Shifts of agonist concentration-response curves by allosteric modulators were globally fitted to an operational model of allosterism (Leach et al., 2007):

$$y = basal + \frac{(E_m - basal)(\tau_A[A](K_B + \alpha\beta[B]) + \tau_B[B]K_A)^n}{(\tau_A[A](K_B + \alpha\beta[B]) + \tau_B[B]K_A)^n + ([A]K_B + K_AK_B + K_A[B] + \alpha[A][B])^n}$$

where *A* is the molar concentration of the orthosteric agonist; *B* is the molar concentration of the allosteric modulator; K_A is the equilibrium dissociation constant of the orthosteric agonist, and K_B is the equilibrium dissociation constant of allosteric modulator. Affinity modulation is governed by the cooperativity factor α, and efficacy modulation is governed by β. The parameters τ_A and τ_B relate to the ability of orthosteric agonist and allosteric ligands, respectively, to directly activate the receptor. *Basal,* E_m and *n* represent

the basal system response, maximal possible system response and the transducer function that links occupancy to response.

Alternatively, a simplified version of this model was applied to estimate a composite cooperativity parameter (αβ) for PAMs (Leach et al., 2007):

$$y = basal + \frac{(E_m - basal)(\tau_A[A](K_B + \alpha\beta[B]) + \tau_B[B]K_A)^n}{(\tau_A[A](K_B + \alpha\beta[B]) + \tau_B[B]K_A)^n + (K_A(K_B + [B]))^n}$$

where all parameters are as described above.

For the simulation of $mGlu_4$ PAM effects, the logK_A of L-AP4 for $mGlu_4$ was set to -6.759 according to literature values (Monastyrskaia et al., 1999), and was assumed to be unaltered at $mGlu_{2/4}$ heterocomplexes. For PHCCC and 4PAM-2, logτ_B was set to -100 due to the lack of allosteric agonist activity but was allowed to float for compounds exhibiting allosteric agonism (VU0155041, Lu-AF29134). For the simulation of MNI-137, the logK_A of DCG-IV for $mGlu_2$ was set to -6.959 according to literature values (Schweitzer et al., 2000), and was assumed to be unaltered at $mGlu_{2/4}$ heterocomplexes; logτ_B was set to -100.

Transient transfections

Two days before the assay, combinations of pIRES-hyg3-rat $mGlu_2$, pIRES-hyg3-rat $mGlu_4$, and pIRES-hyg3-rat $mGlu_7$ were co-transfected with ratios of 0 μg:1 μg, 0.1 μg:1 μg, 0.2 μg:1 μg, 0.5 μg:1μg or 1 μg:1μg of DNA into HEK/GIRK cells using Fugene 6 (Promega, Fitchburg, WI) according to the manufacturer's protocol. After 24 hours, cells

were trypsinized and plated in 384-well poly D-lysine-coated plates using assay media. Plates were then tested the next day using the thallium flux assay as described above.

Whole-cell patch-clamp recordings

Whole-cell patch-clamp recordings were performed using coronal slices prepared from 15- to 19-day-old Sprague-Dawley rats of mixed gender (Charles River, Wilmington, MA). Animals were anesthetized with isoflurane and brains were removed and submerged into ice-cold cutting solution (in mM: 220 sucrose, 2.5 KCl, 1.25 NaH_2PO_4, 26.2 $NaHCO_3$, 10 D-glucose, 0.5 $CaCl_2$, 8 $MgCl_2$). Coronal slices containing the striatum were cut at 300 μm using a vibratome (Leica VT 1200S) or a compresstome (Precisionary Instruments, Greenville, NC). Slices were transferred to a holding chamber containing ACSF (in mM: 126 NaCl, 2.5 KCl, 1.2 NaH_2PO_4, 25 $NaHCO_3$, 11 D-glucose, 2.4 $CaCl_2$, 1.2 $MgCl_2$) supplemented with 5 μM glutathione, for slice viability, for 25 min at 32°C. All buffers were continuously bubbled with 95% O_2/5% CO_2. Subsequently, slices were maintained at room temperature for at least 30 minutes in ACSF, then transferred to a submersion recording chamber where they were perfused with room temperature ACSF at a rate of 2 ml/min. Neurons were visualized with a 40× water immersion lens with Hoffman modulation contrast optics coupled with an Olympus BX50WI upright microscope (Olympus, Lake Success, NY). Borosilicate glass patch electrodes were pulled using a Flaming/Brown micropipette puller (Sutter Instruments, CA) and had a resistance of 4-6 MΩ when filled with an intracellular solution containing (in mM: 123 potassium gluconate, 7 KCl, 0.025 $CaCl_2$, 1 $MgCl_2$, 10 HEPES, 0.1 EGTA, 2 magnesium-ATP, 0.2 sodium-GTP; pH adjusted to 7.3 with 1 N KOH; 295 mOsm).

Whole-cell recordings were made from medium spiny neurons which were visually identified and then confirmed by determining the current-voltage relationship of positive or negative current injections; a MultiClamp 700B amplifier (Molecular Devices, Sunnyvale, CA) was used for current-clamp recordings. Data were digitized with a DigiData 1331 system (Molecular Devices, Sunnyvale, CA) and acquired using pClamp10.2 (Molecular Devices, Sunnyvale, CA). EPSPs were evoked in medium spiny neurons by placing a bipolar electrode in the white matter between the cortex and striatum. After formation of a whole-cell configuration, membrane potential was recorded and current was injected to maintain resting membrane potential at -75 mV and changes in membrane potential were recorded. Compounds were diluted in ACSF and bath applied as noted. Data were analyzed using Clampfit 10.2 (Molecular Devices, Sunnyvale, CA).

Drugs

Glutamate, DCG-IV, CBiPES and LY487379 was purchased from Tocris Biosciences (Ellisville, Missouri). L-AP4, LY379268 and *N*-Phenyl-7-(hydroxyimino)cyclopropa[*b*]chromen-1a-carboxamide (PHCCC) were purchased from Abcam Biochemicals (Cambridge, UK). cis-2-[[(3,5-Dichlorophenyl)amino]carbonyl]cyclohexanecarboxylic acid (VU0155041), *N*-(4-(*N*-(2-chlorophenyl)sulfamoyl)phenyl)picolinamide (4PAM-2), (1S,2R)-N1-(3,4-dichlorophenyl)cyclohexane-1,2-dicarboxamide (Lu AF21934) and biphenylindanone A

(BINA) were synthesized in-house. Synthesis of VU0155041, BINA, and MNI-137 was performed according to methods in the following references: (Galici et al., 2006; Hemstapat et al., 2007; Niswender et al., 2008b).

Synthesis of 4PAM-2 and Lu AF21934 was performed according to methods described below:

General. All NMR spectra were recorded on a 400 MHz AMX Bruker NMR spectrometer. ^{1}H chemical shifts are reported in δ values in ppm downfield with the deuterated solvent as the internal standard. Data are reported as follows: chemical shift, multiplicity (s = singlet, d = doublet, t = triplet, q = quartet, br = broad, m = multiplet), integration, coupling constant (Hz). Low resolution mass spectra were obtained on an Agilent 1200 series 6130 mass spectrometer with electrospray ionization. High resolution mass spectra were recorded on a Waters Q-TOF API-US plus Acquity system with electrospray ionization. Analytical thin layer chromatography was performed on EM Reagent 0.25 mm silica gel 60-F plates. Analytical HPLC was performed on an Agilent 1200 series with UV detection at 214 nm and 254 nm along with ELSD detection. LC/MS: Restek-C18, 3.2x30mm, 2 min gradient, 10%[0.05%TFA/CH_3CN]:90%[0.05%TFA/H_2O] to 100%[0.1%TFA/CH_3CN] or Phenomenex-C18, 2.1 X 30 mm, 1 min gradient, 7%[0.1%TFA/CH_3CN]:93%[0.1%TFA/H_2O] to 95%[0.1%TFA/CH_3CN]. Preparative purification was performed on a custom HP1100 purification system with collection triggered by mass detection. Solvents for extraction, washing and chromatography were

HPLC grade. All reagents were purchased from Aldrich Chemical Co. and were used without purification.

4PAM-2 (*N*-(4-(*N*-(2-chlorophenyl)sulfamoyl)phenyl)picolinamide):

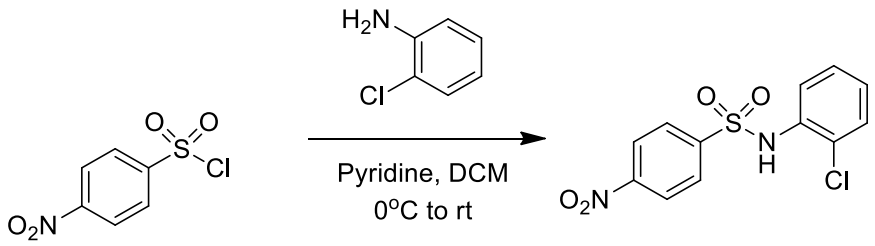

1

To a solution of 2-chloroaniline (0.95 mL, 9.02 mmol, 1.0 eq) in pyridine (5 mL) and DCM (5 mL) at 0°C was added 4-nitrobenzenesulfonylchloride (2.0g, 9.02 mmol, 1.0eq). After 15 min, the cold bath was removed. After an additional 24 h at rt, the rxn was added to 1N HCl (aq) (50 mL) and DCM (50 mL). The organic layer was separated, washed with 1N HCl (aq) (20 mL), H_2O (2 x 20 mL), brine (20 mL) and dried ($MgSO_4$). The mixture was filtered and concentrated to afford **1** (2.73g, 97%). The residue was carried through without further purification.

R_f 0.85 (50% EtOAc/hexanes);

LCMS: R_t=1.403 min, M+H=313.0; >98% @ 215 and 254 nm

^{1}H NMR (400 MHz, $CDCl_3$): δ 8.27 (d, J = 9.0 Hz, 2H), 7.92 (d, J = 9.0 Hz, 2H), 7.70 (dd, J = 8.1, 1.4 Hz, 1H), 7.32-7.26 (m, 2H), 7.13 (ddd, J = 8.8, 8.8, 1.5 Hz, 1H), 7.01 (br s, 1H)

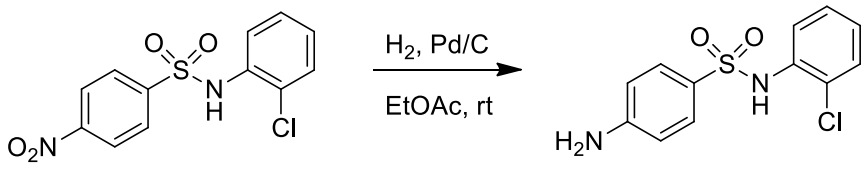

1 **2**

To a solution of **1** (2.73g, 8.73 mmol, 1.0eq) in EtOAc (40 mL) was added 5% Pd/C (~150 mg). The rxn atmosphere was evacuated and purged with H_2 balloon (1 atm). The rxn was followed by TLC. After 4h, the rxn mixture was filtered through Celite and concentrated to provide a white solid (2.45g, 99%).

R_f 0.50 (50% EtOAc/hexanes);

^{1}H NMR (400 MHz, $CDCl_3$): δ 7.64 (dd, J = 8.2, 1.4 Hz, 1H), 7.54 (d, J = 8.7 Hz, 2H), 7.24-7.19 (m, 2H), 7.01 (ddd, J = 7.8, 7.8, 1.5 Hz, 1H), 6.91 (br s, 1H), 6.58 (d, J = 8.8 Hz, 2H), 4.11 (br s, 2H)

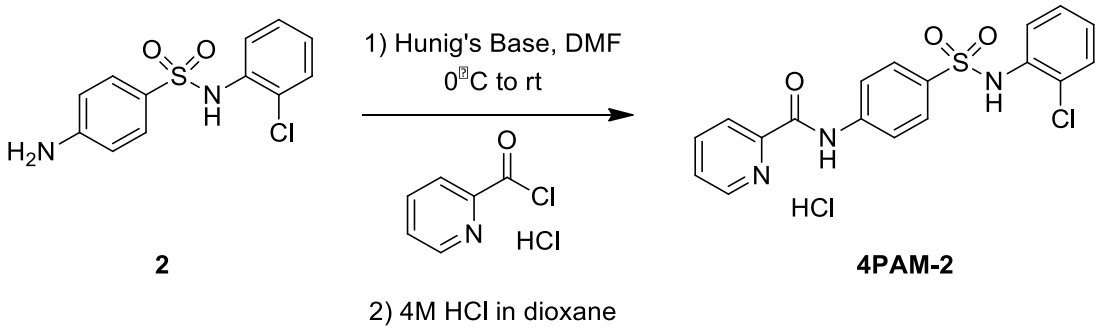

2 **4PAM-2**

To a solution of **2** (2.45g, 8.66 mmol, 1.0eq) in DMF (16 mL) and Hunig's Base (3.64 mL, 25.98 mmol, 3.0eq) at 0°C was added picolinoyl chloride hydrochloride (1.70g, 9.53 mmol, 1.1eq). After 15 min, the ice bath was removed. After an additional 24h at rt, the rxn was added to EtOAc:H_2O (1:1, 100 mL). The organic layer was separated and washed with H_2O (2 x 50 mL), brine (50 mL), dried ($MgSO_4$) and concentrated. The residue was purified by reverse phase liquid column chromatography (40-80%

acetonitrile: H_2O with 0.1% trifluoroacetic acid). The collected fractions were added to EtOAc:$NaHCO_3$(aq) (1:1, 100 mL). The organic layer was separated and washed with H_2O (50 mL), brine (50 mL), dried ($MgSO_4$), filtered and concentrated to afford a white solid. The white solid was dissolved in DCM (25 mL) and 4N HCl in dioxane (5 mL) was added. After 5 min, the solvent was removed to yield **4PAM-2** as an HCl salt (1.06 g, 32% yield).

LCMS: R_t=1.455 min, M+H=387.8; >98% @ 215 and 254 nm

^{1}H NMR (400 MHz, *d*-DMSO): δ 11.01 (s, 1H), 9.92 (s, 1H), 8.77 (d, J = 4.2 Hz, 1H), 8.18 (d, J = 7.6 Hz, 1H), 8.10 (d, J = 8.7 Hz, 2H), 8.09-8.08 (m, 1H), 7.73-7.71 (m, 1H), 7.71 (d, J = 8.8 Hz, 2H), 7.41 (dd, J = 7.8, 1.2 Hz, 1H), 7.32-7.26 (m, 2H), 7.23-7.19 (m, 1H);

HRMS, calc'd for $C_{18}H_{14}N_3O_3NaSCl$ ($M+Na^+$), 410.0342; found 410.0339.

Lu AF21934 (N^1-(3,4-dichlorophenyl)cyclohexane-1,2-dicarboxamide):

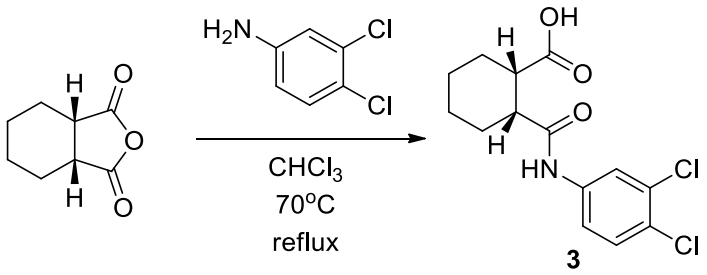

3

Into a 50 mL round bottom flask, containing a magnetic stir bar, was weighed 1.3751 mmol (212 mg) of cyclohexyldicarboxylic anhydride (predominantly cis) followed by 6 mL chloroform. To this solution was added 0.9167 mmol (148.5 mg) of 3,4-dichloroaniline. After being fitted with a reflux column the reaction mixture was heated in an oil bath to reflux at 70°C for 2 h, with magnetic stirring. Over this time a white

solid crashed out of the reaction mixture. After cooling the reaction to ambient temperature, the solid was isolated via vacuum filtration and washed with cold chloroform to obtain 434.8 mg of the desired product, **3** (78.4% yield) as a crystalline white powder.

LCMS: R_t= 0.741 min, M+H=315.7; >98% @ 215 and 254 nm;

HRMS calcd for $C_{14}H_{15}Cl_2NO_3$[M+H]: 315.0667 found 315.0668;

^{1}H NMR (400 MHz, methyl sulfoxide-d_6 calibrated to 2.54) δ10.02 (s, 1H), 7.99 (d, J = 2.39 Hz, 1H), 7.53 (d, J = 8.79 Hz, 1H), 7.46 (dd, J = 8.87, 2.43 Hz, 1H), 2.92 (q, J = 4.78 Hz, 1H), 2.64-2.60 (m, 1H), 2.12-2.03 (m, 1H), 1.99-1.94 (m, 1H), 1.76-1.61 (m, 3H), 1.41-1.29 (m, 3H).

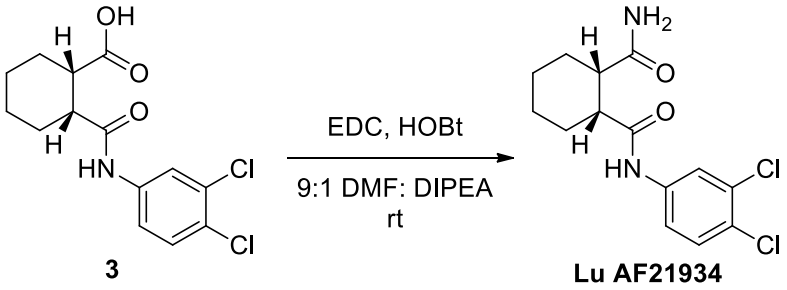

3 **Lu AF21934**

To a 4 mL vial were weighed 0.3115 mmol (98.5 mg) compound **3**, 0.9345 mmol (98.5 mg) ammonium chloride, 0.3738 mmol (71.5 mg) 1-ethyl-3-(3-dimethylaminopropyl)carbodiimide, and 0.3115 mmol (42.1 mg) hydroxybenzotriazole, followed by 3 mL of 9:1 dimethylformamide:diisopropylethylamine. The reaction vial was rotated at room temperature overnight. The reaction was diluted with ethyl acetate (~5 mL) and washed with brine. The organic phase was separated and dried over sodium sulfate. Solvent was removed under reduced pressure and the crude product was purified via flash column chromatography. Product-containing fractions were combined and the

solvents removed under reduced pressure to obtain 31 mg of the desired product, **Lu AF21934** (31.5% yield) as an off-white powder.

LCMS: 0.690 min, M+H=314.7; >98% @ 215 and 254 nm;

HRMS calcd for $C_{14}H_{16}Cl_2N_2O_2$[M+H]: 316.0507 found 316.0507;

^{1}H NMR (400 MHz, methyl sulfoxide-d_6 calibrated to 2.54): δ9.92 (s, 1H), 8.01 (d, J = 2.27 Hz, 1H), 7.51 (d, J = 8.91 Hz, 1H), 7.44 (dd, J = 8.88, 2.42, 1H), 7.06 (s, 1H), 6.72 (s, 1H), 2.80 (q, J = 4.83 Hz, 1H), 2.50-2.46 (m, 1H), 2.15-1.98 (m, 1H), 1.70-1.48 (m, 1H), 1.39-1.23 (m, 1H).

Animal studies

Animals were maintained in accordance with the guidelines of the American Association for the Accreditation of Laboratory Animal Care under a 12 hour light/dark cycle (lights on 06:00 to 18:00) with free access to food and water. All experiments were approved by Vanderbilt University's Institutional Animal Care and Use Committee, and conformed to guidelines established by the National Research Council Guide for the Care and Use of Laboratory Animals. All efforts were made to minimize animal suffering and the number of animals used.

Statistical analysis

All data shown represent Mean±SEM value for at least three replicates. Statistical significance between groups was determined using unpaired Student's t tests or ANOVA (with Dunnett's or Bonferroni's post-test) as specified in each Figure Legend.

Results

$mGlu_4$ interacts with $mGlu_2$ to form heterocomplexes both *in vitro* and in brain tissue

PHCCC is the first described $mGlu_4$ positive allosteric modulator (PAM) (Maj et al., 2003; Marino et al., 2003) and has been used to probe the activity of $mGlu_4$ at various synapses in the basal ganglia and other brain regions (Jones et al., 2008; Marino et al., 2003; Valenti et al., 2005). The efficacy of PHCCC at striatopallidal and STN-SNc synapses is consistent with its symptomatic and disease modifying effects in PD animal models (Battaglia et al., 2006; Marino et al., 2003). In addition to striatopallidal and STN-SNc synapses, immunohistochemistry studies reveal that $mGlu_4$ is expressed at corticostriatal synapses, which represent the primary input to the basal ganglia from the motor cortex (Corti et al., 2002). Consistent with expression studies, Bennouar et al. recently reported that the $mGlu_4$ PAM Lu AF21934 reduces corticostriatal transmission (Bennouar et al., 2012). To further understand the role of $mGlu_4$ in regulation of basal ganglia function, we evaluated the ability of PHCCC to reduce corticostriatal transmission. In agreement with previous results (Pisani et al., 1997), 100 μM L-AP4, a group III selective mGlu receptor agonist, reduced evoked excitatory postsynaptic potentials (eEPSPs) measured in striatal medium spiny neurons following stimulation in

the corpus callosum (42.8 ± 5.8% of baseline; Figure 3.1A). To determine if PHCCC could potentiate the response to L-AP4, a concentration of L-AP4 that resulted in a small reduction in the eEPSP amplitude was identified. 500 nM L-AP4 resulted in reduction in the eEPSP amplitude that was at the threshold for detection (90.5 ± 6.2% of baseline; Figure 3.1B). Surprisingly, PHCCC did not potentiate the response to L-AP4 at this synapse; 30 μM PHCCC, followed by the co-addition of 30 μM PHCCC + 500 nM L-AP4, resulted in no change in eEPSP amplitude (90.1 ± 7.1% of baseline; Figure 3.1C) relative to 500 nM L-AP4 alone.

The lack of effect of PHCCC was surprising and contrasts with the ability of this compound to potentiate $mGlu_4$ activity at other synapses (Jones et al., 2008; Marino et al., 2003; Valenti et al., 2005). In addition, this finding does not align with the ability of the structurally distinct $mGlu_4$–selective PAM Lu AF21934 to potentiate $mGlu_4$ agonist effects at corticostriatal synapses (Bennouar et al., 2012). Interestingly, both the group II mGlu agonist LY379268 (Picconi et al., 2002) and the $mGlu_2$ PAM cyPPTS (Johnson et al., 2005) inhibit excitatory transmission at corticostriatal synapses via a presynaptic mechanism of action, suggesting that $mGlu_2$ receptors are also expressed on corticostriatal terminals. Recent studies including time-resolved FRET and co-expression studies have shown that $mGlu_2$ and $mGlu_4$ form heterodimers *in vitro* (Doumazane et al., 2011a; Kammermeier, 2012) and we hypothesized that $mGlu_4$-containing heteromers may be expressed on corticostriatal terminals and may not display the same response to PHCCC as that observed with $mGlu_4$ homomers.

To test this hypothesis, an $mGlu_{2/4}$ cell line was constructed by transfecting rat $mGlu_4$ into rat $mGlu_2$/HEK cells stably expressing G Protein Inwardly Rectifying Potassium (GIRK) channels, which allows assessment of receptor activity using a GIRK-mediated thallium flux assay (Niswender et al., 2008a). We established that the resulting $mGlu_{2/4}$ cell line expressed similar amounts of both $mGlu_2$ and $mGlu_4$ protein compared to the parental cell lines expressing either receptor alone (Figure 3.2). We then assessed the physical interaction between $mGlu_2$ and $mGlu_4$ using co-immunoprecipitation techniques. $mGlu_4$ antibodies immunoprecipitated $mGlu_4$ protein (~240 kDa in dimeric form) from the cell lysate of the $mGlu_4$ and $mGlu_{2/4}$ cell lines (Figure 3.3B). A band of approximately 100 kDa was present in all of the immunoprecipitation (IP) samples and obscured specific identification of monomeric receptor protein; this band was present in IP samples without any cell lysate (data not shown), suggesting that it resulted from the antibody itself. In cells co-expressing $mGlu_2$ and $mGlu_4$, $mGlu_2$ proteins were co-precipitated along with $mGlu_4$ by $mGlu_4$ antibody-coupled beads (Figure 3.3D; ~100 kDa and ~240 kDa for monomeric and dimeric forms, respectively). In contrast, precipitation using the protein A/G beads alone did not yield any specific bands. Additionally, precipitated $mGlu_2$ was not detected in IPs from the control $mGlu_2$ or $mGlu_4$ cell line. To eliminate the possibility that $mGlu_2$ and $mGlu_4$ proteins nonspecifically aggregated after the cells were lysed, we mixed the cell lysates from the $mGlu_2$-expressing cell line and the $mGlu_4$-expressing cell line and subjected the mixed sample to co-IP. The absence of precipitated $mGlu_2$ in this mixed sample indicated that $mGlu_{2/4}$ complexes were formed before, but not during or after, the lysis process. We further confirmed the physical interaction between $mGlu_2$ and $mGlu_4$ by swapping the bait and prey in additional co-IP

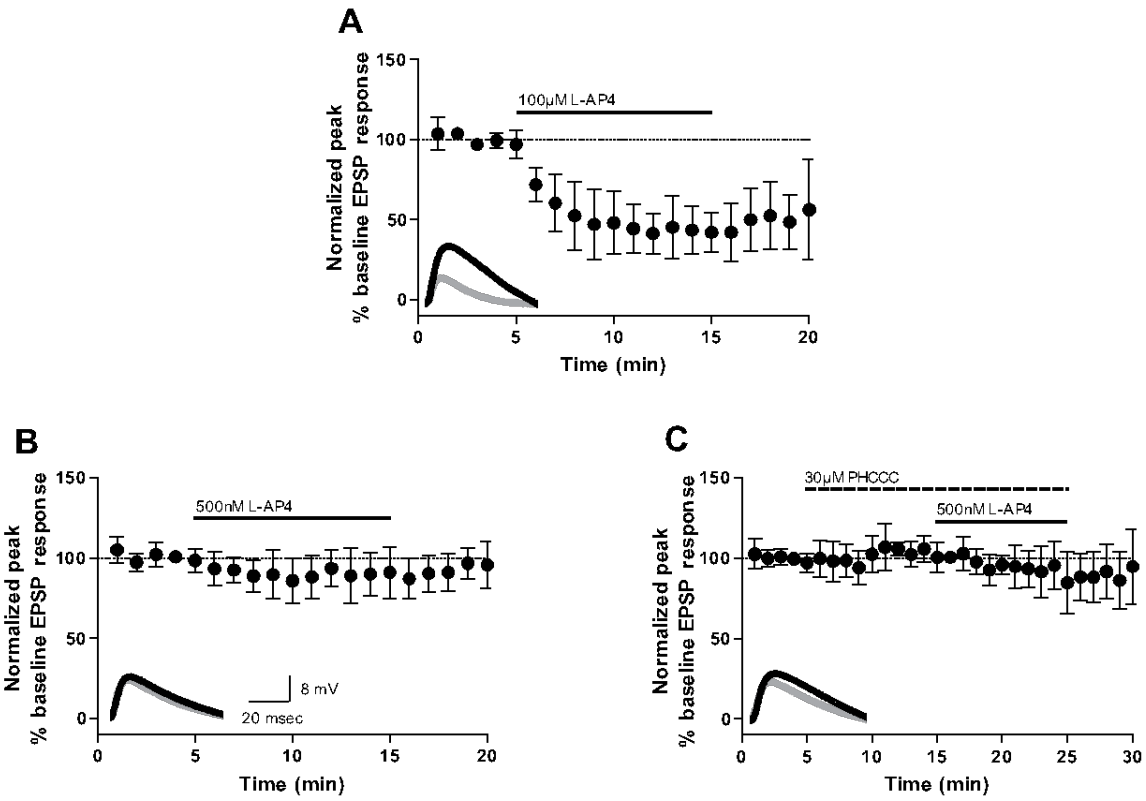

Figure 3.1. The $mGlu_4$ PAM PHCCC fails to potentiate L-AP4-induced decreases in evoked EPSPs at corticostriatal synapses. EPSPs were recorded in medium spiny neurons following stimulation of the white matter between the cortex and striatum with a bipolar electrode. All compounds were bath applied. Data are normalized to the average baseline EPSP amplitude. Insets are sample traces from an individual, representative experiment (black – averaged traces from minute prior to L-AP4 application; gray – averaged traces from last minute of L-AP4 application). Slices were treated with 100 μM L-AP4 (**A**), 500 nM L-AP4 (**B**) or 30 μM PHCCC followed by co-application of 30 μM PHCCC and 500 nM L-AP4 (**C**). Solid and dashed lines represent time of compound additions. Values represent mean ± SEM (n=5).

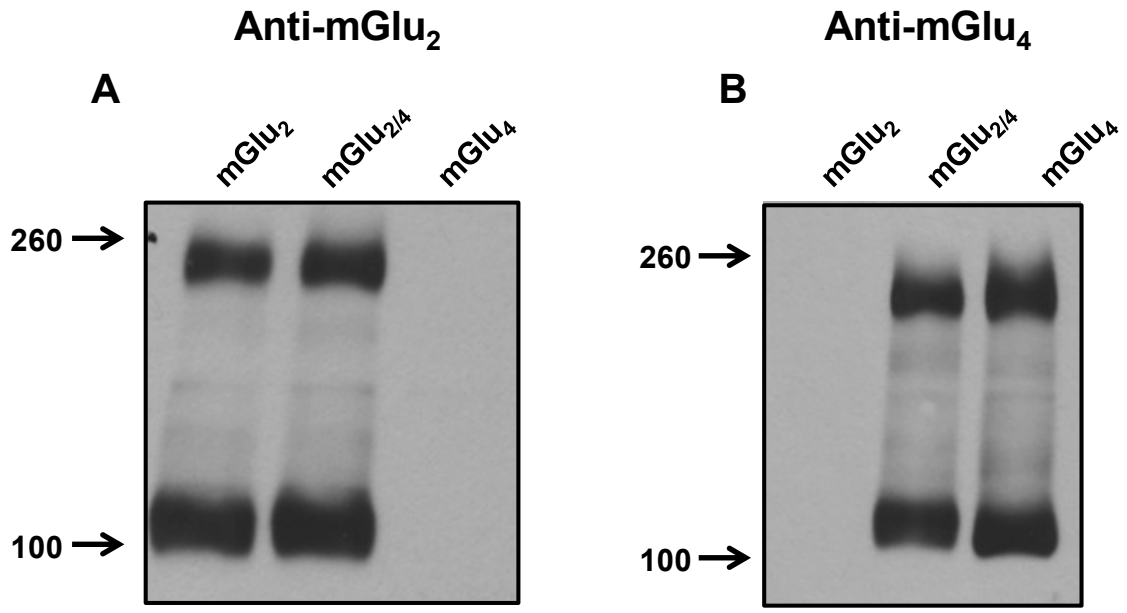

Figure 3.2. Similar expression levels of $mGlu_2$ and $mGlu_4$ in various cell lines. 15 μg of cell lysates from $mGlu_2$, $mGlu_{2/4}$ and $mGlu_4$ cell lines were prepared as described. Receptor expression was analyzed by western blots using anti-$mGlu_2$ (panel **A**, 1:1000 dilution) and anti-$mGlu_4$ (panel **B**; 1:1000 dilution) antibodies.

experiments. When $mGlu_2$ was used as the bait, $mGlu_4$ proteins were also co-immunoprecipitated by $mGlu_2$ antibodies only in the cell line that expressed both receptors (Figure 3.3H). These data support the hypothesis that $mGlu_2$ specifically interacts in some manner with $mGlu_4$ *in vitro* and can be co-immunoprecipitated with antibodies recognizing the native receptor proteins.

After optimizing conditions for co-immunoprecipitation of $mGlu_2$ and $mGlu_4$ in cell lines, we tested the hypothesis that these receptors interact in brain tissue. Both $mGlu_2$ and $mGlu_4$ are expressed in dorsal striatum and medial prefrontal cortex of Sprague-Dawley rats, as indicated by the immuno-reactive monomeric and dimeric bands in tissue lysates (Figure 3.4, input). While both $mGlu_4$ antibodies and a rabbit IgG control generated antibody bands at around 100 kDa, $mGlu_4$ antibodies were able to precipitate dimeric $mGlu_4$ from the dorsal striatum and medial prefrontal cortex (~240 kDa in dimeric form; Figure 3.4A and B). Conversely, immunoprecipitation using rabbit IgG did not yield any $mGlu_4$-specific bands. In addition, when detected using $mGlu_2$-specific antibodies, we found that $mGlu_2$ proteins were co-immunoprecipitated by $mGlu_4$ antibodies in both monomeric and dimeric forms (~100 kDa and 240 kDa respectively), but not by rabbit IgG (Figure 3.4C and D). Similar results were also obtained in mouse dorsal striatum and medial prefrontal cortex (Figure 4E-H). Taken together, these data present the first evidence consistent with the existence of mGlu heteromers *in vivo* and suggest that $mGlu_{2/4}$ heteromers may participate in the regulation of CNS function.

$mGlu_{2/4}$ heteromer differentially regulate the effect of $mGlu_4$ allosteric modulators

To further test the hypothesis that the lack of efficacy of PHCCC at the corticostriatal synapse was due to expression of $mGlu_4$-containing heteromers, the pharmacology of $mGlu_{2/4}$ receptors was extensively characterized using the thallium flux assay (Niswender et al., 2008a). In these studies, the initial slopes (starting 5 seconds after thallium addition and then measured over a 10 second time span) of inward flux of thallium are calculated and plotted as agonist-induced concentration-response curves (samples traces of thallium flux assays are shown in Figure 3.5A-C and represent the data used to generate the L-AP4 curves in panel 3.5F). Glutamate, the orthosteric agonist for both $mGlu_2$ and $mGlu_4$, exhibited a pEC_{50} value of 6.22±0.03 in the $mGlu_{2/4}$ cell line. This potency was similar to the pEC_{50} of glutamate at $mGlu_2$ (6.08±0.03) compared to that of $mGlu_4$ (4.79±0.03) (Figure 3.5D, Table 3.1). To further characterize each of the subtypes in the heterocomplex, more selective agonists were utilized for $mGlu_2$ (LY379268) or $mGlu_4$ (L-AP4) (Figure 5E and F). In the $mGlu_{2/4}$ cell line, the $mGlu_2$ agonist LY379268 elicited a full agonist response with a slightly reduced potency comparing to cells expressing $mGlu_2$ alone (Figure 3.5E, Table 3.1). Likewise, L-AP4, the $mGlu_4$ selective agonist, induced an agonist response with similar potency in cells expressing $mGlu_{2/4}$ and $mGlu_4$ alone. Unlike LY379268, L-AP4 was only able to elicit about 70% of the maximum response generated by glutamate in $mGlu_{2/4}$ cells. Additionally, we observed a significant decrease in the Hill slope of the curve fits for both LY379268 and L-AP4 in $mGlu_{2/4}$-co-expressing cells (Table 3.1), indicating an interaction between the two proteins and supporting the hypothesis that the $mGlu_{2/4}$ complex possesses distinct pharmacological properties.

We then investigated whether $mGlu_2$ and $mGlu_4$ agonist sites interact with each other in $mGlu_{2/4}$-expressing cells. A serial dilution of L-AP4 was applied either alone or in the presence of 0.5 nM or 1 nM LY379268. In the $mGlu_4$ cell line, neither concentration of LY379268 produced any effect on L-AP4 responses compared to buffer control (Figure 3. 6A). When assessed in the $mGlu_{2/4}$ cell line, LY379268 dose-dependently shifted the L-AP4 dose response curve to the left (Figure 3.6B), suggesting a potentiating effect by co-activation of the $mGlu_2$ subunit. In support of an interaction between subunits, 0.1, 10 and 100 nM L-AP4 dramatically potentiate the responses induced by LY379268 as well (Figure 3.6C and D).

After assessing the activity of orthosteric agonists in cells expressing either receptor alone or expressing the combination, we moved to an analysis of potential effects on the pharmacology of allosteric modulators for $mGlu_4$ and $mGlu_2$ (structures shown in Figure 3.7). Advantages if focusing our studies on $mGlu_2$ and $mGlu_4$ are that 1) these receptors are co-expressed in many brain regions, and 2) there are a number of orthosteric and allosteric ligands that differentiate between $mGlu_2$ and $mGlu_4$, allowing us to generate a tool set of ligands appropriate for native tissue studies. 10 μM PHCCC induced a 4.7±0.02 fold leftward shift of the L-AP4 response in cells expressing $mGlu_4$ alone

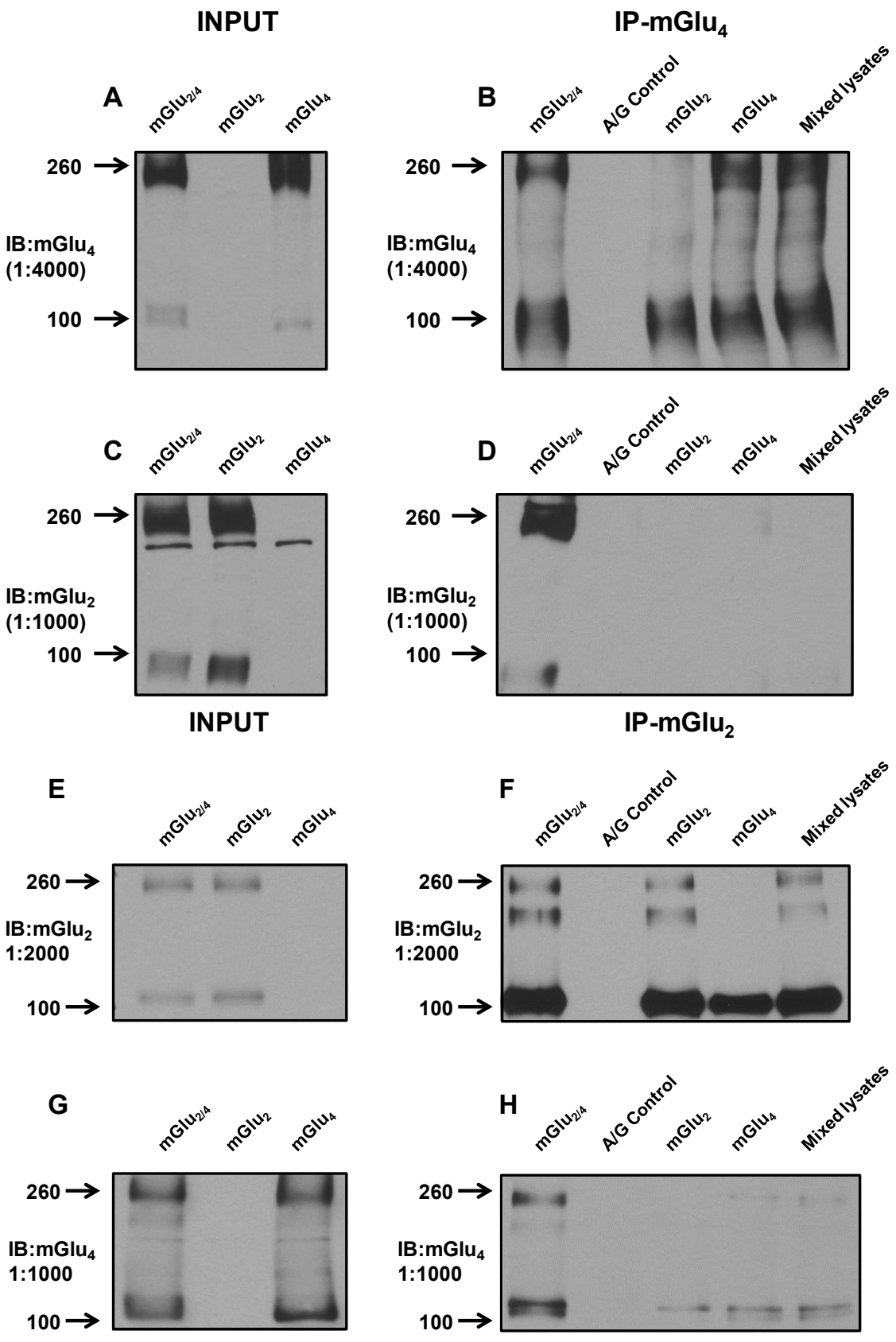
INPUT
IP-mGlu4
A
B
C
D
E
F
G
H
mGlu2/4
mGlu2
mGlu4
A/G Control
Mixed lysates
260
100
IB:mGlu4
(1:4000)
IB:mGlu2
(1:1000)
IB:mGlu2
1:2000
IB:mGlu4
1:1000

Figure 3.3. $mGlu_2$ and $mGlu_4$ are co-immunoprecipitated from Human Embryonic Kidney (HEK) cells. $mGlu_4$ antibodies (A-D) or $mGlu_2$ antibodies (E-H) were used for co-immunoprecipitation. Cell lysates from $mGlu_{2/4}$, $mGlu_2$, and $mGlu_4$ cell lines, together with lysates from $mGlu_2$ cells and $mGlu_4$ cells that were mixed after lysis, were subjected to co-IP experiments. Cell lysates from $mGlu_{2/4}$ cells were also precipitated by protein A/G beads without antibody as a negative control (A/G control). Precipitated proteins from different samples were analyzed by western blots. Cell lysates before co-IP experiments were loaded as indication of IP input (left side panels). Molecular sizes of $mGlu_2$ or $mGlu_4$ (~100 kDa and ~240 kDa for monomeric and dimeric forms, respectively) are indicated with arrows.

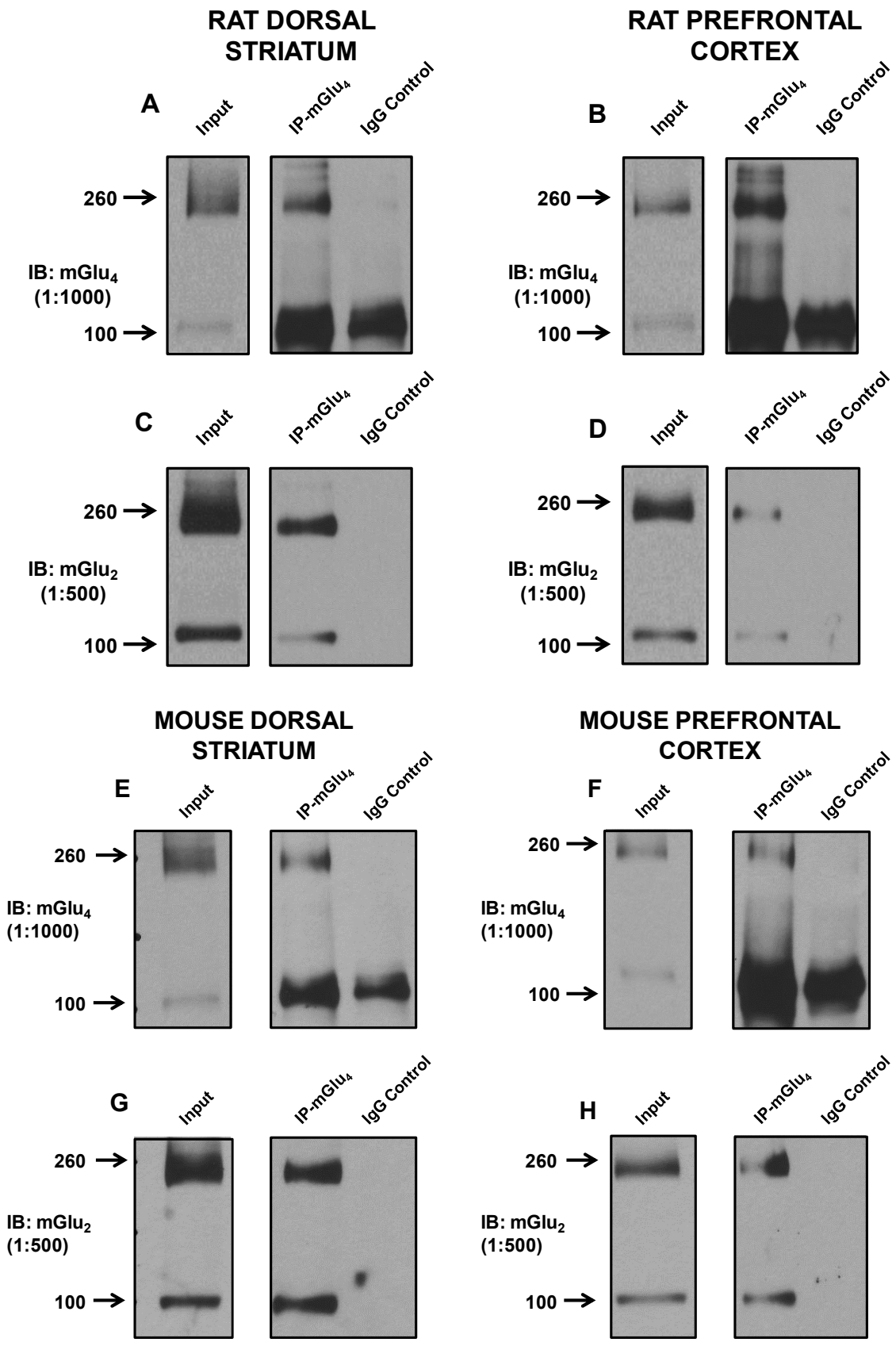
RAT DORSAL STRIATUM
RAT PREFRONTAL CORTEX
A
B
C
D
Input
IP-mGlu4
IgG Control
260
100
IB: mGlu4 (1:1000)
IB: mGlu2 (1:500)
MOUSE DORSAL STRIATUM
MOUSE PREFRONTAL CORTEX
E
F
G
H

Figure 3.4. $mGlu_4$ antibodies co-immunoprecipitate $mGlu_2$ protein from rodent dorsal striatum and medial prefrontal cortex. Dorsal striatum and medial prefrontal cortex extracts from rat (A-D) or mouse (E-H) samples were prepared as described and tissue lysates were precipitated using anti-$mGlu_4$ antibody (IP-$mGlu_4$) or rabbit IgG (IgG Control). The precipitated proteins were analyzed via western blots and tissue lysates before IP experiments were loaded as IP input. Molecular sizes of $mGlu_2$ or $mGlu_4$ (~100 kDa and ~240 kDa for monomeric and dimeric forms, respectively) are indicated with arrows.

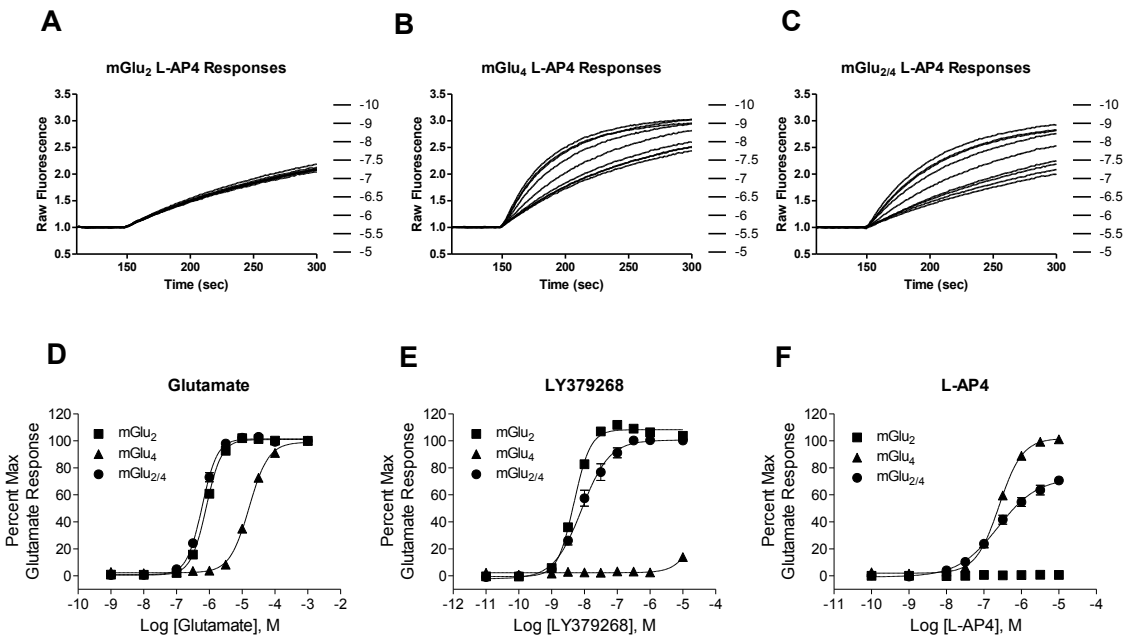

Figure 3.5. Orthosteric agonist responses are distinct in $mGlu_2$, $mGlu_4$ or $mGlu_{2/4}$-expressing cell lines. A-C, sample traces of L-AP4 responses in $mGlu_2$, $mGlu_4$ and $mGlu_{2/4}$ cells with concentrations ranging from 0.1 nM to 10 μM. The initial slopes of the raw traces were used to generate concentration response curves shown in F. D-F, serial dilutions of glutamate (D), the group II agonist LY379268 (E) and the group III agonist L-AP4 (F) were applied to HEK/GIRK/$mGlu_2$ (■), HEK/GIRK/$mGlu_4$ (▲) and HEK/GIRK/$mGlu_{2/4}$ (●) cell lines and GIRK-mediated thallium flux was measured according to protocols described above. Reponses were normalized to the maximal response induced by 1 mM glutamate in each individual cell line, and pEC_{50} values for concentration- response curves are shown in Table 1. All values represent mean ± SEM ($n \geq 3$).

	$mGlu_2$			$mGlu_4$			$mGlu_{2/4}$		
	pEC_{50}	% Glu Max	Hill Slope	pEC_{50}	% Glu Max	Hill Slope	pEC_{50}	% Glu Max	Hill Slope
Glutamate	6.08±0.03	101.0±0.8	1.88±0.08	4.79±0.03	99.1±0.5	1.50±0.03	6.22±0.03[a]	101.4±0.6	2.01±0.04
LY379268	8.32±0.02	108.3±0.9	1.73±0.05	>5.0	N/A	N/A	8.04±0.10[b]	101.9±0.9[c]	1.10±0.10[d]
L-AP4	N/A	N/A	N/A	6.60±0.03	100.9±1.1	1.42±0.03	6.64±0.05	72.8±2.0[e]	0.91±0.02[f]

Table 3.1. Potencies and efficacies of orthosteric agonists in various cell lines. Data represent the Mean±SEM of at least three experiments performed in duplicate. [a]$p=0.0034$ for $mGlu_2$ versus $mGlu_{2/4}$ lines; [b]$p=0.0161$ for $mGlu_2$ versus $mGlu_{2/4}$ lines; [c]$p=0.0049$ for $mGlu_2$ versus $mGlu_{2/4}$ lines; [d]$p<0.0001$ for $mGlu_2$ versus $mGlu_{2/4}$ lines; [e]$p<0.0001$ for $mGlu_4$ versus $mGlu_{2/4}$ lines; [f]$p<0.0001$ for $mGlu_4$ versus $mGlu_{2/4}$ lines. Unpaired Student's T test ($n\geq3$, two-tailed).

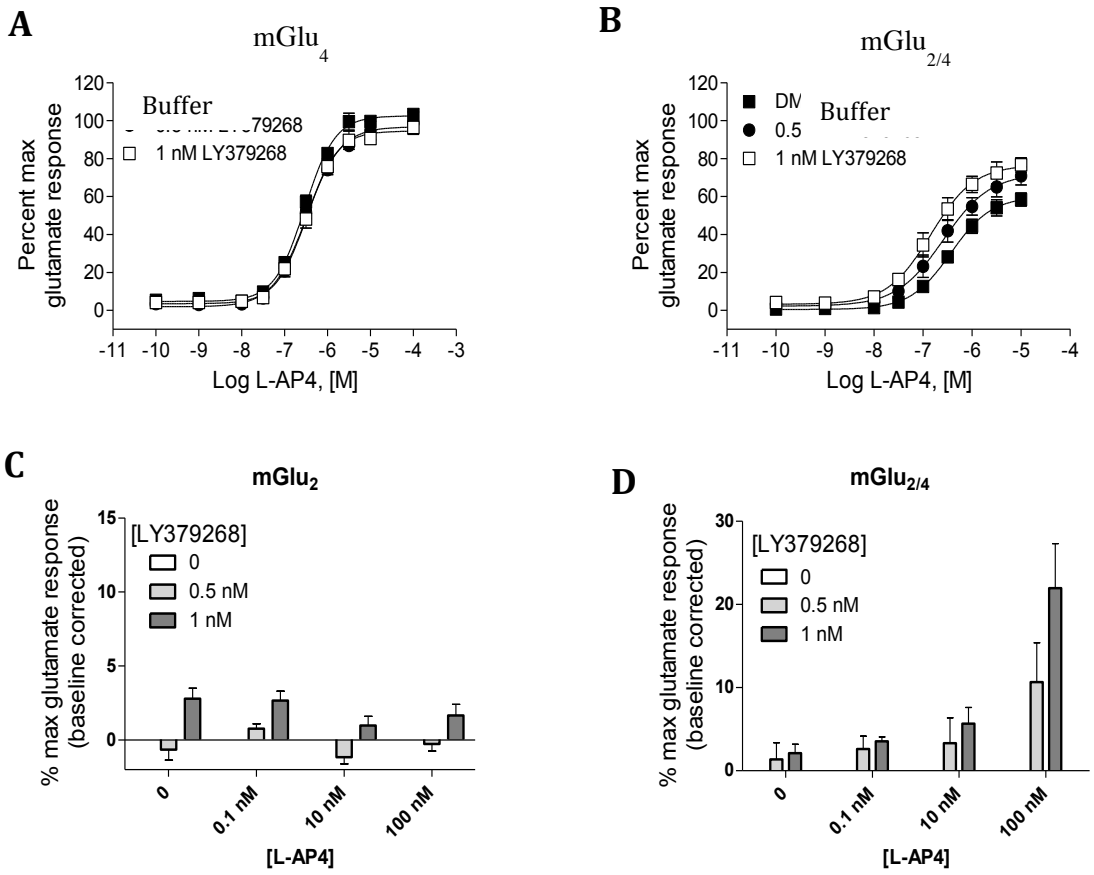

Figure 3.6. Orthosteric agonist of $mGlu_2$ and $mGlu_4$ potentiates effect of each other in $mGlu_{2/4}$-expressing cell line. Buffer control (■), 0.5 nM (●) or 1 nM LY379268 (□) were added 140 s before addition of serial dilutions of L-AP4. GIRK channel-mediated thallium flux was measured as described in HEK/GIRK/$mGlu_2$, HEK/GIRK/$mGlu_4$ or HEK/GIRK/$mGlu_{2/4}$ cell line and was normalized to the maximal response induced by 1 mM glutamate. A and B, L-AP4 dose response curves were plotted in the absence or presence of LY379268 in $mGlu_4$ or $mGlu_{2/4}$ cells. C and D, the responses induced by 0, 0.5 or 1 nM LY379268 were plotted in the absence or presence of L-AP4 in $mGlu_2$ or $mGlu_{2/4}$ cells. Basal responses induced by 0.1, 10 or 100 nM L-AP4 alone were deducted.

(Figure 3.8A). In contrast, PHCCC only induced a negligible shift of the L-AP4 response in the $mGlu_{2/4}$ cell line (1.7±0.04 fold, Figure 3.8B). When assessed using glutamate, 10 μM PHCCC shifted the concentration-response curve to the left by 3.5±0.53 fold in $mGlu_4$ cells (Figure 3.8C) but did not potentiate the glutamate response in cells expressing both $mGlu_2$ and $mGlu_4$ (1.0±0.04 fold; Figure 3.8D). This loss of efficacy in the $mGlu_{2/4}$ cell line is consistent with a previous report (Kammermeier, 2012) and aligns with the lack of significant potentiation of the L-AP4 response we observed with PHCCC at corticostriatal synapses (Figure 3.1C). The inability to potentiate $mGlu_{2/4}$ heteromers was not limited to PHCCC alone. 4PAM-2 is a selective and efficacious PAM of $mGlu_4$ which binds to the same allosteric site as PHCCC (Drolet et al., 2011c). In cells expressing $mGlu_4$ alone, 10 μM 4PAM-2 shifted concentration-response curves of L-AP4 and glutamate by 18.8±2.6 and 15.2±3.1 fold, respectively (Table 3.2). When $mGlu_2$ was co-expressed, however, 4-PAM2 only weakly potentiated the L-AP4 response (2.7±0.2 fold) and was completely ineffective at shifting the glutamate concentration-response curve (1.0±0.02 fold; Table 3.2).

VU0155041 is another $mGlu_4$ PAM derived from a different chemical scaffold compared to PHCCC or 4PAM-2. Consistent with our previous report (Niswender et al., 2008b), VU0155041 (10 μM) shifted the L-AP4 and glutamate concentration-response curves to the left by 3.9±0.3 and 4.0±0.3 fold, respectively, in cells expressing $mGlu_4$ alone (Figures 3.8E and G). Interestingly, VU0155041 also induced leftward shifts in the agonist concentration response curves in the $mGlu_{2/4}$ cell line, shifting the L-AP4 response substantially (9.7±1.0 fold shift), retaining its efficacy in shifting the glutamate response (3.5±0.3 fold shift) (Figure 3.7F and H), and, surprisingly, even showing

significant potentiation of the LY379268 response (4.2±0.12 fold, Table 3.2). As VU0155041 is predicted to bind only to the $mGlu_4$ protein and LY379268 should only activate $mGlu_2$, this finding suggests that there is transactivation between the subunits within the heteromer. We noted a slight decrease in the maximal response induced by the VU0155041/glutamate combination (Figure 3.8H); this was not present when L-AP4 was used as the agonist (Figure 3.8) or when $mGlu_4$ was expressed alone (Figure 3.8G). There are several possibilities that may explain this phenomenon. For example, there could be differences in receptor desensitization induced by the allosteric agonist activity of VU0155041 (Niswender et al., 2008b). When the endogenous agonist activity of VU0155041 was assessed in the absence of orthosteric agonist, the potency of VU0155041 was similar in cells expressing $mGlu_4$ versus those containing $mGlu_{2/4}$ as was the maximal level of potentiation (pEC_{50} value, $mGlu_4$, -5.38±0.17, and $mGlu_{2/4}$ cells, 5.25±0.10 (p=0.5719); maximal response, $mGlu_4$, 40.5±4.8% of glutamate maximal response, and $mGlu_{2/4}$ cells, 38.9±6.3% of glutamate maximal response (p=0.8459)), suggesting differential desensitization is not the cause of this discrepancy. It is possible that the use of glutamate in these experiments may contribute to this change in maximal response as glutamate will activate both $mGlu_2$ and $mGlu_4$. The decrease in the maximal response occurs at glutamate concentrations that would activate both $mGlu_2$ and $mGlu_4$, suggesting that there could be unique responses elicited when both the $mGlu_2$ and $mGlu_4$ orthosteric sites are occupied. The use of L-AP4, however, would not carry such a caveat, and the maximal responses in Figure 3.7F are similar with or without VU0155041. The enhanced ability of VU0155041 to potentiate L-AP4 responses was not due to non-

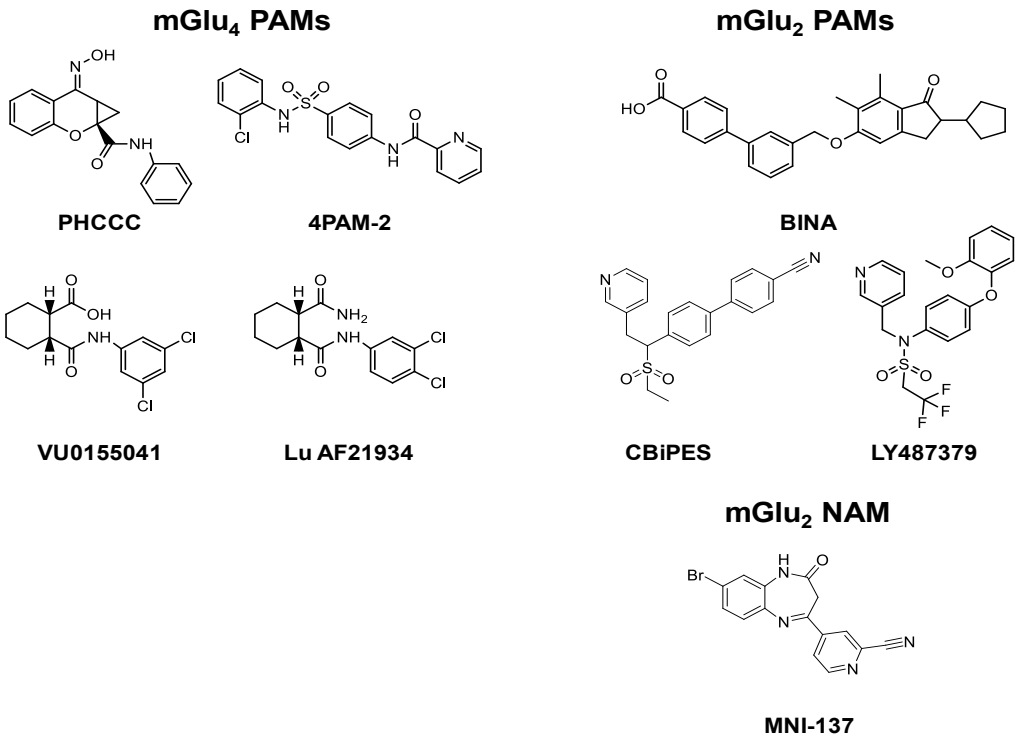

Figure 3.7. Structures of allosteric ligands used in these studies.

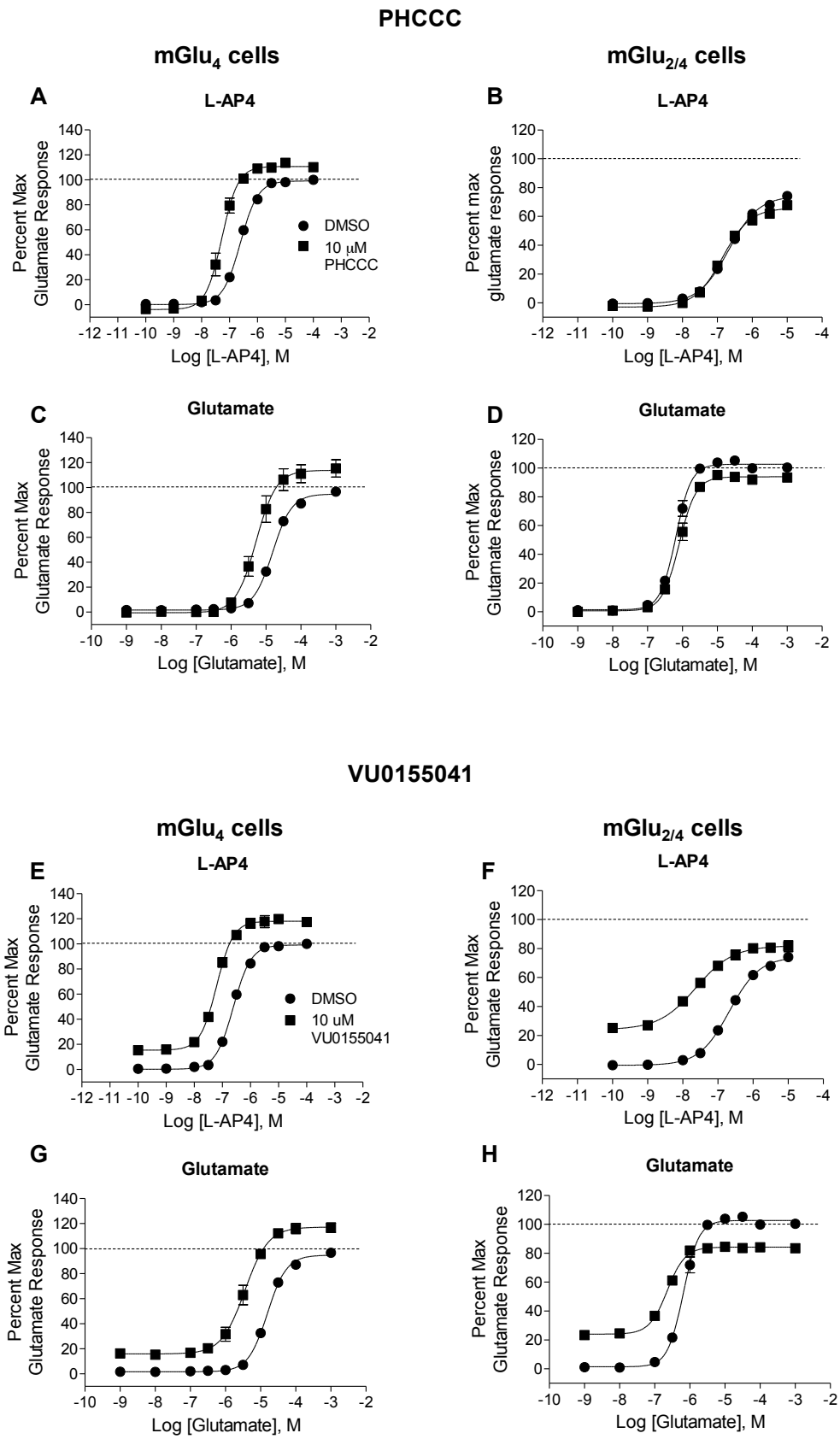
PHCCC
mGlu4 cells
mGlu2/4 cells
A
L-AP4
Percent Max Glutamate Response
DMSO
10 μM PHCCC
Log [L-AP4], M
B
L-AP4
Percent max glutamate response
Log [L-AP4], M
C
Glutamate
Percent Max Glutamate Response
Log [Glutamate], M
D
Glutamate
Percent Max Glutamate Response
Log [Glutamate], M
VU0155041
mGlu4 cells
mGlu2/4 cells
E
L-AP4
Percent Max Glutamate Response
DMSO
10 uM VU0155041
Log [L-AP4], M
F
L-AP4
Percent Max Glutamate Response
Log [L-AP4], M
G
Glutamate
Percent Max Glutamate Response
Log [Glutamate], M
H
Glutamate
Percent Max Glutamate Response
Log [Glutamate], M

Figure 3.8. The efficacies of PHCCC and VU0155041 are differentially regulated by $mGlu_{2/4}$ co-expression. A-H, 10 μM compound (■) or DMSO (●) were added 140 s before addition of serial dilutions of L-AP4 or glutamate. GIRK channel-mediated thallium flux was measured as described in HEK/GIRK/$mGlu_4$ (left panels) and HEK/GIRK/$mGlu_{2/4}$ (right panels) cell lines. Reponses were normalized to the maximal response induced by 1 mM glutamate in each individual cell line. pEC_{50} values for dose response curves in panels A-D without or with PHCCC were: A, 6.61±0.11 vs. 7.28±0.11 ($p=0.0115$); B, 6.63±0.06 vs. 6.85±0.05 ($p=0.0557$); C, 4.77±0.05 vs. 5.27±0.10 ($p=0.0017$); D, 6.11±0.05 vs. 6.09±0.06 ($p=0.8383$). pEC_{50} values for dose response curves in panel E-H without or with VU0155041 were: E, 6.61±0.11 vs. 7.21±0.08 ($p=0.0113$); F, 6.63±0.06 vs. 7.61±0.07 ($p=0.0004$); G, 4.77±0.05 vs. 5.36±0.04 ($p<0.0001$); H, 6.11±0.05 vs. 6.64±0.02 ($p<0.0001$). All values represent mean ± SEM ($n\geq3$).

	$mGlu_2$		$mGlu_4$		$mGlu_{2/4}$		
	Glutamate	LY379268	Glutamate	L-AP4	Glutamate	LY379268	L-AP4
10 μM PHCCC	0.9±0.03	1.0±0.04	3.5±0.53	4.7±0.02	1.0±0.04[a]	0.8±0.07	1.7±0.04[b]
10 μM 4PAM-2	0.9±0.03	0.9±0.05	15.2±3.10	18.8±2.58	1.0±0.02[c]	0.9±0.07	2.7±0.21[d]
10 μM VU0155041	0.9±0.02	0.9±0.02	4.0±0.26	3.9±0.29	3.5±0.30	4.1±0.12[e]	9.7±1.00[f]
10 μM Lu AF21934	1.0±0.03	1.0±0.02	3.4±0.14	3.9±0.08	2.7±0.17[g]	1.7±0.10[h]	8.2±0.96[i]

Table 3.2. The ability of $mGlu_4$ PAMs to left-shift agonist concentration-response curves is distinct for different groups of PAMs. Data represent the Mean SEM of at least three experiments performed in duplicate. [a]$p=0.0009$ for $mGlu_4$ versus $mGlu_{2/4}$ lines; [b]$p<0.0001$ for $mGlu_4$ versus $mGlu_{2/4}$ lines; [c]$p=0.0003$ for $mGlu_4$ versus $mGlu_{2/4}$ lines; [d]$p=0.0034$ for $mGlu_4$ versus $mGlu_{2/4}$ lines; [e]$p<0.0001$ for $mGlu_2$ versus $mGlu_{2/4}$ lines; [f]$p=0.0054$ for $mGlu_4$ versus $mGlu_{2/4}$ lines; [g]$p=0.0175$ for $mGlu_4$ versus $mGlu_{2/4}$ lines; [h]$p<0.0001$ for $mGlu_2$ versus $mGlu_{2/4}$ lines; [i]$p=0.0021$ for $mGlu_4$ versus $mGlu_{2/4}$ lines. Unpaired student's t-test ($n\geq3$, two-tailed). Note the ability of VU0155041 to shift responses of the $mGlu_2$ agonist, LY379268.

selective activity of VU0155041 on $mGlu_2$ receptors (Table 3.2, (Niswender et al., 2008b)). These results reveal that VU0155041 can be used as a chemical probe to potentiate responses to activation of $mGlu_{2/4}$ heterodimers.

The marked distinction between VU0155041 and PHCCC led us to speculate that the divergence in effect between the two PAMs may arise from their different chemical structures or binding sites; PHCCC and 4-PAM2 have been reported to bind to the same site on $mGlu_4$ while VU0155041 appears to bind to a distinct site on the $mGlu_4$ protein ((Drolet et al., 2011c), assessed using a racemic mixture of VU0155041 regioisomers). Consistent with this hypothesis, the VU0155041-related compound, Lu AF21934, also exhibited an enhanced ability to potentiate L-AP4 responses (3.9±0.1 fold for $mGlu_4$ cells alone and 8.2±1.0 fold for $mGlu_{2/4}$ cells) and retained the ability to potentiate glutamate responses (3.4±0.1 fold, $mGlu_4$ cells; 2.7±0.2 fold, $mGlu_{2/4}$ cells, Table 3.2) in cells co-expressing both receptors.

To gain further insight into the mechanism of the pharmacological changes, the ability of increasing amounts of compound to induce progressive leftward shifts in agonist concentration-response curves was measured using each individual $mGlu_4$ PAM and the operational model of allosterism was applied to compare the affinity (log K_B) and cooperativity (log $\alpha\beta$-a combined parameter that represents the effects of a modulator on affinity (α) as well as effects on efficacy (β)) of PAMs in cells expressing $mGlu_4$ alone vs. $mGlu_{2/4}$. As shown in Table 3.3, the estimated affinity of PHCCC was similar in $mGlu_{2/4}$ cells compared to cells expressing $mGlu_4$ alone. However, the positive cooperativity of PHCCC decreased significantly, from 0.57 ± 0.03 in the $mGlu_4$ cell line

to 0.12 ± 0.02 in $mGlu_{2/4}$ cell line (p=0.0017). Similar to PHCCC, 4PAM-2 also demonstrated a significant decrease in positive cooperativity in $mGlu_{2/4}$ cells (log $\alpha\beta$: 1.29±0.04 in $mGlu_4$ vs. 0.82±0.02 in $mGlu_{2/4}$ cells, p=0.0006); again, the affinity of the compound was not significantly different in the cell line expressing both receptors (Table 3.3). In contrast, VU0155041 and Lu AF21934 exhibited significant changes in affinity (Log K_B -5.27±0.01 vs. -4.78±0.13 for VU0155041, p=0.0188 and -5.88±0.04 vs. -5.26±0.09 for Lu AF21934, p=0.0042) as well as increases in positive cooperativity (log $\alpha\beta$ 0.95 ± 0.05 vs. 1.83 ± 0.27 for VU0155041, p=0.0334 and 0.66 ± 0.03 versus 1.7 ± 0.11 for Lu AF21934, p=0.0008) in $mGlu_{2/4}$ expressing cells compared to cells expressing $mGlu_4$ alone. These data suggest the altered pharmacology of $mGlu_4$ PAMs is due to differential changes in their positive cooperativity.

The lack of efficacy of PHCCC and 4PAM-2 suggests that the $mGlu_{2/4}$ cell line in which we performed our studies contains few or no $mGlu_4$ homomers, indicating that $mGlu_{2/4}$ interactions may be dominant and actually preferred. To further probe the interactions between the receptors, we transiently transfected either increasing amounts of $mGlu_2$ alone, increasing amounts of $mGlu_2$ in the presence of a constant amount of $mGlu_4$, or increasing amounts of $mGlu_2$ in the presence of another group III mGlu, $mGlu_7$. $mGlu_7$ was chosen as Kammermeir previously reported that $mGlu_2$ and $mGlu_7$ do not appear to interact in the same fashion as $mGlu_2$ and $mGlu_4$, suggesting that there is some specificity to the interaction (Kammermeier, 2012). In these studies, we observed gradual increases in the maximal LY379268 response when $mGlu_2$ was expressed alone in increasing amounts (data not shown); at the concentrations used here, we saw no significant

differences in the potency (Figure 3.9A) or Hill slope (Figure 3.9B) of the LY379268 response when $mGlu_2$ was assessed in the absence of other mGlus. In the presence of $mGlu_7$, responses appeared similar to those in which $mGlu_2$ alone was expressed, with no differences in LY379268 potency or Hill slope (Figure 3.9A and B). In the presence of $mGlu_4$, however, the potency of LY379268 was progressively shifted to the left when $mGlu_2$ levels were increased; additionally, the Hill slope of the curve fit also progressively increased, indicating alterations in cooperativity between the subunits. These differences suggest that the $mGlu_{2/4}$ combination appears to be distinct from that of $mGlu_{2/7}$, indicating some specificity in this interaction and confirming previous work by Kammermeier.

To further demonstrate that the altered pharmacology of $mGlu_4$ PAMs was due to $mGlu_{2/4}$ interaction, we tested the activity of $mGlu_4$ PAMs after transient transfection of increasing amounts of $mGlu_2$ in the presence of a constant amount of $mGlu_4$. In these experiments, a 30 μM concentration of each PAM was used. In cells transfected with just $mGlu_4$, 30 μM of PHCCC induced 7.2±1.5 and 8.5±0.3 fold leftward shifts of the glutamate or L-AP4 concentration-response curves, respectively. However, in cells co-transfected with 0.1, 0.2 and 0.5 μg $mGlu_2$ DNA, the shift of the L-AP4 response progressively decreased to 5.8±1.2, 3.5±0.6 and 3.4±0.2 fold, and in cells transfected with equal amounts of $mGlu_2$ and $mGlu_4$, the shift was only 1.9±0.5 fold (Figure 3.9C and Table 3.4). In addition, the shift of the glutamate response, even with only 0.1 μg of $mGlu_2$ DNA present (10% of the amount of $mGlu_4$) drastically decreased to only 1.3±0.1 fold (Figure 3.8D), suggesting a quite dramatic and dominant effect induced by the

presence of $mGlu_2$. As with the responses observed with PHCCC, 4PAM-2 demonstrated similar efficacy changes in transiently transfected cells, which is consistent with our findings in the stable cell lines and the observation that these two PAMs bind to the same allosteric pocket. Interestingly, the potentiation induced by VU0155041 and Lu AF21934 remained similar as the amount of $mGlu_2$ increased, further supporting the observation that distinct classes of $mGlu_4$ PAMs are differentially regulated by $mGlu_{2/4}$ interactions. It should be noted that, in these experiments, the similarity in potencies and Hill slopes of LY379268 in $mGlu_{2/4}$-expressing cells when the $mGlu_{2:4}$ ratio is 1:1, compared to cells expressing $mGlu_2$ alone, suggest that $mGlu_2$ homomers may exist along with $mGlu_{2/4}$ heteromers in these experiments. In contrast, our data also suggest that $mGlu_{2/4}$ heteromers are the dominant entity for $mGlu_4$ in these experiments. This interpretation is supported by the lack of potentiation induced by PHCCC and 4PAM-2 when glutamate is used as the agonist and the ratio of $mGlu_2$ to $mGlu_4$ is 1:10, suggesting that co-expression of even small amounts of $mGlu_2$ dramatically regulates activity of $mGlu_4$.

Co-addition of $mGlu_2$ PAM and $mGlu_4$ PAM does not result in further potentiation

We were also intrigued to investigate the cooperatvity of $mGlu_2$ PAM and $mGlu_4$ PAM and examined if co-addition of these compounds led to further potentiation in $mGlu_{2/4}$ cells compared to the effect induced by single PAM. 1 μM BINA, an $mGlu_2$ PAM, was applied either alone or in combination with $mGlu_4$ PAM VU0155041 (Figure 3.10A). 1 μM BINA, when added alone, induced allosteric agonist activity as can be seen by the elevated baseline of the dose response curve, and produced a 2.9±0.8 fold shift of the glutamate response. Consistent with previous data, 10 μM VU0155041 was able to shift

	Log K_B		Log $\alpha\beta$	
	$mGlu_4$ cells	**$mGlu_{2/4}$ cells**	**$mGlu_4$ cells**	**$mGlu_{2/4}$ cells**
PHCCC	−5.46 ± 0.23	−5.47 ±0.09	0.94 ± 0.06	0.51 ± 0.01[a]
4PAM-2	−6.32 ± 0.04	−6.44 ±0.06	1.29 ± 0.04	0.82 ± 0.02[b]
VU0155041	−5.27 ± 0.01	−4.78 ± 0.13[c]	0.95 ± 0.05	1.83 ± 0.27[d]
Lu AF21934	−5.88 ± 0.04	−5.26 ± 0.09[e]	0.66 ± 0.03	1.70 ± 0.11[f]

Table 3.3. Analysis of $mGlu_4$ PAMs using the operational model of allosterism reveals differential alterations in affinity or cooperativity for distinct groups of PAMs. Data were generated by progressive fold shift experiments using increasing concentrations of four $mGlu_4$ PAMs (ranging from 0 to 30 μM) prior to application of a full concentration-response range of L-AP4 (ranging from 0.1 nM to 10 μM). The logK_A of L-AP4 for $mGlu_4$ was set to -6.759 according to literature values (Monastyrskaia et al., 1999). For PHCCC and 4PAM-2, logτ_B was set to -100 due to the lack of allosteric agonist activity but was allowed to float for compounds exhibiting allosteric agonism (VU0155041, Lu AF29134). Data represent the Mean±SEM of at least three experiments performed in duplicate. [a]p=0.0017 between $mGlu_4$ cells and $mGlu_{2/4}$ cells; [b]p= 0.0006 between $mGlu_4$ cells and $mGlu_{2/4}$ cells; [c]p=0.0188 between $mGlu_4$ cells and $mGlu_{2/4}$ cells; [d]p=0.0334 between $mGlu_4$ cells and $mGlu_{2/4}$ cells; [e]p=0.0042 between $mGlu_4$ cells and $mGlu_{2/4}$ cells; [f]p=0.0008 between $mGlu_4$ cells and $mGlu_{2/4}$ cells. Unpaired student's t-test (n≥3, two-tailed).

	Glutamate CRC					L-AP4 CRC				
DNA ($mGlu_4$+$mGlu_2$, µg)	**1+0**	**1+0.1**	**1+0.2**	**1+0.5**	**1+1**	**1+0**	**1+0.1**	**1+0.2**	**1+0.5**	**1+1**
PHCCC	7.2±1.5	1.3±0.1***	1.7±0.1***	1.3±0.01***	1.2±0.1***	8.5±0.3	5.8±1.2*	3.5±0.6**	3.4±0.2***	1.9±0.5***
4-PAM2	10.0±1.1	1.5±0.1***	1.6±0.2***	1.3±0.04***	1.3±0.1***	14.7±2.6	9.6±3.2	5.2±0.2*	4.8±1.2*	2.4±0.5**
VU0155041	4.4±0.8	4.8±0.4	5.3±0.9	4.9±0.1	4.1±0.3	6.3±2.1	8.8±3.8	3.7±0.7	7.6±0.5	3.9±0.6
Lu AF21934	3.7±0.9	4.6±0.5	5.3±0.7	4.4±0.4	3.9±0.1	2.6±0.4	3.6±1.2	3.5±0.8	4.2±0.4	2.1±1.0

Table 3.4. Differential leftward fold shifts of glutamate or L-AP4 concentration-response curves are induced by different PAMs after transient expression of increasing amounts of $mGlu_2$ (0, 0.1, 0.2, 0.5 or 1 µg) with a constant amount (1 µg) of $mGlu_4$. Data represent the Mean ± SEM of three independent experiments performed in duplicate. Data were analyzed using one way ANOVA and Dunnett's Multiple Comparison Test comparing to cells transfected with $mGlu_4$ alone: $^{*}p<0.05$, $^{**}p<0.01$, $^{***}p<0.001$.

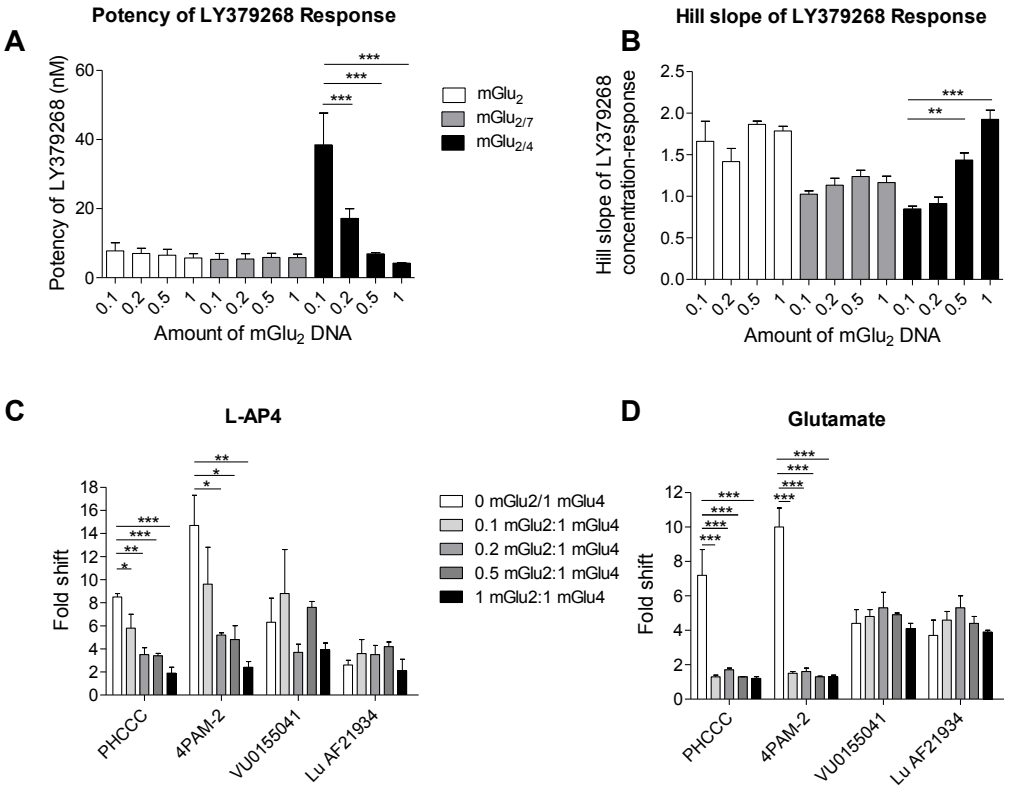

Figure 3.9. Co-expression of varying amounts of $mGlu_2$ and $mGlu_4$ regulates responses to both orthosteric and allosteric ligands. HEK/GIRK cells were transfected with 0, 0.1, 0.2, 0.5 or 1 μg $mGlu_2$ DNA in the absence or presence of co-transfection of 1 μg of vector control, 1 μg $mGlu_7$, or 1 μg $mGlu_4$. A and B. Potencies and Hill slope of the LY379268 response were determined; responses were unaffected by empty vector or $mGlu_7$ but dramatically altered in the presence of $mGlu_4$. C and D. The fold shifts induced by 30 μM of PHCCC, 4PAM-2, VU0155041 or Lu AF21934 are summarized for L-AP4 (C) and glutamate (D) using bar graphs. Values represent mean ± SEM (n=3). Statistics were performed using 1way ANOVA, Bonferroni's Multiple Comparison Test was used for A and B and Dunnett's Multiple Comparison Test was used for C and D. * denotes $p < 0.05$; ** denotes $p<0.01$ and *** denotes $p<0.001$.

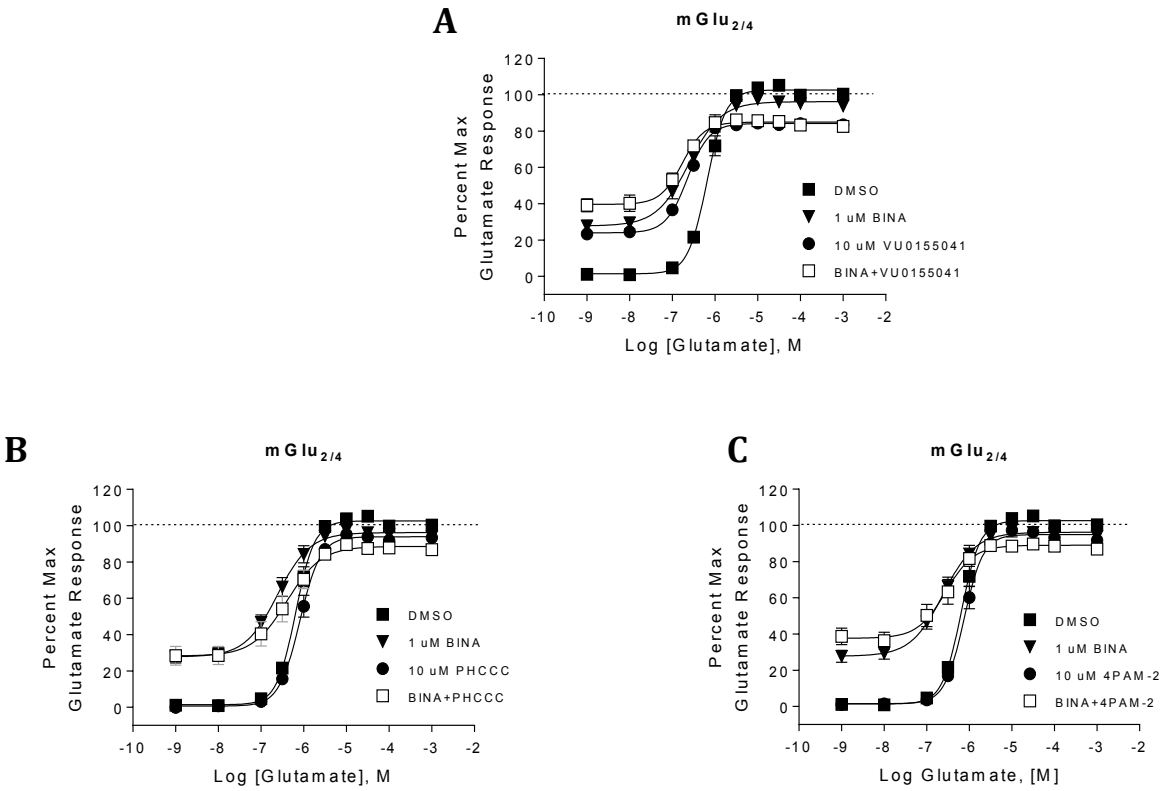

Figure 3.10. Co-addtion of $mGlu_2$ PAM and $mGlu_4$ PAM does not result in further potentiation. A-C**,** DMSO control (■), 1 μM BINA (▼), 10 μM $mGlu_4$ PAM (●, VU0155041, PHCCC or 4PAM-2) or BINA plus $mGlu_4$ PAM (□) were added 140 s before addition of serial dilutions of glutamate. GIRK channel-mediated thallium flux was measured as described in HEK/GIRK/$mGlu_{2/4}$ cell line and was normalized to the maximal response induced by 1 mM glutamate. pEC_{50} values for dose response curves of DMSO and 1 μM BINA were 6.10±0.05 and 6.48±0.16, respectively. pEC_{50} values for dose response curves of $mGlu_4$ PAM and BINA plus $mGlu_4$ PAM in panels A-C were: A, 6.64±0.02 vs. 6.79±0.05; B, 6.09±0.06 vs. 6.44±0.15; C, 6.12±0.05 vs. 6.60±0.14. All values represent mean ± SEM (n≥3).

glutamate dose response curve to the left by 3.5±0.3 fold. When added together, the induced fold shift was 5.0±0.3 fold, considerably lower than the expected value if the $mGlu_2$ PAM and $mGlu_4$ PAM exhibited an additive or cooperative effect. As shown in Table 3.2, PHCCC or 4PAM-2 was not able to shift glutamate responses when added alone in $mGlu_{2/4}$ cells (Figure 3.10 B and C). The effect of these two $mGlu_4$ PAMs were then assessed to determine if their efficacies could be modified in the presence of BINA. Co-addition of BINA resulted in a fold shift value that is not significantly higher than BINA alone (2.61±0.81 for PHCCC and 3.37±0.96 for 4PAM-2), suggesting no cooperative effect between $mGlu_2$ and $mGlu_4$ PAM sites.

Allosteric modulators of $mGlu_2$ are also differentially regulated upon formation of $mGlu_{2/4}$ heteromer

We also sought to investigate the influence of $mGlu_{2/4}$ interaction on $mGlu_2$ allosteric modulators. CBiPES and LY487379 are two PAMs from the pyridylmethylsulfonamide series that selectively potentiate $mGlu_2$ (Johnson et al., 2003; Johnson et al., 2005), whereas BINA was identified from a different chemical scaffold (Galici et al., 2006). We took advantage of these structurally distinct compounds and compared their efficacy in cells expressing $mGlu_2$ alone versus cells co-expressing $mGlu_2$ and $mGlu_4$. As shown in Table 3.5, none of the $mGlu_2$ PAMs potentiated responses to the $mGlu_4$ agonist L-AP4 in either $mGlu_4$ or $mGlu_{2/4}$-expressing cells. 1 μM BINA induced a 6.7 ±0.6 fold leftward shift of the glutamate concentration-response curve in $mGlu_2$ cells (Figure 3.11A). However, this number significantly decreased, to 3.0 ± 0.5 fold, in cells expressing both

$mGlu_2$ and $mGlu_4$ (Figure 3.11B). Likewise, the fold shift of the LY379628 response significantly decreased from 4.0 ±1.1 fold in $mGlu_2$ cells to 1.7 ± 0.2 fold in $mGlu_{2/4}$ cells (Figure 3.11C, D). In contrast, the ability of the $mGlu_2$ PAMs LY487379 and CBiPES to potentiate either glutamate or LY379268 responses was not significantly altered (Figure 3.11E-L), suggesting that distinct $mGlu_2$ PAMs also possess different pharmacological profiles when $mGlu_2$ is expressed alone relative to when $mGlu_2$ and $mGlu_4$ are co-expressed.

In contrast to what was observed with VU0155041/Lu AF21934 and their ability to potentiate LY379268 responses, we did not see potentiation of L-AP4 responses with any of the $mGlu_2$ PAMs. Each of the $mGlu_2$ PAMs used here exhibits similar potentiation of $mGlu_2$ responses compared to the responses of VU0155041 and Lu AF21934 at $mGlu_4$ (3-6 fold), suggesting that our assay system should be sensitive enough to detect potentiation of an $mGlu_4$ agonist response. However, in contrast to responses to $mGlu_4$ agonists, we would note that there is possibly some masking of potentiation due to expression of $mGlu_2$ homodimers in our cells. Each of the $mGlu_2$ PAMs used here shows some degree of allosteric agonist activity, which may complicate measurement of the signal when L-AP4 is used as the orthosteric agonist. In contrast to $mGlu_4$, where we hypothesize most of the receptors are in heteromeric form, this may result in a loss of sensitivity. Additionally, these compounds could be engaging distinct sites on each receptor that translate to distinct abilities to induce potentiation. Our data actually are most consistent with the hypothesis that the two halves of the heteromer may not function symmetrically or may differentially interact with signaling components, such as G-

proteins. If correct, this might suggest that one half of the dimer may be more sensitive to potentiation (or antagonism). While this remains to be determined experimentally for $mGlu_{2/4}$ heteromers and will require an assay system in which absolutely no $mGlu_2$ homomers are present, it could eventually contribute to signaling differences induced downstream of heteromic receptors when specific modulators are used.

Unlike PHCCC, all $mGlu_2$ PAMs evaluated had some activity at both $mGlu_2$ and $mGlu_{2/4}$, suggesting that either these cells express some level of homomeric $mGlu_2$ or that the effect on potentiation is not as dramatic as that observed with the $mGlu_4$ PAMs examined thusfar; regardless, the ability of these PAMs to each retain some degree of potentiation indicates that these compounds may not be useful as selective probes for differentiating homomeric versus heteromeric receptors in native systems.

In addition to the evaluation of the efficacy of $mGlu_2$ PAMs, we also assessed the efficacy of MNI-137, a selective group II mGlu NAM, on $mGlu_2$ versus $mGlu_{2/4}$ responses (Figure 3.12). For these studies, we chose to use the group II agonist DCG-IV, as LY379268 will weakly activate $mGlu_4$ at the higher concentrations needed to assess whether any potential interaction was competitive or noncompetitive in nature. In cells expressing $mGlu_2$ alone, increasing concentrations of MNI-137 non-competitively antagonized activation of $mGlu_2$ by DCG-IV, completely abolishing the response (Figure 3.10A). Consistent with its previously reported selectivity profile (Hemstapat et al., 2007), MNI-137 showed no significant effect in blocking L-AP4 responses in cells expressing $mGlu_4$ alone (Figure 3.10B). In $mGlu_{2/4}$ cells, MNI-137 was still able to

	$mGlu_2$		$mGlu_4$		$mGlu_{2/4}$		
	Glutamate	LY379268	Glutamate	L-AP4	Glutamate	LY379268	L-AP4
1 μM BINA	6.7±0.6	4.0±1.0	0.9±0.03	0.9±0.1	3.0±0.5[a]	1.7±0.2[b]	1.2±0.2
1 μM LY487379	3.2±0.2	2.1±0.3	0.9±0.02	1.0±0.1	2.7±0.3	2.1±0.3	1.0±0.05
1 μM CBiPES	6.2±0.3	3.0±0.02	0.8±0.1	0.9±0.04	5.1±0.3	2.8±0.7	0.9±0.2

Table 3.5. The efficacy of $mGlu_2$ PAMs to left-shift agonist concentration-response curves differs between classes of PAMs. Data represent the Mean ± SEM of three independent experiments performed in duplicate. [a]$p=0.0003$ for $mGlu_2$ versus $mGlu_{2/4}$ lines; [b]$p=0.0466$ for $mGlu_2$ versus $mGlu_{2/4}$ lines. Unpaired student's t-test ($n\geq3$, two-tailed).

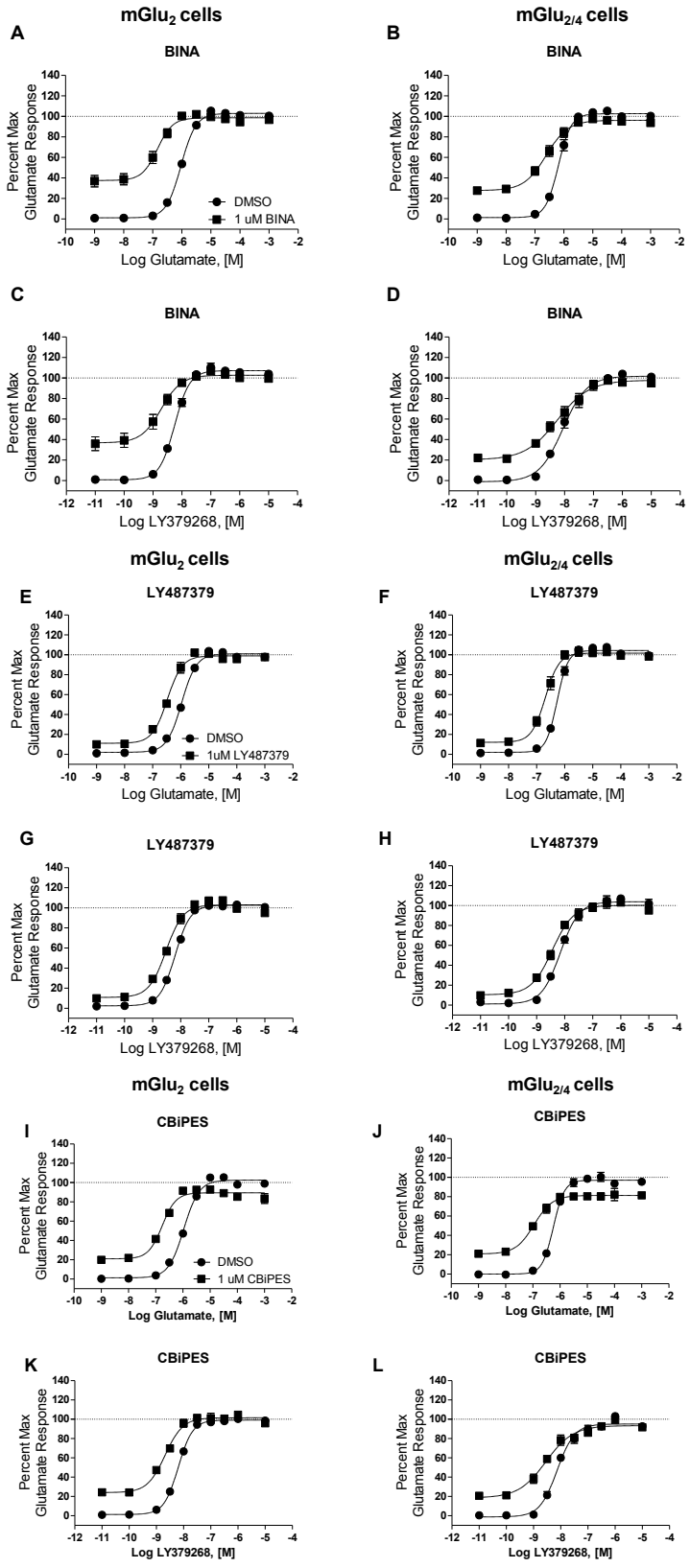
mGlu2 cells
A
BINA
Percent Max Glutamate Response
DMSO
1 uM BINA
Log Glutamate, [M]
mGlu2/4 cells
B
BINA
Percent Max Glutamate Response
Log Glutamate, [M]
C
BINA
Percent Max Glutamate Response
Log LY379268, [M]
D
BINA
Percent Max Glutamate Response
Log LY379268, [M]
mGlu2 cells
E
LY487379
Percent Max Glutamate Response
DMSO
1uM LY487379
Log Glutamate, [M]
mGlu2/4 cells
F
LY487379
Percent Max Glutamate Response
Log Glutamate, [M]
G
LY487379
Percent Max Glutamate Response
Log LY379268, [M]
H
LY487379
Percent Max Glutamate Response
Log LY379268, [M]
mGlu2 cells
I
CBiPES
Percent Max Glutamate Response
DMSO
1 uM CBiPES
Log Glutamate, [M]
mGlu2/4 cells
J
CBiPES
Percent Max Glutamate Response
Log Glutamate, [M]
K
CBiPES
Percent Max Glutamate Response
Log LY379268, [M]
L
CBiPES
Percent Max Glutamate Response
Log LY379268, [M]

Figure 3.11. The efficacies of $mGlu_2$ PAMs are also differentially regulated by $mGlu_{2/4}$ co-expression. 1 μM compound (■) or DMSO (●) were added 140 s before addition of serial dilutions of glutamate or LY379268. GIRK channel-mediated thallium flux was measured as described in HEK/GIRK/$mGlu_2$ (left panels) and HEK/GIRK/$mGlu_{2/4}$ (right panels) cell lines. Reponses were normalized to the maximal response induced by 1 mM glutamate in each individual cell line. pEC_{50} values for concentration response curves in panels A-D without or with BINA were: A, 6.01±0.03 vs. 6.81±0.05 ($p<0.0001$); B, 6.18±0.04 vs. 6.59±0.10 ($p<0.0001$); C, 8.25±0.02 vs. 8.79±0.10 ($p<0.0001$); D, 8.02±0.09 vs. 8.22±0.13 ($p=0.0058$). pEC_{50} values for dose response curves in panel E-H without or with LY487379 were: E, 5.96±0.01 vs. 6.47±0.03 ($p<0.0001$); F, 6.27±0.01 vs. 6.69±0.05 ($p<0.0001$); G, 8.20±0.02 vs. 8.52±0.05 ($p=0.0003$); H, 8.15±0.03 vs. 8.45±0.05 ($p=0.0009$). pEC_{50} values for dose response curves in panel I-L without or with CBiPES were: I, 5.97±0.01 vs. 6.76±0.02 ($p<0.0001$); J, 6.25±0.01 vs. 6.96±0.03 ($p<0.0001$); K, 8.20±0.01 vs. 8.68±0.01 ($p<0.0001$); L, 8.13±0.05 vs. 8.54±0.08 ($p=0.0132$). All values represent mean ± SEM ($n\geq3$) and statistics were performed using unpaired t test.

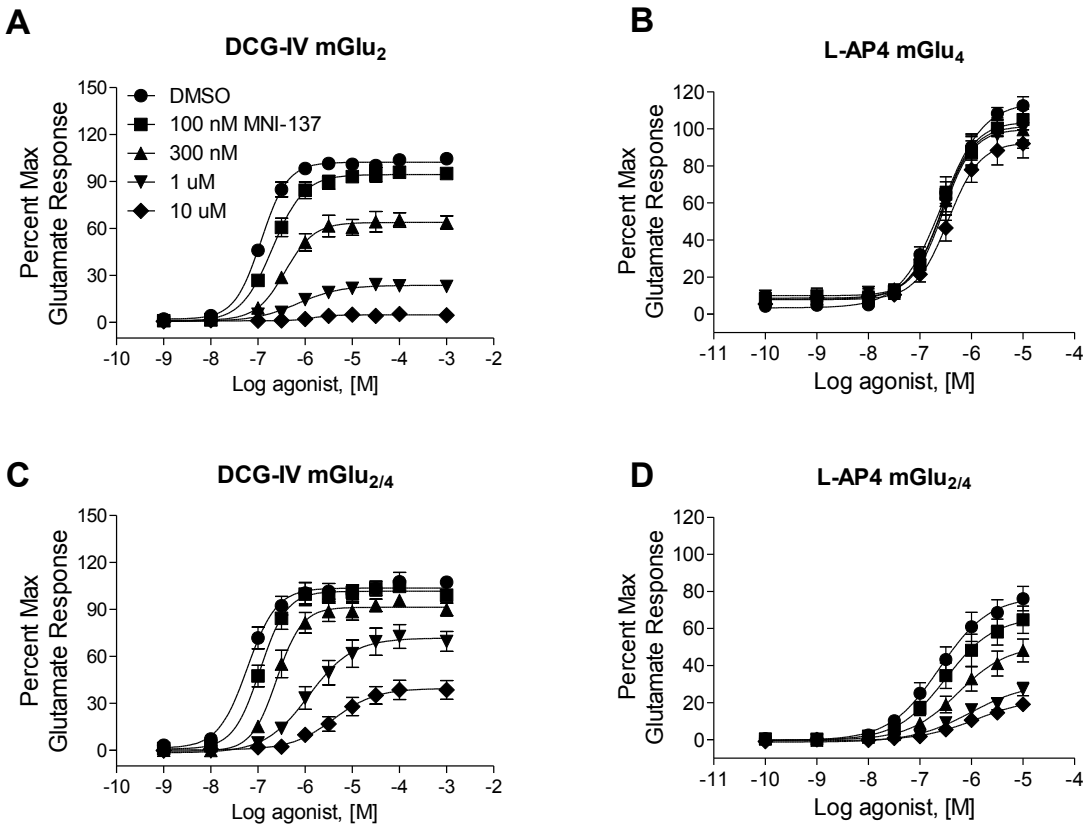

Figure 3.12. MNI-137 exhibits reduced efficacy when $mGlu_4$ and $mGlu_2$ are co-expressed and non-competitively antagonizes $mGlu_4$-mediated responses in $mGlu_{2/4}$-expressing cells. A and B, the effect of MNI-137 on DCG-IV responses were tested in the $mGlu_2$ or $mGlu_{2/4}$ cell line. C and D, the effect of MNI-137 on L-AP4 responses was tested in $mGlu_4$ or $mGlu_{2/4}$ cell line. DMSO (●) or 100 nM, 300 nM, 1 μM or 10 μM MNI-137 were added 140 s before addition of serial dilutions of LY379268 or L-AP4. GIRK channel-mediated thallium flux was measured as described and responses were normalized to the maximal response induced by 1 mM glutamate in each individual cell line. All values represent mean ± SEM (n=3).

antagonize DCG-IV responses in a non-competitive manner (Figure 3.12C). Analysis using the operational model of allosterism suggested that the affinity of MNI-137 was slightly higher in $mGlu_{2/4}$ cells. In addition, MNI-137 demonstrates increased cooperativity for affinity modulation but decreased cooperativity for efficacy modulation at $mGlu_{2/4}$ (Table 3.6), evidenced by an inability to completely abolish the response to DCG-IV. Surprisingly, MNI-137 was also able to noncompetitively block activation of the $mGlu_4$ subunit induced by stimulation with L-AP4, further supporting a structural and functional inter-subunit interaction within the $mGlu_{2/4}$ complex and suggesting that MNI-137 binding to $mGlu_2$ can negatively modulate the function of $mGlu_4$. Since MNI-137 does not block responses to L-AP4 unless $mGlu_2$ is co-expressed with $mGlu_4$, this NAM provides an excellent tool to evaluate responses to L-AP4 that may be mediated by $mGlu_{2/4}$ in native systems.

$mGlu_{2\text{ and }4}$ allosteric modulators exhibit unique pharmacological effect at the corticostriatal synapse

The unique pharmacology of VU0155041 and MNI-137 on $mGlu_{2/4}$-elicited responses suggests that these compounds provide a pair of tool compounds that can be utilized to provide evidence for the existence of $mGlu_{2/4}$ heteromers in native systems. Therefore, the effect of these two compounds were tested at the corticostriatal synapses by Meredith Noetzel and Kari Johnson in our laboratory. Treatment of slices with 10 μM VU0155041, followed by the co-addition of 10 μM VU0155041 and 500 nM L-AP4, resulted in a robust decrease in the eEPSP amplitude (51.3 ± 4.0% of baseline; Figure 3.13) relative to that observed with 500 nM L-AP4 alone (90.5 ± 6.2 % of baseline; Figure 3.1). These results, together with the lack of efficacy of PHCCC at the corticostriatal synapse, suggest that, in a native system, the potentiation of the L-AP4 responses by $mGlu_4$ PAMs mimics the differential responses observed in cells co-expressing $mGlu_2$ and $mGlu_4$.

Parameters	$mGlu_2$	$mGlu_{2/4}$
Log K_B	−6.82±0.04	−7.18±0.03[a]
Log α	−0.47±0.05	−0.74±0.05[b]
Log β	−100	−0.69±0.04

Table 3.6. MNI-137 exhibits enhanced affinity but decreased efficacy in modulating DCV-IV responses in $mGlu_{2/4}$ cells compared to cells expressing $mGlu_2$ alone. Data were analyzed using the operational model of allosterism as described in the Materials and Methods. The logK_A of DCG-IV for $mGlu_2$ was set to -6.959 according to literature values; logτ_B was set to -100. Data represent the Mean ± SEM of three independent experiments performed in duplicate. [a]p=0.0028 between $mGlu_2$ cells and $mGlu_{2/4}$ cells; [b]p=0.0206 between $mGlu_2$ cells and $mGlu_{2/4}$ cells. Unpaired student's t-test (n≥3, two-tailed).

Furthermore, these results suggest that homomeric $mGlu_4$ receptors, which would be predicted to respond to PHCCC, are expressed at extremely low abundance, if at all, in these synaptic terminals.

If $mGlu_{2/4}$ heteromeric receptors play a dominant role in regulating transmission at corticostriatal synapses, we would also predict that the $mGlu_2$ and $mGlu_{2/4}$ NAM MNI-137 would inhibit the effect of L-AP4 at this synapse. Treatment of slices with L-AP4 (100 μM) robustly inhibited the amplitude of electrically evoked EPSPs in striatal MSNs (62.3 ± 4.8% of baseline, Figure 3.14A). Bath application of MNI-137 (10 μM) for 10 min produced a small increase in EPSP amplitude (112.7 ± 3.5% of baseline, Figure 3.14B). Following pretreatment with MNI-137, 10 min bath application of L-AP4, in combination with MNI-137, returned EPSP amplitudes to baseline values (100.1 ± 3.4% of baseline, Figure 3.14B) and produced significantly less inhibition of EPSP amplitude compared with L-AP4 alone. The average inhibition of EPSP amplitude for L-AP4 alone was 37.1 ± 5.8%, whereas the L-AP4-induced inhibition of EPSP amplitude following MNI-137 treatment was only 12.5 ± 2.7% ($P<0.05$, unpaired *t* test, Figure 3.14C). These results indicate that an $mGlu_2$ NAM can regulate the responses of an $mGlu_4$ agonist at corticostriatal synapses, providing additional evidence for $mGlu_{2/4}$ heteromer expression in vivo.

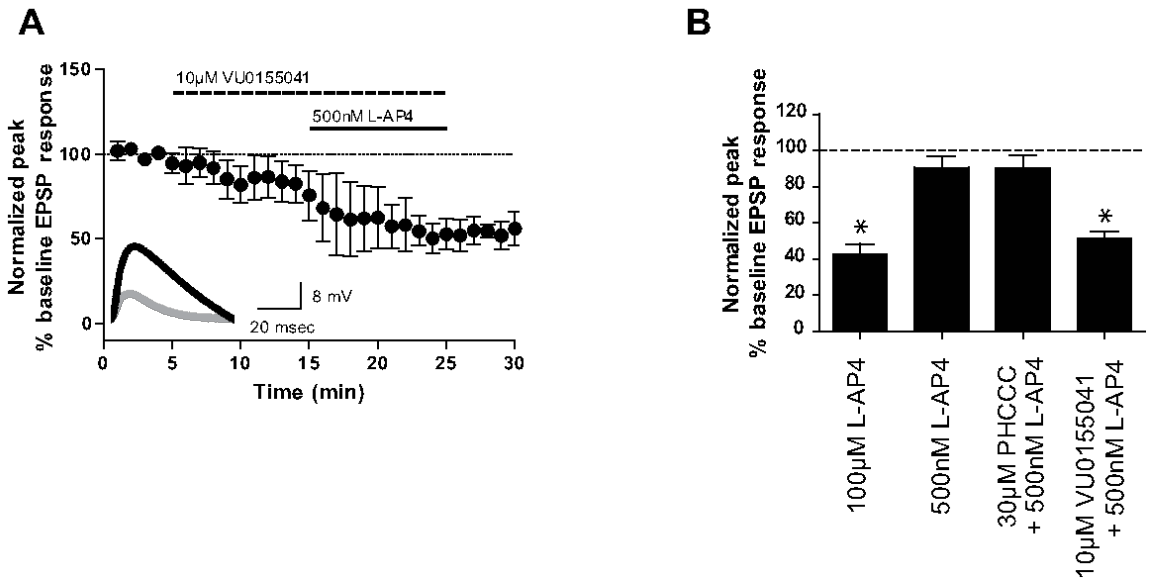

Figure 3.13. In contrast to PHCCC, VU0155041 potentiates the L-AP4-induced decrease in evoked EPSPs at the corticostriatal synapse. EPSPs were recorded in medium spiny neurons following stimulation of the white matter between the cortex and striatum with a bipolar electrode. All compounds were bath applied. Data are normalized to the average baseline EPSP amplitude. Insets are sample traces from an individual experiment (black – averaged traces from minute prior to L-AP4 application; gray – averaged traces from last minute of L-AP4 application). Slices were treated with 10 μM VU0155041 followed by co-application of 10 μM VU0155041 and 500 nM L-AP4. Two slices exhibited responses when VU0155041 was applied alone. Solid and dashed lines represent time of compound additions (A). Bar graphs summarizing the normalized peak EPSP response measured during the last two minutes of compound addition (B). Values represent mean ± SEM (n=5). * denotes $p < 0.05$ when compared to 500 nM L-AP4 using Dunnett's Multiple Comparison Test.

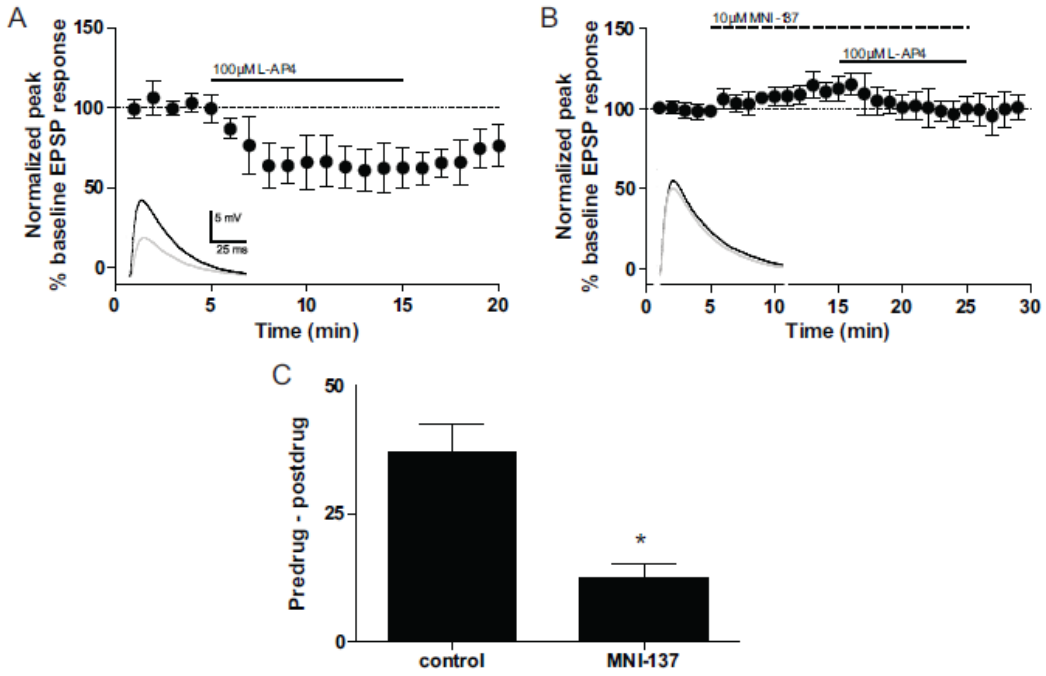

Figure 3.14. MNI-137 blocks L-AP4-induced inhibition of corticostriatal transmission. EPSPs were recorded in medium spiny neurons following stimulation of the white matter between the cortex and striatum with a bipolar electrode. Data are normalized to the average baseline EPSP amplitude. Insets represent sample traces from a representative experiment (black – averaged traces from minute prior to L-AP4 application; gray – averaged traces from last minute of L-AP4 application). Slices were treated with 100 μM L-AP4 alone (A) or following a 10 minute pretreatment with 10 μM MNI-137 (B). (C) Bar graph representation of the inhibition of corticostriatal transmission by L-AP4 in the absence (control) and presence of MNI-137. The difference between EPSP amplitudes during the minute prior to L-AP4 application and the last minute of L-AP4 application were calculated for each cell, and the average difference for each treatment group is shown in the bar graph. Data represent mean ± SEM (n=5-7). * denotes $P < 0.05$, unpaired t test.

Discussion

As recombinant cell lines are used to identify and characterize allosteric reagents, it is important to recognize potential discrepancies between *in vitro* and *in vivo* properties of these novel compounds. For example, MMPIP, an allosteric antagonist of $mGlu_7$, inhibits $mGlu_7$ activity in recombinant cell lines (Mitsukawa et al., 2005; Niswender et al., 2010; Suzuki et al., 2007) ; however, when applied to brain slices, it fails to inhibit $mGlu_7$-mediated L-AP4 responses at SC-CA1 synapses (Niswender et al., 2010). We show here that PHCCC fails to potentiate $mGlu_4$ at corticostriatal synapses, despite its well-established efficacy *in vitro* and at other synapses. These data suggest that the activity of allosteric compounds may be context-specific and could be dramatically altered by the *in vivo* environment, such as differential expression of signaling pathway components or variations in receptor assembly.

By performing co-IP experiments in dorsal striatum and medial prefrontal cortex from both rat and mouse, our data demonstrate $mGlu_{2/4}$ interaction in native tissue. The detection of $mGlu_{2/4}$ heteromers in dorsal striatum is consistent with electrophysiology data that both $mGlu_2$ and $mGlu_4$ act presynaptically to reduce excitatory transmission at corticostriatal synapses (Bennouar et al., 2012; Johnson et al., 2005), although $mGlu_2$ and $mGlu_4$ may colocalize on other axon terminals in the striatum as well. Similarly, our medial prefrontal cortex samples contain many axon terminals where $mGlu_2$ and $mGlu_4$ might colocalize. While we cannot conclude the precise localization of $mGlu_{2/4}$ heteromers in this region, physiological evidence suggests that presynaptic expression of

$mGlu_2$ and $mGlu_4$ at thalamocortical synapses (Benneyworth et al., 2007; Marek et al., 2000; Zhang and Marek, 2007) is also a potential source of the $mGlu_{2/4}$ heterocomplexes.

We have observed altered efficacies of $mGlu_4$ PAMs in cells co-expressing $mGlu_2$ and $mGlu_4$ (Figure 3.8 and Table 3.2). These data are consistent with Kammermeier's finding in *in vitro* cultured neurons co-injected with $mGlu_2$ and $mGlu_4$ cDNA (Kammermeier, 2012). We have also shown that effects of $mGlu_2$ allosteric modulators can also be significantly altered. Modeling of $mGlu_4$ PAM interactions using the operational model of allosterism suggests that binding to two distinct allosteric pockets results in differential pharmacological profile changes with regards to affinity and cooperativity. This suggests that these allosteric binding pockets may encounter differential conformation changes upon heterointeraction of the two receptor subunits, although more detailed structural studies are needed.

In our experiments, $mGlu_2$ and $mGlu_4$ were co-transfected without being forced to form an interaction. Advantages of this approach are that it avoids tagging of the receptors, which may affect pharmacology, and that it more closely mimics the receptor assembly in an *in vivo* environment where mGlu homomers and heteromers may co-exist. At the receptor levels expressed in our stable cell lines, the pharmacology of orthosteric agonists, such as LY379268 and L-AP4, was not dramatically altered in the $mGlu_{2/4}$ line (Figure 3.5). However, although both agonists elicited a response alone, the Hill slopes of the concentration-response curves were significantly decreased compared to cells expressing a single mGlu subtype, suggesting an interaction between the subunits. We did observe

differences in the ability of LY379268 and L-AP4 to achieve maximal responses (LY379268 was a full agonist while L-AP4 only achieved a 70% maximal response), which could result from the presence of $mGlu_2$ homodimers under these experimental conditions. In contrast, our data appear to be consistent with little to no expression of $mGlu_4$ homodimers in our $mGlu_{2/4}$ cell line. For example, the fact that PHCCC and 4PAM-2 exhibit significantly decreased/no efficacy in potentiating L-AP4 responses suggests that most $mGlu_4$ subunits in $mGlu_{2/4}$ cell line appear to be in a complexed form. While we cannot definitively conclude that the receptors are forming strict heterodimers (as opposed to oligomers) in our system, the work of Doumazane et al. suggests that $mGlu_2$ and $mGlu_4$ appear to form heterodimers, rather than higher order oligomers, *in vitro* (Doumazane et al., 2011a).

To overcome the caveat of $mGlu_2$ homodimers in the stable cell line, we performed transient transfection experiments with a constant amount of $mGlu_4$ or $mGlu_7$ and variable amounts of $mGlu_2$. Results from these studies suggest that expression of $mGlu_4$ specifically results in changes in the potency and cooperativity of an $mGlu_2$ orthosteric agonist, and that alterations in $mGlu_4$ PAM pharmacology are dependent on the amount of $mGlu_2$ co-expression. Quite strikingly, 1/10 of the amount of $mGlu_2$ compared to $mGlu_4$ resulted in a nearly complete loss of potentiation of the glutamate response by PHCCC and 4PAM-2, suggesting that the heterointeractions may be dominant.

We would note that, when $mGlu_2$ and $mGlu_4$ were co-transfected in similar amounts, the potency and Hill slope of the LY379268 response was the same as when $mGlu_2$ is

expressed alone. The lack of effect of PHCCC and 4-PAM2, along with the similarities in Hill slope and potency once the amount of $mGlu_2$ equals that of $mGlu_4$, suggests that the interpretation that there are homomeric pools of $mGlu_2$ and heteromeric $mGlu_{2/4}$ under these conditions are most consistent with the current data. These data also recapitulate Kammermeier's finding that $mGlu_2$ homodimers existed when $mGlu_2$ and $mGlu_4$ were transfected with a 1:1 ratio but not a 1:3 ratio (Kammermeier, 2012).

It has previously been shown that heterodimerization/hetero-interactions of receptors can substantially alter the effect of pharmacological reagents. For example, Gonzalez-Maeso et al. reported that 5-HT_{2A} receptors interact with $mGlu_2$ and form functional complexes in cerebral cortex (Gonzalez-Maeso et al., 2008). In the presence of this 5-HT_{2A}/$mGlu_2$ complex, hallucinogenic 5-HT_{2A} agonists triggered unique cellular responses, which may contribute to the pathogenesis of psychosis. The combination of unique orthosteric and allosteric ligands for $mGlu_2$ and $mGlu_4$ now allows us to pharmacologically interrogate the functional expression of $mGlu_4$-containing heteromers at synapses in the CNS. For example, we found that VU0155041 potentiated L-AP4 responses at corticostriatal synapses, whereas PHCCC, which binds to a distinct allosteric site, showed no effect (Figure 3.1 and 3.13). In addition, the $mGlu_2$ NAM MNI-137 was able to block L-AP4 induced responses at the corticostriatal synapse, recapitulating the pharmacological profile of this compound in the $mGlu_{2/4}$ cell line.

Although the results reported here cannot be seen as definitive evidence of $mGlu_{2/4}$ heterodimer formation in the CNS and could be explained by other potential mechanisms, such as involvement of other partner proteins, multiple lines of evidence are consistent with functional existence of predominantly $mGlu_{2/4}$ heteromers at corticostriatal synapses: 1) time-resolved FRET studies by Doumazane et al. indicate that $mGlu_2$ and $mGlu_4$ form strict heterodimers when expressed in the same cells, 2) our co-immunoprecipitation data using rodent striatal tissue demonstrate some type of physical interaction between $mGlu_2$ and $mGlu_4$ in this brain region, and 3) pharmacological properties at corticostriatal synapses recapitulate the results seen in the $mGlu_{2/4}$ recombinant cell line. Regardless of the mechanism, these studies provide compelling evidence that the function of mGlu receptors can be context-dependent and that $mGlu_4$ may display fundamentally distinct responses to selective allosteric modulators at different synapses upon coexpression of other mGlu receptor subtypes.

CHAPTER IV

GENERAL DISCUSSION AND FUTURE DIRECTION

Functional selectivity and therapeutic implications of mGlu allosteric modulators

Seven transmembrane receptors (7TMRs) are intrinsic plasma membrane proteins that function as information transducers to pass stimuli from binding of natural ligands to activation of cytosolic signaling cascades. The fundamental mechanism of these actions is conformational changes of the receptors. Receptor proteins are dynamic molecules that are "breathing" and keep changing conformations, which are stabilized by natural ligands and synthetic orthosteric/allosteric reagents. Traditionally, these conformations are classified into "fully on", "partially on" or "off" conformations using criteria of G protein activation.

In addition to G proteins, however, numerous cytosolic proteins interact with various domains on the 7TMRs and constitute a part in the whole "breathing system". These proteins include arrestins and 7TMR interacting proteins, many of which are PDZ domain proteins. β-arrestin is able to recruit signaling molecules and induce long-lasting activation of ERK. Some examples of PDZ domain proteins include Na^+/H^+ exchange regulator factor 1 and PICK1. As each receptor conformation possesses a specific energy map, the affinities to signaling molecules also varies. It has recently been shown by bioluminescence resonance energy transfer that G protein and non-G protein pathways

are directly correlated with unique receptor conformations (Galandrin et al., 2008). Therefore, a ligand may not elicit responses in all signaling pathways and theoretically, no two ligands would produce the same receptor behavior in terms of signaling and receptor regulation. And such phenomenon is termed "functional selectivity" (Gesty-Palmer and Luttrell, 2011).

Even naturally occurring ligands may exhibit functionally selective effect. CCL19 and CCL20 represent the first examples, which induce different receptor desensitization profile on CCR7 receptor (Kohout et al., 2004). Other examples of orthosteric ligands stem from serotonin (5-HT) receptors. Orthosteric ligands at the 5-HT_{2A} and 5-HT_{2C} receptors have revealed different rank orders of agonists to stimulate phospholipase C versus phospholipase A2 pathways (Berg et al., 1998). In addition, there are now examples of ligands with inverse agonist properties in certain pathways but clear agonist activity in others (De Deurwaerdere et al., 2004). It has been observed as well, that compounds classified as "antagonists" can induce desensitization, internalization, and downregulation of receptors, a property that might be considered "agonistic" in nature (discussed in (Urban et al., 2007)).

These observations deviate from "linear efficacy" and has breached the traditional view of signal propagation via the receptors. To better quantify such biased effects, useful measurements have been proposed to describe agonist effects. The term activity ratio, calculated using Max/$EC_{50,}$ serves to characterize the ability of a certain agonist to activate a given signaling pathway (Ehlert, 2005). When two pathways are compared, the

relative activity ratios can thus be used to determine preference of one pathway over the other as a measurement of signaling bias.

As the search for more selective and "drug-like" 7TMR ligands has grown, the development of allosteric ligands has emerged. As these compounds bind to alternate sites on a 7TMR compared to the endogenous ligand, it might be expected that they could as well place the receptor in a unique structural conformation that might not be achieved, or at least favored, in their absence and result in preferential regulation of certain pathways in the presence of an allosteric ligand. For example, the $mGlu_5$ PAM *N*-{4-chloro-2-[(1,3-dioxo-1,3-dihydro-2*H*-isoindol-2-yl) methyl]phenyl}-2-hydroxybenzamide (CPPHA), which binds to an alternate site on the $mGlu_5$ receptor versus other PAMs (O'Brien et al., 2004), exhibits differential effects on calcium mobilization and ERK1/2 phosphorylation downstream of $mGlu_5$ activation in cultured cortical astrocytes (Zhang et al., 2005). This is in contrast to the PAM 3,3′-difluorobenzaldazine (DFB), which potentiates both responses similarly. Additionally, the study in Chapter II has introduced a second mechanism of functional selectivity where $mGlu_4$ PAMs usually do not induce biased signaling yet can exhibit functional selective effects upon co-activation of a G_q coupled receptor. This indicates that the pharmacodynamics of compounds could be far more complicated in native environment and the substantial calcium response induced by $mGlu_4$ PAMs could be of importance in the physiological and pathological conditions.

Functional selectivity could be used for rational design of drugs to maximize their therapeutic effects. In a case where functional selectivity may have therapeutic relevance, activation of the GPR109 receptor by nicotinic acid is effective is beneficial for dyslipidemia by lowering triglycerides and elevating high-density lipoprotein. However, serious side effects were observed in patients including cutaneous flushing (Pike, 2005). It has been shown that activation of the receptor by nicotinic acid activates the G_i signaling pathway, as well as phospholipase A2 activation followed by recruitment of β-arrestins. Studies using β-arrestin1 knockout mice revealed reduced dermal side effects while maintaining beneficial efficacies. In addition, MK-0354, a biased ligand that is devoid of β-arrestin recruitment, decreases serum levels of free fatty acids without inducing cutaneous flushing, and may represent an improved option for the treatment of dyslipidemia (Lai et al., 2008; Walters et al., 2009).

β-arrestin signaling, however, can also be associated with additional therapeutic effects. For example, the β-adrenergic receptor blocker carvedilol acts as an inverse agonist in cAMP pathways but as an agonist in stimulating β-arrestin-mediated ERK phosphorylation (Wisler et al., 2007); this compound clinically shows advantages over other β-blockers in the treatment of heart failure. Another example comes from parathyroid hormone (PTH) receptor. Intermittent Activation of PTH receptor increases bone mass by stimulating osteoblasts. However, bone resorption can also occur through the coupling of osteoblasts to osteoclasts, which is not desired for the treatment of osteoporosis. Studies using β-arrestin2 knockout mice suggest that β-arrestin pathway limits PTH-induced osteoclastogenesis and contributes to increased bone mass (Ferrari et

al., 2005). Indeed, a biased agonist, D-Trp(12),Tyr(34))-PTH(7-34) (also named PTH-betaarr), activates β-arrestin but not classic G protein signaling and induces bone formation without bone resorption, offering improved therapy for osteoporosis (Gesty-Palmer et al., 2009).

As to the biased signaling described in Chapter II, calcium is involved in various cellular functions including enzyme activation, signal-transduction, and electrophysiological responses. In the central nervous system, intracellular calcium mobilization is vital for neurotransmitter release and synaptic plasticity, including long-term potentiation and long-term depression. It is well studied that massive calcium mobilization mediated by 7TMR cross-talk can have significant physiological implications. For example, $mGlu_1$-mediated calcium mobilization in Purkinje neurons is enhanced by concomitant activation of GABAB receptor (Kamikubo et al., 2007). Induction of such a calcium signal is suggested to act as a co-incidence detector for parallel- and climbing-fiber inputs, and is required for long-term depression at parallel-fiber–Purkinje cell synapses (Hirono et al., 2001; Wang et al., 2000). Similarly, potentiated calcium release by cross-talk between group I and group II mGluRs is shown to be critical for LTD in the perirhinal cortex under resting-membrane potentials (Cho et al., 2000). Therefore, signaling bias induced by $mGlu_4$ PAMs could be utilized to treat disease conditions where calcium signaling of a G_q coupled receptor is desired in $mGlu_4$-coexpressing cells but not in other tissues. On the other hand, however, an inappropriate intracellular calcium surge could induce apoptosis via activation of calpain (Camins et al., 2009). Therefore, caution may

need to be taken when $mGlu_4$ PAMs are used in combination with other G_q receptor agonists.

As more allosteric modulators are pursued in the hopes of achieving highly selective drug leads with good pharmacokinetic properties, further complexity induced by signal bias will continue to develop. While functional selectivity clearly complicates the use of compounds as general tools for probing receptor function and the progression of drugs with these properties through clinical development, there is great promise in this approach to eventually tailor drug therapy to a particular pathway or subset of signaling cascades to enhance therapeutic efficacy and/or reduce side effects.

Receptor assembly-selective modulators of mGlu

As mentioned above, allosterism of the receptor by ligands/modulators and interacting cytosolic proteins is essential for the signal transduction from environment into the cells. In addition to the guest allosterism and cytosolic allostery induced by these factors, receptor dimerization/oligomerization, as well as the lipid environment, comprise important components for the lateral allostery of 7TMRs (Kenakin and Miller, 2010).

Although oligomerization of family A 7TMRs is a topic of extensive debate, family B 7TMRs have recently been shown to form stable homodimers with the interacting interface at TM4 (Harikumar et al., 2008; Harikumar et al., 2007). In addition, family C

7TMRs (including mGlus) have shown compelling evidence for dimerization/oligomerization via both covalent and non-covalent bonds (Ray and Hauschild, 2000; Romano et al., 2001).

As it is common to consider small molecules as receptor modulators, large receptor protomers may also induce conformational change to other protomers. It is thus important to realize two-way transmission by which receptor assembly can alter the behavior of small molecule modulators as well. This effect has been well established in cell line settings. Using the angiotensin receptor as an example, the agonist angiotensin II exhibits significantly increased efficacy when the receptor form a heterocomplex with bradykinin-2 receptor (AbdAlla et al., 2000). Receptor dimerization may also affect intracellular signaling pathways. The G protein coupling of dopamine D_2 receptor switches from $G_{i/o}$ to $G_{q/11}$ when dimerized with dopamine D_1 receptor (Rashid et al., 2007). In addition, SKF83959, a compound with no effect on either D_1 or D_2 monomer, activates the D_1/D_2 heterodimer toward $G_{q/11}$ (Rashid et al., 2007).

As dimerization/oligomerization of receptors clearly complicated the use of pharmaceutical reagents in *in vivo* settings. While selective compounds for receptor heterodimers help to avoid off-target effects, reagents that target all receptor assemblies may produce superior pharmaceutical efficacy. The results decribed in Chapter III also shed light on targeting distinct mGlu receptor assembly for drug development purposes. Taking PD as an example, highly selective $mGlu_4$ PAMs have been developed from different chemical series and exhibit robust efficacy in preclinical rodent models.

Interestingly, both PHCCC and VU0155041 have been shown to reverse reserpine-induced akinesia in rodents, suggesting that the anti-parkinsonian effects induced by $mGlu_4$ PAMs may not be dependent on their activity at corticostriatal synapses and the assembly of $mGlu_{2/4}$ heterodimer. However, corticostriatal synapses have been shown to be overactive in dopamine-depleted animals, which contributes to the loss of spines of striatal medium spiny neurons in PD (Garcia et al., 2010). The work of Picconi et al. demonstrates that dysregulated plasticity at these synapses, such as long-term depression and depotentiation, may underlie the mechanism of L-DOPA-induced dyskinesia (Picconi et al., 2011; Picconi et al., 2003). Therefore, $mGlu_4$ PAMs that potentiate $mGlu_{2/4}$ heteromers may potentially provide additional therapeutic benefits, such as restoring morphology of striatal neurons and reversing L-DOPA-induced dyskinesias. In contrast, PAMs with selectivity for homodimers over heteromers might be beneficial for targeting $mGlu_4$ activation in regions predominantly expressing $mGlu_4$ alone if activation of heteromers proves to engender side effects. Additionally, selective $mGlu_{2/4}$ modulators without $mGlu_2$ or $mGlu_4$ activity might also be of interest to achieve selective modulatory effect without affecting receptor homomers expressed in other regions.

Although the signaling pathway of $mGlu_{2/4}$ heterodimers does not deviate from the $G_{i/o}$ coupling of each individual subtype, whether hetero-assembly lead to biased signal is of interest to explore. The effect of heterodimerization on other signaling cascades, especially arrestin binding, receptor desensitization, and internalization is worth further examination. Additionally, binding of modulators to one protomer on the heterodimers may also affect the pharmacology of allosteric sites on the other protomer. Detailed

studies using binding assays and functional assays are required to answer this question. Beside receptor dimerization, the effects of other interacting proteins and lipid bilayer composition on mGlu allosteric modulators are also largely unknown.

In addition to $mGlu_{2/4}$, other combinations of mGlu subtypes are co-localized in the CNS as well. For instance, $mGlu_4$ and $mGlu_8$ are co-expressed at the lateral olfactory tract-piriform cortex synapse and suppress synaptic transmission (Jones et al., 2008). $mGlu_1$ and $mGlu_5$ are co-expressed in several neuronal populations including CA1 hippocampal pyramidal cells, striatal cholinergic interneurons, STN glutamatergic neurons and SNr GABAergic neurons (reviewed in (Valenti et al., 2002)). In addition, both $mGlu_7$ and $mGlu_8$ receptors modulate the Schaffer collateral-CA1 synapse in neonatal rats (Ayala et al., 2008). Although the assembly of other mGlu heteromers has yet to be determined *in vivo*, previous studies showing aberrant activity of mGlu-selective compounds may eventually be explained by heteromer-specific pharmacology (Ayala et al., 2008; Niswender et al., 2010). As characterization of other combinations of mGlu heteromers are underway, localizing mGlu homomers and heteromers will help elucidate the complexity of mGlu receptor signaling and function and eventually contribute to rational development of therapeutic reagents that target specific tissues through selective modulation of individual receptor assemblies.

$mGlu_{2/4}$ heteromer as a biomarker for Parkinson's Disease

As defined by the National Institutes of Health, a biomarker is a parameter that is objectively measured and evaluated as an indicator of normal biological processes, pathogenic processes, or pharmacologic responses to a therapeutic intervention (Group, 2001). Biomarkers for PD are of critical importance for patient treatment, since neuroprotective therapy starting at an advanced stage (after motor symptoms develop) is usually unsuccessful in progressive neurodegenerative diseases when compared to early stages.

An ideal biomarker for PD should be able to facilitate PD treatment in the following aspects: 1) Aid in the early diagnosis of PD, preferably in a premotor period; 2) Accurately reflect disease progression; 3) Aid in therapeutic assignment of patients; and 4) Aid in accessing therapeutic efficacy of an intervention.

Since its first description, the diagnosis of PD has been made based on motor deficits and associated non-motor symptoms. Recently, however, a number of biomarkers have been developed to aid in the diagnosis of PD, which can be further divided into pathological biomarkers, biochemical biomarkers, genetic biomarkers, electrophysiological biomarkers and imaging biomarkers. A recent study discovered that α-synuclein and Lewy bodies exist in the gut biopsies of PD patients that were obtained several years before the onset of motor symptoms (Shannon et al., 2012), serving as a potential pathological biomarker for early PD detection. Schmid et al. has shown that biochemical

profiling of the post-translational modification of α-synuclein in the cerebrospinal fluid or blood plasma might be a more relevant biomarker than total α-synuclein level (Schmid et al., 2013). Altered levels of brain-derived neurotrophic factor (BDNF) have been reported in the circulation (serum or plasma) of patients with PD. However, BDNF might not serve as a specific biomarker since decreased levels of this neurotrophic factor were also observed in other neurodegenerative disorders, including Alzheimer's disease and Huntington's disease, as well as mood disorders (major depression and bipolar disorder) (Teixeira et al., 2010). Mutations in five genes, such as α-synuclein, Parkin, PTEN-induced kinase 1 (PINK1), DJ-1 and Leucine-rich repeat kinase 2 (LRRK2)] have been shown to lead to PD (Klein and Lohmann-Hedrich, 2007). However, these cases only account for 2–3% of all PD patients (Klein and Lohmann-Hedrich, 2007), and, even in these patients, age and environmental exposures greatly affect disease progression. Electrophysiologically, Hohlefeld et al. reported long-range temporal correlation of oscillation activities in subthalamic nucleus of PD patients, which can be modulated by levodopa treatment (Hohlefeld et al., 2012). However, the surgical procedures needed to measure neuronal activity in patients limited the usage of this parameter as a biomarker. In contrast, non-invasive imaging approaches have demonstrated great potential as a biomarker for PD diagnosis and treatment. For example, imaging of the dopamine transporter (DAT) with Single Photon Emission Computer Tomography (SPECT) is a main diagnostic imaging procedure for the assessment of patients with parkinsonism (Varrone and Halldin, 2012).

Although with caveats, these existing biomarkers have brought valuable advances in PD diagnosis and the drug development process, including early proof-of-concept studies and dosing regimen determination. As PD is much more complicated than a single-cause disease, it is equally important to assign patients to suitable therapeutic interventions, and ideally, as quickly as possible to prevent further neurodegeneration. Unfortunately, no such biomarker has yet been developed. $mGlu_4$ PAMs have been validated as potential therapeutic agents for PD with one possible mechanism being reduction of excessive GABA release at striatopallidal synapses (Marino et al., 2003; Valenti et al., 2003), thereby rebalancing basal ganglia circuitry. In addition, activation of $mGlu_4$ inhibits glutamate release onto substantia nigra dopamine neurons (Valenti et al., 2005), which has been proposed to protect against excitotoxicity. However, our study described in Chapter III reveals that the efficacy of $mGlu_4$ PAMs are differentially regulated by formation of $mGlu_{2/4}$ heterodimers, with PHCCC losing efficacy and VU0155041 retaining efficacy at the corticostriatal synapse. In addition, transient transfection experiment using cell lines suggests that the regulatory effect is dependent on the expression level of $mGlu_2$. Due to the heterogeneity within PD population, it is conceivable that $mGlu_2$ expression levels in the basal ganglia circuitry could vary among PD patients and may suggest that $mGlu_4$ PAMs that are ideal for some patients may not benefit others with high $mGlu_2$ expression colocalized with $mGlu_4$. Therefore, with help from future development of selective and powerful imaging reagents for $mGlu_2$ and $mGlu_4$, the expression pattern of $mGlu_2$ and $mGlu_4$ within the basal represent an attractive biomarker in PD clinical trials and future clinical practice.

BIBLIOGRAPHY

AbdAlla, S., Lother, H., and Quitterer, U. (2000). AT1-receptor heterodimers show enhanced G-protein activation and altered receptor sequestration. Nature *407*, 94-98.

Acher, F.C., and Bertrand, H.O. (2005). Amino acid recognition by Venus flytrap domains is encoded in an 8-residue motif. Biopolymers *80*, 357-366.

Attucci, S., Carla, V., Mannaioni, G., and Moroni, F. (2001). Activation of type 5 metabotropic glutamate receptors enhances NMDA responses in mice cortical wedges. Br J Pharmacol *132*, 799-806.

Ayala, J.E., Chen, Y., Banko, J.L., Sheffler, D.J., Williams, R., Telk, A.N., Watson, N.L., Xiang, Z., Zhang, Y., Jones, P.J.*, et al.* (2009). mGluR5 positive allosteric modulators facilitate both hippocampal LTP and LTD and enhance spatial learning. Neuropsychopharmacology *34*, 2057-2071.

Ayala, J.E., Niswender, C.M., Luo, Q., Banko, J.L., and Conn, P.J. (2008). Group III mGluR regulation of synaptic transmission at the SC-CA1 synapse is developmentally regulated. Neuropharmacology *54*, 804-814.

Battaglia, G., Busceti, C.L., Molinaro, G., Biagioni, F., Traficante, A., Nicoletti, F., and Bruno, V. (2006). Pharmacological activation of mGlu4 metabotropic glutamate receptors reduces nigrostriatal degeneration in mice treated with 1-methyl-4-phenyl-1,2,3,6-tetrahydropyridine. J Neurosci *26*, 7222-7229.

Benneyworth, M.A., Xiang, Z., Smith, R.L., Garcia, E.E., Conn, P.J., and Sanders-Bush, E. (2007). A selective positive allosteric modulator of metabotropic glutamate receptor subtype 2 blocks a hallucinogenic drug model of psychosis. Mol Pharmacol *72*, 477-484.

Bennouar, K.E., Uberti, M.A., Melon, C., Bacolod, M.D., Jimenez, H.N., Cajina, M., Kerkerian-Le Goff, L., Doller, D., and Gubellini, P. (2012). Synergy between l-DOPA and a novel positive allosteric modulator of metabotropic glutamate receptor 4: Implications for Parkinson's disease treatment and dyskinesia. Neuropharmacology.

Bennouar, K.E., Uberti, M.A., Melon, C., Bacolod, M.D., Jimenez, H.N., Cajina, M., Kerkerian-Le Goff, L., Doller, D., and Gubellini, P. (2013). Synergy between L-DOPA and a novel positive allosteric modulator of metabotropic glutamate receptor 4: implications for Parkinson's disease treatment and dyskinesia. Neuropharmacology *66*, 158-169.

Beqollari, D., and Kammermeier, P.J. (2008). The mGlu(4) receptor allosteric modulator N-phenyl-7-(hydroxyimino)cyclopropa[b]chromen-1a-carboxamide acts as a direct agonist at mGlu(6) receptors. European journal of pharmacology *589*, 49-52.

Beqollari, D., and Kammermeier, P.J. (2010). Venus fly trap domain of mGluR1 functions as a dominant negative against group I mGluR signaling. J Neurophysiol *104*, 439-448.

Berg, K.A., Maayani, S., Goldfarb, J., Scaramellini, C., Leff, P., and Clarke, W.P. (1998). Effector pathway-dependent relative efficacy at serotonin type 2A and 2C receptors: evidence for agonist-directed trafficking of receptor stimulus. Mol Pharmacol *54*, 94-104.

Bertaso, F., Zhang, C., Scheschonka, A., de Bock, F., Fontanaud, P., Marin, P., Huganir, R.L., Betz, H., Bockaert, J., Fagni, L.*, et al.* (2008). PICK1 uncoupling from mGluR7a causes absence-like seizures. Nat Neurosci *11*, 940-948.

Besong, G., Battaglia, G., D'Onofrio, M., Di Marco, R., Ngomba, R.T., Storto, M., Castiglione, M., Mangano, K., Busceti, C.L., Nicoletti, F.R.*, et al.* (2002). Activation of

group III metabotropic glutamate receptors inhibits the production of RANTES in glial cell cultures. J Neurosci *22*, 5403-5411.

Betts, M.J., O'Neill, M.J., and Duty, S. (2012). Allosteric modulation of the group III mGlu(4) receptor provides functional neuroprotection in the 6-hydroxydopamine rat model of Parkinson's disease. British journal of pharmacology *166*, 2317-2330.

Beurrier, C., Lopez, S., Revy, D., Selvam, C., Goudet, C., Lherondel, M., Gubellini, P., Kerkerian-LeGoff, L., Acher, F., Pin, J.P.*, et al.* (2009). Electrophysiological and behavioral evidence that modulation of metabotropic glutamate receptor 4 with a new agonist reverses experimental parkinsonism. FASEB J *23*, 3619-3628.

Bjarnadottir, T.K., Gloriam, D.E., Hellstrand, S.H., Kristiansson, H., Fredriksson, R., and Schioth, H.B. (2006). Comprehensive repertoire and phylogenetic analysis of the G protein-coupled receptors in human and mouse. Genomics *88*, 263-273.

Bockaert, J., Dumuis, A., Fagni, L., and Marin, P. (2004). GPCR-GIP networks: a first step in the discovery of new therapeutic drugs? Current opinion in drug discovery & development *7*, 649-657.

Bradley, S.R., Standaert, D.G., Rhodes, K.J., Rees, H.D., Testa, C.M., Levey, A.I., and Conn, P.J. (1999). Immunohistochemical localization of subtype 4a metabotropic glutamate receptors in the rat and mouse basal ganglia. J Comp Neurol *407*, 33-46.

Bridges, T.M., and Lindsley, C.W. (2008). G-protein-coupled receptors: from classical modes of modulation to allosteric mechanisms. ACS Chem Biol *3*, 530-541.

Brock, C., Oueslati, N., Soler, S., Boudier, L., Rondard, P., and Pin, J.P. (2007). Activation of a dimeric metabotropic glutamate receptor by intersubunit rearrangement. J Biol Chem *282*, 33000-33008.

Camins, A., Crespo-Biel, N., Junyent, F., Verdaguer, E., Canudas, A.M., and Pallas, M. (2009). Calpains as a target for therapy of neurodegenerative diseases: putative role of lithium. Current drug metabolism *10*, 433-447.

Celanire, S., Bolea, C., Bruckner, S., Liverton, N., Charvin, D., Hess, F., Poli, S., Bournique, B., Fonsi, M., Polsky-Fisher, S.*, et al.* (2011). Discovery and Characterization of Novel Metabotropic Glutamate Receptor 4 (mGluR4) Allosteric Potentiators. Current Neuropharmacology *9*, 9.

Chaudhari, N., Landin, A.M., and Roper, S.D. (2000). A metabotropic glutamate receptor variant functions as a taste receptor. Nat Neurosci *3*, 113-119.

Chen, J.J., and Swope, D.M. (2007). Pharmacotherapy for Parkinson's disease. Pharmacotherapy *27*, 161S-173S.

Chen, Y., Goudet, C., Pin, J.P., and Conn, P.J. (2008). N-{4-Chloro-2-[(1,3-dioxo-1,3-dihydro-2H-isoindol-2-yl)methyl]phenyl}-2-hydroxybe nzamide (CPPHA) acts through a novel site as a positive allosteric modulator of group 1 metabotropic glutamate receptors. Mol Pharmacol *73*, 909-918.

Cho, K., Kemp, N., Noel, J., Aggleton, J.P., Brown, M.W., and Bashir, Z.I. (2000). A new form of long-term depression in the perirhinal cortex. Nat Neurosci *3*, 150-156.

Choi, K.Y., Chang, K., Pickel, J.M., Badger, J.D., 2nd, and Roche, K.W. (2011). Expression of the metabotropic glutamate receptor 5 (mGluR5) induces melanoma in transgenic mice. Proc Natl Acad Sci U S A *108*, 15219-15224.

Comps-Agrar, L., Kniazeff, J., Brock, C., Trinquet, E., and Pin, J.P. (2012). Stability of GABAB receptor oligomers revealed by dual TR-FRET and drug-induced cell surface targeting. FASEB J *26*, 3430-3439.

Conn, P.J., Christopoulos, A., and Lindsley, C.W. (2009). Allosteric modulators of GPCRs: a novel approach for the treatment of CNS disorders. Nat Rev Drug Discov *8*, 41-54.

Conn, P.J., and Pin, J.P. (1997). Pharmacology and functions of metabotropic glutamate receptors. Annu Rev Pharmacol Toxicol *37*, 205-237.

Corti, C., Aldegheri, L., Somogyi, P., and Ferraguti, F. (2002). Distribution and synaptic localisation of the metabotropic glutamate receptor 4 (mGluR4) in the rodent CNS. Neuroscience *110*, 403-420.

Corti, C., Restituito, S., Rimland, J.M., Brabet, I., Corsi, M., Pin, J.P., and Ferraguti, F. (1998). Cloning and characterization of alternative mRNA forms for the rat metabotropic glutamate receptors mGluR7 and mGluR8. Eur J Neurosci *10*, 3629-3641.

Dale, L.B., Bhattacharya, M., Seachrist, J.L., Anborgh, P.H., and Ferguson, S.S. (2001). Agonist-stimulated and tonic internalization of metabotropic glutamate receptor 1a in human embryonic kidney 293 cells: agonist-stimulated endocytosis is beta-arrestin1 isoform-specific. Mol Pharmacol *60*, 1243-1253.

De Deurwaerdere, P., Navailles, S., Berg, K.A., Clarke, W.P., and Spampinato, U. (2004). Constitutive activity of the serotonin2C receptor inhibits in vivo dopamine release in the rat striatum and nucleus accumbens. J Neurosci *24*, 3235-3241.

Dev, K.K., Nakanishi, S., and Henley, J.M. (2001). Regulation of mglu(7) receptors by proteins that interact with the intracellular C-terminus. Trends Pharmacol Sci *22*, 355-361.

Doumazane, E., Scholler, P., Zwier, J.M., Eric, T., Rondard, P., and Pin, J.P. (2011a). A new approach to analyze cell surface protein complexes reveals specific heterodimeric metabotropic glutamate receptors. FASEB J *25*, 66-77.

Doumazane, E., Scholler, P., Zwier, J.M., Trinquet, E., Rondard, P., and Pin, J.P. (2011b). A new approach to analyze cell surface protein complexes reveals specific heterodimeric metabotropic glutamate receptors. FASEB J *25*, 66-77.

Drolet, R., Tugusheva, K., Liverton, N., Vogel, R., Reynolds, I.J., Hess, F.J., Renger, J.J., Kern, J.T., Celanire, S., Tang, L.*, et al.* (2011a). Binding property characterization of a novel mGlu4 positive allosteric modulator. Society for Neuroscience Abstracts.

Drolet, R., Tugusheva, K., Liverton, N., Vogel, R., Reynolds, I.J., Hess, F.J., Renger, J.J., Kern, J.T., Celanire, S., Tang, L.*, et al.* (2011b). Binding property characterization of a novel mGluR4 positive allosteric modulator. In Society for Neuroscience (Washington, DC: 2011 Neuroscience Meeting Planner).

Drolet, R., Tugusheva, K., Liverton, N., Vogel, R., Reynolds, I.J., Hess, F.J., Renger, J.J., Kern, J.T., Celanire, S., Tang, L.*, et al.* (2011c). Binding property characterization of a novel mGluR4 positive allosteric modulator. In Society for Neuroscience (Washington, DC: 2011 Neuroscience Meeting Planner).

Ehlert, F.J. (2005). Analysis of allosterism in functional assays. J Pharmacol Exp Ther *315*, 740-754.

El Moustaine, D., Granier, S., Doumazane, E., Scholler, P., Rahmeh, R., Bron, P., Mouillac, B., Baneres, J.L., Rondard, P., and Pin, J.P. (2012). Distinct roles of metabotropic glutamate receptor dimerization in agonist activation and G-protein coupling. Proceedings of the National Academy of Sciences of the United States of America *109*, 16342-16347.

Engers, D.W., Gentry, P.R., Williams, R., Bolinger, J.D., Weaver, C.D., Menon, U.N., Conn, P.J., Lindsley, C.W., Niswender, C.M., and Hopkins, C.R. (2010). Synthesis and

SAR of novel, 4-(phenylsulfamoyl)phenylacetamide mGlu4 positive allosteric modulators (PAMs) identified by functional high-throughput screening (HTS). Bioorg Med Chem Lett *20*, 5175-5178.

Enz, R. (2012). Structure of metabotropic glutamate receptor C-terminal domains in contact with interacting proteins. Front Mol Neurosci *5*, 52.

Esseltine, J.L., Willard, M.D., Wulur, I.H., Lajiness, M.E., Barber, T.D., and Ferguson, S.S. (2013). Somatic mutations in GRM1 in cancer alter metabotropic glutamate receptor 1 intracellular localization and signaling. Mol Pharmacol *83*, 770-780.

Fagni, L., Ango, F., Perroy, J., and Bockaert, J. (2004). Identification and functional roles of metabotropic glutamate receptor-interacting proteins. Seminars in cell & developmental biology *15*, 289-298.

Fallarino, F., Volpi, C., Fazio, F., Notartomaso, S., Vacca, C., Busceti, C., Bicciato, S., Battaglia, G., Bruno, V., Puccetti, P.*, et al.* (2010). Metabotropic glutamate receptor-4 modulates adaptive immunity and restrains neuroinflammation. Nat Med *16*, 897-902.

Fazio, F., Lionetto, L., Molinaro, G., Bertrand, H.O., Acher, F., Ngomba, R.T., Notartomaso, S., Curini, M., Rosati, O., Scarselli, P.*, et al.* (2012). Cinnabarinic acid, an endogenous metabolite of the kynurenine pathway, activates type 4 metabotropic glutamate receptors. Mol Pharmacol *81*, 643-656.

Fell, M.J., Witkin, J.M., Falcone, J.F., Katner, J.S., Perry, K.W., Hart, J., Rorick-Kehn, L., Overshiner, C.D., Rasmussen, K., Chaney, S.F.*, et al.* (2011). N-(4-((2-(trifluoromethyl)-3-hydroxy-4-(isobutyryl)phenoxy)methyl)benzyl)-1-methy l-1H-imidazole-4-carboxamide (THIIC), a novel metabotropic glutamate 2 potentiator with potential

anxiolytic/antidepressant properties: in vivo profiling suggests a link between behavioral and central nervous system neurochemical changes. J Pharmacol Exp Ther *336*, 165-177.

Ferraguti, F., Klausberger, T., Cobden, P., Baude, A., Roberts, J.D., Szucs, P., Kinoshita, A., Shigemoto, R., Somogyi, P., and Dalezios, Y. (2005). Metabotropic glutamate receptor 8-expressing nerve terminals target subsets of GABAergic neurons in the hippocampus. J Neurosci *25*, 10520-10536.

Ferrari, S.L., Pierroz, D.D., Glatt, V., Goddard, D.S., Bianchi, E.N., Lin, F.T., Manen, D., and Bouxsein, M.L. (2005). Bone response to intermittent parathyroid hormone is altered in mice null for {beta}-Arrestin2. Endocrinology *146*, 1854-1862.

Francesconi, A., and Duvoisin, R.M. (1998). Role of the second and third intracellular loops of metabotropic glutamate receptors in mediating dual signal transduction activation. J Biol Chem *273*, 5615-5624.

Francesconi, A., and Duvoisin, R.M. (2004). Divalent cations modulate the activity of metabotropic glutamate receptors. J Neurosci Res *75*, 472-479.

Galandrin, S., Oligny-Longpre, G., Bonin, H., Ogawa, K., Gales, C., and Bouvier, M. (2008). Conformational rearrangements and signaling cascades involved in ligand-biased mitogen-activated protein kinase signaling through the beta1-adrenergic receptor. Mol Pharmacol *74*, 162-172.

Galici, R., Jones, C.K., Hemstapat, K., Nong, Y., Echemendia, N.G., Williams, L.C., de Paulis, T., and Conn, P.J. (2006). Biphenyl-indanone A, a positive allosteric modulator of the metabotropic glutamate receptor subtype 2, has antipsychotic- and anxiolytic-like effects in mice. J Pharmacol Exp Ther *318*, 173-185.

Garcia, B.G., Neely, M.D., and Deutch, A.Y. (2010). Cortical regulation of striatal medium spiny neuron dendritic remodeling in parkinsonism: modulation of glutamate release reverses dopamine depletion-induced dendritic spine loss. Cereb Cortex *20*, 2423-2432.

Gesty-Palmer, D., Flannery, P., Yuan, L., Corsino, L., Spurney, R., Lefkowitz, R.J., and Luttrell, L.M. (2009). A beta-arrestin-biased agonist of the parathyroid hormone receptor (PTH1R) promotes bone formation independent of G protein activation. Science translational medicine *1*, 1ra1.

Gesty-Palmer, D., and Luttrell, L.M. (2011). Refining efficacy: exploiting functional selectivity for drug discovery. Advances in pharmacology *62*, 79-107.

Gomeza, J., Joly, C., Kuhn, R., Knopfel, T., Bockaert, J., and Pin, J.P. (1996). The second intracellular loop of metabotropic glutamate receptor 1 cooperates with the other intracellular domains to control coupling to G-proteins. J Biol Chem *271*, 2199-2205.

Gonzalez-Maeso, J., Ang, R.L., Yuen, T., Chan, P., Weisstaub, N.V., Lopez-Gimenez, J.F., Zhou, M., Okawa, Y., Callado, L.F., Milligan, G.*, et al.* (2008). Identification of a serotonin/glutamate receptor complex implicated in psychosis. Nature *452*, 93-97.

Goudet, C., Gaven, F., Kniazeff, J., Vol, C., Liu, J., Cohen-Gonsaud, M., Acher, F., Prezeau, L., and Pin, J.P. (2004). Heptahelical domain of metabotropic glutamate receptor 5 behaves like rhodopsin-like receptors. Proc Natl Acad Sci U S A *101*, 378-383.

Goudet, C., Kniazeff, J., Hlavackova, V., Malhaire, F., Maurel, D., Acher, F., Blahos, J., Prezeau, L., and Pin, J.P. (2005). Asymmetric functioning of dimeric metabotropic glutamate receptors disclosed by positive allosteric modulators. J Biol Chem *280*, 24380-24385.

Goudet, C., Vilar, B., Courtiol, T., Deltheil, T., Bessiron, T., Brabet, I., Oueslati, N., Rigault, D., Bertrand, H.O., McLean, H.*, et al.* (2012). A novel selective metabotropic glutamate receptor 4 agonist reveals new possibilities for developing subtype selective ligands with therapeutic potential. FASEB J *26*, 1682-1693.

Gregory, K.J., Noetzel, M.J., and Niswender, C.M. (2013). Pharmacology of metabotropic glutamate receptor allosteric modulators: structural basis and therapeutic potential for CNS disorders. Prog Mol Biol Transl Sci *115*, 61-121.

Gregory, K.J., Noetzel, M.J., Rook, J.M., Vinson, P.N., Stauffer, S.R., Rodriguez, A.L., Emmitte, K.A., Zhou, Y., Chun, A.C., Felts, A.S.*, et al.* (2012). Investigating metabotropic glutamate receptor 5 allosteric modulator cooperativity, affinity, and agonism: enriching structure-function studies and structure-activity relationships. Molecular pharmacology *82*, 860-875.

Group, B.D.W. (2001). Biomarkers and surrogate endpoints: preferred definitions and conceptual framework. Clinical pharmacology and therapeutics *69*, 89-95.

Gu, Z., Liu, W., Wei, J., and Yan, Z. (2012). Regulation of N-methyl-D-aspartic acid (NMDA) receptors by metabotropic glutamate receptor 7. J Biol Chem *287*, 10265-10275.

Guo, J., and Ikeda, S.R. (2005). Coupling of metabotropic glutamate receptor 8 to N-type Ca2+ channels in rat sympathetic neurons. Mol Pharmacol *67*, 1840-1851.

Hampson, D.R., Huang, X.P., Pekhletski, R., Peltekova, V., Hornby, G., Thomsen, C., and Thogersen, H. (1999). Probing the ligand-binding domain of the mGluR4 subtype of metabotropic glutamate receptor. The Journal of biological chemistry *274*, 33488-33495.

Harikumar, K.G., Happs, R.M., and Miller, L.J. (2008). Dimerization in the absence of higher-order oligomerization of the G protein-coupled secretin receptor. Biochimica et biophysica acta *1778*, 2555-2563.

Harikumar, K.G., Pinon, D.I., and Miller, L.J. (2007). Transmembrane segment IV contributes a functionally important interface for oligomerization of the Class II G protein-coupled secretin receptor. J Biol Chem *282*, 30363-30372.

Havlickova, M., Blahos, J., Brabet, I., Liu, J., Hruskova, B., Prezeau, L., and Pin, J.P. (2003). The second intracellular loop of metabotropic glutamate receptors recognizes C termini of G-protein alpha-subunits. J Biol Chem *278*, 35063-35070.

Hemstapat, K., Da Costa, H., Nong, Y., Brady, A.E., Luo, Q., Niswender, C.M., Tamagnan, G.D., and Conn, P.J. (2007). A novel family of potent negative allosteric modulators of group II metabotropic glutamate receptors. J Pharmacol Exp Ther *322*, 254-264.

Hermans, E., and Challiss, R.A. (2001). Structural, signalling and regulatory properties of the group I metabotropic glutamate receptors: prototypic family C G-protein-coupled receptors. Biochem J *359*, 465-484.

Hirono, M., Yoshioka, T., and Konishi, S. (2001). GABA(B) receptor activation enhances mGluR-mediated responses at cerebellar excitatory synapses. Nat Neurosci *4*, 1207-1216.

Hlavackova, V., Goudet, C., Kniazeff, J., Zikova, A., Maurel, D., Vol, C., Trojanova, J., Prezeau, L., Pin, J.P., and Blahos, J. (2005). Evidence for a single heptahelical domain being turned on upon activation of a dimeric GPCR. EMBO J *24*, 499-509.

Hlavackova, V., Zabel, U., Frankova, D., Batz, J., Hoffmann, C., Prezeau, L., Pin, J.P., Blahos, J., and Lohse, M.J. (2012). Sequential inter- and intrasubunit rearrangements during activation of dimeric metabotropic glutamate receptor 1. Sci Signal *5*, ra59.

Hohlefeld, F.U., Huebl, J., Huchzermeyer, C., Schneider, G.H., Schonecker, T., Kuhn, A.A., Curio, G., and Nikulin, V.V. (2012). Long-range temporal correlations in the subthalamic nucleus of patients with Parkinson's disease. Eur J Neurosci *36*, 2812-2821.

Iacovelli, L., Bruno, V., Salvatore, L., Melchiorri, D., Gradini, R., Caricasole, A., Barletta, E., De Blasi, A., and Nicoletti, F. (2002). Native group-III metabotropic glutamate receptors are coupled to the mitogen-activated protein kinase/phosphatidylinositol-3-kinase pathways. J Neurochem *82*, 216-223.

Iacovelli, L., Salvatore, L., Capobianco, L., Picascia, A., Barletta, E., Storto, M., Mariggio, S., Sallese, M., Porcellini, A., Nicoletti, F.*, et al.* (2003). Role of G protein-coupled receptor kinase 4 and beta-arrestin 1 in agonist-stimulated metabotropic glutamate receptor 1 internalization and activation of mitogen-activated protein kinases. J Biol Chem *278*, 12433-12442.

Jankovic, J. (2008). Parkinson's disease: clinical features and diagnosis. J Neurol Neurosurg Psychiatry *79*, 368-376.

Johnson, K.A., Conn, P.J., and Niswender, C.M. (2009). Glutamate receptors as therapeutic targets for Parkinson's disease. CNS Neurol Disord Drug Targets *8*, 475-491.

Johnson, M.P., Baez, M., Jagdmann, G.E., Jr., Britton, T.C., Large, T.H., Callagaro, D.O., Tizzano, J.P., Monn, J.A., and Schoepp, D.D. (2003). Discovery of allosteric potentiators for the metabotropic glutamate 2 receptor: synthesis and subtype selectivity of N-(4-(2-

methoxyphenoxy)phenyl)-N-(2,2,2- trifluoroethylsulfonyl)pyrid-3-ylmethylamine. J Med Chem *46*, 3189-3192.

Johnson, M.P., Barda, D., Britton, T.C., Emkey, R., Hornback, W.J., Jagdmann, G.E., McKinzie, D.L., Nisenbaum, E.S., Tizzano, J.P., and Schoepp, D.D. (2005). Metabotropic glutamate 2 receptor potentiators: receptor modulation, frequency-dependent synaptic activity, and efficacy in preclinical anxiety and psychosis model(s). Psychopharmacology (Berl) *179*, 271-283.

Joly, C., Gomeza, J., Brabet, I., Curry, K., Bockaert, J., and Pin, J.P. (1995). Molecular, functional, and pharmacological characterization of the metabotropic glutamate receptor type 5 splice variants: comparison with mGluR1. J Neurosci *15*, 3970-3981.

Jones, C.K., Bubser, M., Thompson, A.D., Dickerson, J.W., Turle-Lorenzo, N., Amalric, M., Blobaum, A.L., Bridges, T.M., Morrison, R.D., Jadhav, S.*, et al.* (2011). The mGlu4 positive allosteric modulator VU0364770 produces efficacy alone and in combination with L-DOPA or an adenosine A2A antagonist in preclinical rodent models of Parkinson's disease. J Pharmacol Exp Ther.

Jones, C.K., Bubser, M., Thompson, A.D., Dickerson, J.W., Turle-Lorenzo, N., Amalric, M., Blobaum, A.L., Bridges, T.M., Morrison, R.D., Jadhav, S.*, et al.* (2012). The metabotropic glutamate receptor 4-positive allosteric modulator VU0364770 produces efficacy alone and in combination with L-DOPA or an adenosine 2A antagonist in preclinical rodent models of Parkinson's disease. J Pharmacol Exp Ther *340*, 404-421.

Jones, P.J., Xiang, Z., and Conn, P.J. (2008). Metabotropic glutamate receptors mGluR4 and mGluR8 regulate transmission in the lateral olfactory tract-piriform cortex synapse. Neuropharmacology *55*, 440-446.

Kamikubo, Y., Tabata, T., Kakizawa, S., Kawakami, D., Watanabe, M., Ogura, A., Iino, M., and Kano, M. (2007). Postsynaptic GABAB receptor signalling enhances LTD in mouse cerebellar Purkinje cells. J Physiol *585*, 549-563.

Kammermeier, P.J. (2012). Functional and pharmacological characteristics of metabotropic glutamate receptors 2/4 heterodimers. Mol Pharmacol *82*, 438-447.

Kenakin, T. (2005). New concepts in drug discovery: collateral efficacy and permissive antagonism. Nat Rev Drug Discov *4*, 919-927.

Kenakin, T., and Miller, L.J. (2010). Seven transmembrane receptors as shapeshifting proteins: the impact of allosteric modulation and functional selectivity on new drug discovery. Pharmacological reviews *62*, 265-304.

Keov, P., Sexton, P.M., and Christopoulos, A. (2011). Allosteric modulation of G protein-coupled receptors: a pharmacological perspective. Neuropharmacology *60*, 24-35.

Kinney, G.G., O'Brien, J.A., Lemaire, W., Burno, M., Bickel, D.J., Clements, M.K., Chen, T.B., Wisnoski, D.D., Lindsley, C.W., Tiller, P.R.*, et al.* (2005). A novel selective positive allosteric modulator of metabotropic glutamate receptor subtype 5 has in vivo activity and antipsychotic-like effects in rat behavioral models. J Pharmacol Exp Ther *313*, 199-206.

Kinoshita, A., Ohishi, H., Neki, A., Nomura, S., Shigemoto, R., Takada, M., Nakanishi, S., and Mizuno, N. (1996). Presynaptic localization of a metabotropic glutamate receptor, mGluR8, in the rhinencephalic areas: a light and electron microscope study in the rat. Neurosci Lett *207*, 61-64.

Klein, C., and Lohmann-Hedrich, K. (2007). Impact of recent genetic findings in Parkinson's disease. Current opinion in neurology *20*, 453-464.

Klunk, W.E., McClure, R.J., and Pettegrew, J.W. (1991). Possible roles of L-phosphoserine in the pathogenesis of Alzheimer's disease. Molecular and chemical neuropathology / sponsored by the International Society for Neurochemistry and the World Federation of Neurology and research groups on neurochemistry and cerebrospinal fluid *15*, 51-73.

Kniazeff, J., Bessis, A.S., Maurel, D., Ansanay, H., Prezeau, L., and Pin, J.P. (2004). Closed state of both binding domains of homodimeric mGlu receptors is required for full activity. Nat Struct Mol Biol *11*, 706-713.

Kohout, T.A., Nicholas, S.L., Perry, S.J., Reinhart, G., Junger, S., and Struthers, R.S. (2004). Differential desensitization, receptor phosphorylation, beta-arrestin recruitment, and ERK1/2 activation by the two endogenous ligands for the CC chemokine receptor 7. J Biol Chem *279*, 23214-23222.

Kosinski, C.M., Risso Bradley, S., Conn, P.J., Levey, A.I., Landwehrmeyer, G.B., Penney, J.B., Jr., Young, A.B., and Standaert, D.G. (1999). Localization of metabotropic glutamate receptor 7 mRNA and mGluR7a protein in the rat basal ganglia. J Comp Neurol *415*, 266-284.

Krupnick, J.G., and Benovic, J.L. (1998). The role of receptor kinases and arrestins in G protein-coupled receptor regulation. Annu Rev Pharmacol Toxicol *38*, 289-319.

Kubo, Y., Miyashita, T., and Murata, Y. (1998). Structural basis for a Ca2+-sensing function of the metabotropic glutamate receptors. Science *279*, 1722-1725.

Kunishima, N., Shimada, Y., Tsuji, Y., Sato, T., Yamamoto, M., Kumasaka, T., Nakanishi, S., Jingami, H., and Morikawa, K. (2000). Structural basis of glutamate recognition by a dimeric metabotropic glutamate receptor. Nature *407*, 971-977.

Lai, E., Waters, M.G., Tata, J.R., Radziszewski, W., Perevozskaya, I., Zheng, W., Wenning, L., Connolly, D.T., Semple, G., Johnson-Levonas, A.O.*, et al.* (2008). Effects of a niacin receptor partial agonist, MK-0354, on plasma free fatty acids, lipids, and cutaneous flushing in humans. Journal of clinical lipidology *2*, 375-383.

Lamb, J.P., Engers, D.W., Niswender, C.M., Rodriguez, A.L., Venable, D.F., Conn, P.J., and Lindsley, C.W. (2011). Discovery of molecular switches within the ADX-47273 mGlu5 PAM scaffold that modulate modes of pharmacology to afford potent mGlu5 NAMs, PAMs and partial antagonists. Bioorg Med Chem Lett *21*, 2711-2714.

Le Poul, E., Bolea, C., Girard, F., Poli, S., Charvin, D., Campo, B., Bortoli, J., Bessif, A., Luo, B., Koser, A.J.*, et al.* (2012). A potent and selective metabotropic glutamate receptor 4 positive allosteric modulator improves movement in rodent models of Parkinson's disease. J Pharmacol Exp Ther *343*, 167-177.

Leach, K., Sexton, P.M., and Christopoulos, A. (2007). Allosteric GPCR modulators: taking advantage of permissive receptor pharmacology. Trends Pharmacol Sci *28*, 382-389.

Lee, S.B., Shin, S.H., Hepler, J.R., Gilman, A.G., and Rhee, S.G. (1993). Activation of phospholipase C-beta 2 mutants by G protein alpha q and beta gamma subunits. J Biol Chem *268*, 25952-25957.

Li, X.M., Li, C.C., Yu, S.S., Chen, J.T., Sabapathy, K., and Ruan, D.Y. (2007). JNK1 contributes to metabotropic glutamate receptor-dependent long-term depression and short-term synaptic plasticity in the mice area hippocampal CA1. Eur J Neurosci *25*, 391-396.

Lipnik-Stangelj, M., and Carman-Krzan, M. (2004a). Activation of histamine H1-receptor enhances neurotrophic factor secretion from cultured astrocytes. Inflamm Res *53*, 245-252.

Lipnik-Stangelj, M., and Carman-Krzan, M. (2004b). Histamine-stimulated nerve growth factor secretion from cultured astrocyctes is blocked by protein kinase C inhibitors. Inflamm Res *53 Suppl 1*, S57-58.

Litschig, S., Gasparini, F., Rueegg, D., Stoehr, N., Flor, P.J., Vranesic, I., Prezeau, L., Pin, J.P., Thomsen, C., and Kuhn, R. (1999). CPCCOEt, a noncompetitive metabotropic glutamate receptor 1 antagonist, inhibits receptor signaling without affecting glutamate binding. Mol Pharmacol *55*, 453-461.

Lundstrom, L., Bissantz, C., Beck, J., Wettstein, J.G., Woltering, T.J., Wichmann, J., and Gatti, S. (2011). Structural determinants of allosteric antagonism at metabotropic glutamate receptor 2: mechanistic studies with new potent negative allosteric modulators. Br J Pharmacol *164*, 521-537.

Luttrell, L.M., Ferguson, S.S., Daaka, Y., Miller, W.E., Maudsley, S., Della Rocca, G.J., Lin, F., Kawakatsu, H., Owada, K., Luttrell, D.K.*, et al.* (1999). Beta-arrestin-dependent formation of beta2 adrenergic receptor-Src protein kinase complexes. Science *283*, 655-661.

Macinnes, N., and Duty, S. (2008). Group III metabotropic glutamate receptors act as hetero-receptors modulating evoked GABA release in the globus pallidus in vivo. Eur J Pharmacol *580*, 95-99.

MacInnes, N., Messenger, M.J., and Duty, S. (2004). Activation of group III metabotropic glutamate receptors in selected regions of the basal ganglia alleviates akinesia in the reserpine-treated rat. Br J Pharmacol *141*, 15-22.

Maj, M., Bruno, V., Dragic, Z., Yamamoto, R., Battaglia, G., Inderbitzin, W., Stoehr, N., Stein, T., Gasparini, F., Vranesic, I.*, et al.* (2003). (-)-PHCCC, a positive allosteric modulator of mGluR4: characterization, mechanism of action, and neuroprotection. Neuropharmacology *45*, 895-906.

Malherbe, P., Kratochwil, N., Knoflach, F., Zenner, M.T., Kew, J.N., Kratzeisen, C., Maerki, H.P., Adam, G., and Mutel, V. (2003). Mutational analysis and molecular modeling of the allosteric binding site of a novel, selective, noncompetitive antagonist of the metabotropic glutamate 1 receptor. J Biol Chem *278*, 8340-8347.

Malherbe, P., Kratzeisen, C., Lundstrom, K., Richards, J.G., Faull, R.L., and Mutel, V. (1999). Cloning and functional expression of alternative spliced variants of the human metabotropic glutamate receptor 8. Brain Res Mol Brain Res *67*, 201-210.

Marek, G.J., Wright, R.A., Schoepp, D.D., Monn, J.A., and Aghajanian, G.K. (2000). Physiological antagonism between 5-hydroxytryptamine(2A) and group II metabotropic glutamate receptors in prefrontal cortex. J Pharmacol Exp Ther *292*, 76-87.

Marino, M.J., Williams, D.L., Jr., O'Brien, J.A., Valenti, O., McDonald, T.P., Clements, M.K., Wang, R., DiLella, A.G., Hess, J.F., Kinney, G.G.*, et al.* (2003). Allosteric modulation of group III metabotropic glutamate receptor 4: a potential approach to Parkinson's disease treatment. Proc Natl Acad Sci U S A *100*, 13668-13673.

Marlo, J.E., Niswender, C.M., Days, E.L., Bridges, T.M., Xiang, Y., Rodriguez, A.L., Shirey, J.K., Brady, A.E., Nalywajko, T., Luo, Q.*, et al.* (2009). Discovery and

characterization of novel allosteric potentiators of M1 muscarinic receptors reveals multiple modes of activity. Mol Pharmacol *75*, 577-588.

Mathiesen, J.M., Ulven, T., Martini, L., Gerlach, L.O., Heinemann, A., and Kostenis, E. (2005). Identification of indole derivatives exclusively interfering with a G protein-independent signaling pathway of the prostaglandin D2 receptor CRTH2. Mol Pharmacol *68*, 393-402.

Matsui, T., and Kita, H. (2003). Activation of group III metabotropic glutamate receptors presynaptically reduces both GABAergic and glutamatergic transmission in the rat globus pallidus. Neuroscience *122*, 727-737.

McCool, B.A., Pin, J.P., Harpold, M.M., Brust, P.F., Stauderman, K.A., and Lovinger, D.M. (1998). Rat group I metabotropic glutamate receptors inhibit neuronal Ca2+ channels via multiple signal transduction pathways in HEK 293 cells. J Neurophysiol *79*, 379-391.

Menard, C., and Quirion, R. (2012). Successful cognitive aging in rats: a role for mGluR5 glutamate receptors, homer 1 proteins and downstream signaling pathways. PLoS One *7*, e28666.

Minakami, R., Katsuki, F., Yamamoto, T., Nakamura, K., and Sugiyama, H. (1994). Molecular cloning and the functional expression of two isoforms of human metabotropic glutamate receptor subtype 5. Biochem Biophys Res Commun *199*, 1136-1143.

Mitsukawa, K., Yamamoto, R., Ofner, S., Nozulak, J., Pescott, O., Lukic, S., Stoehr, N., Mombereau, C., Kuhn, R., McAllister, K.H.*, et al.* (2005). A selective metabotropic glutamate receptor 7 agonist: activation of receptor signaling via an allosteric site modulates stress parameters in vivo. Proc Natl Acad Sci U S A *102*, 18712-18717.

Monastyrskaia, K., Lundstrom, K., Plahl, D., Acuna, G., Schweitzer, C., Malherbe, P., and Mutel, V. (1999). Effect of the umami peptides on the ligand binding and function of rat mGlu4a receptor might implicate this receptor in the monosodium glutamate taste transduction. Br J Pharmacol *128*, 1027-1034.

Moreno, J.L., Muguruza, C., Umali, A., Mortillo, S., Holloway, T., Pilar-Cuellar, F., Mocci, G., Seto, J., Callado, L.F., Neve, R.L.*, et al.* (2012). Identification of three residues essential for 5-hydroxytryptamine 2A-metabotropic glutamate 2 (5-HT2A.mGlu2) receptor heteromerization and its psychoactive behavioral function. J Biol Chem *287*, 44301-44319.

Muto, T., Tsuchiya, D., Morikawa, K., and Jingami, H. (2007). Structures of the extracellular regions of the group II/III metabotropic glutamate receptors. Proc Natl Acad Sci U S A *104*, 3759-3764.

Neki, A., Ohishi, H., Kaneko, T., Shigemoto, R., Nakanishi, S., and Mizuno, N. (1996). Pre- and postsynaptic localization of a metabotropic glutamate receptor, mGluR2, in the rat brain: an immunohistochemical study with a monoclonal antibody. Neurosci Lett *202*, 197-200.

Niswender, C.M., and Conn, P.J. (2010). Metabotropic glutamate receptors: physiology, pharmacology, and disease. Annu Rev Pharmacol Toxicol *50*, 295-322.

Niswender, C.M., Johnson, K.A., Luo, Q., Ayala, J.E., Kim, C., Conn, P.J., and Weaver, C.D. (2008a). A novel assay of Gi/o-linked G protein-coupled receptor coupling to potassium channels provides new insights into the pharmacology of the group III metabotropic glutamate receptors. Mol Pharmacol *73*, 1213-1224.

Niswender, C.M., Johnson, K.A., Miller, N.R., Ayala, J.E., Luo, Q., Williams, R., Saleh, S., Orton, D., Weaver, C.D., and Conn, P.J. (2010). Context-dependent pharmacology exhibited by negative allosteric modulators of metabotropic glutamate receptor 7. Mol Pharmacol *77*, 459-468.

Niswender, C.M., Johnson, K.A., Weaver, C.D., Jones, C.K., Xiang, Z., Luo, Q., Rodriguez, A.L., Marlo, J.E., de Paulis, T., Thompson, A.D.*, et al.* (2008b). Discovery, characterization, and antiparkinsonian effect of novel positive allosteric modulators of metabotropic glutamate receptor 4. Mol Pharmacol *74*, 1345-1358.

Niswender, C.M., Lebois, E.P., Luo, Q., Kim, K., Muchalski, H., Yin, H., Conn, P.J., and Lindsley, C.W. (2008c). Positive allosteric modulators of the metabotropic glutamate receptor subtype 4 (mGluR4): Part I. Discovery of pyrazolo[3,4-d]pyrimidines as novel mGluR4 positive allosteric modulators. Bioorg Med Chem Lett *18*, 5626-5630.

Nordstedt, C., and Fredholm, B.B. (1990). A modification of a protein-binding method for rapid quantification of cAMP in cell-culture supernatants and body fluid. Anal Biochem *189*, 231-234.

O'Brien, J.A., Lemaire, W., Wittmann, M., Jacobson, M.A., Ha, S.N., Wisnoski, D.D., Lindsley, C.W., Schaffhauser, H.J., Rowe, B., Sur, C.*, et al.* (2004). A novel selective allosteric modulator potentiates the activity of native metabotropic glutamate receptor subtype 5 in rat forebrain. J Pharmacol Exp Ther *309*, 568-577.

Ohishi, H., Akazawa, C., Shigemoto, R., Nakanishi, S., and Mizuno, N. (1995). Distributions of the mRNAs for L-2-amino-4-phosphonobutyrate-sensitive metabotropic glutamate receptors, mGluR4 and mGluR7, in the rat brain. J Comp Neurol *360*, 555-570.

Ohishi, H., Shigemoto, R., Nakanishi, S., and Mizuno, N. (1993). Distribution of the messenger RNA for a metabotropic glutamate receptor, mGluR2, in the central nervous system of the rat. Neuroscience *53*, 1009-1018.

Pagano, A., Ruegg, D., Litschig, S., Stoehr, N., Stierlin, C., Heinrich, M., Floersheim, P., Prezeau, L., Carroll, F., Pin, J.P.*, et al.* (2000). The non-competitive antagonists 2-methyl-6-(phenylethynyl)pyridine and 7-hydroxyiminocyclopropan[b]chromen-1a-carboxylic acid ethyl ester interact with overlapping binding pockets in the transmembrane region of group I metabotropic glutamate receptors. J Biol Chem *275*, 33750-33758.

Page, G., Khidir, F.A., Pain, S., Barrier, L., Fauconneau, B., Guillard, O., Piriou, A., and Hugon, J. (2006). Group I metabotropic glutamate receptors activate the p70S6 kinase via both mammalian target of rapamycin (mTOR) and extracellular signal-regulated kinase (ERK 1/2) signaling pathways in rat striatal and hippocampal synaptoneurosomes. Neurochem Int *49*, 413-421.

Paquet, M., Ribeiro, F.M., Guadagno, J., Esseltine, J.L., Ferguson, S.S., and Cregan, S.P. (2013). Role of metabotropic glutamate receptor 5 signaling and homer in oxygen glucose deprivation-mediated astrocyte apoptosis. Molecular brain *6*, 9.

Petralia, R.S., Wang, Y.X., Niedzielski, A.S., and Wenthold, R.J. (1996). The metabotropic glutamate receptors, mGluR2 and mGluR3, show unique postsynaptic, presynaptic and glial localizations. Neuroscience *71*, 949-976.

Petralia, R.S., Wang, Y.X., Singh, S., Wu, C., Shi, L., Wei, J., and Wenthold, R.J. (1997). A monoclonal antibody shows discrete cellular and subcellular localizations of mGluR1 alpha metabotropic glutamate receptors. Journal of chemical neuroanatomy *13*, 77-93.

Picconi, B., Bagetta, V., Ghiglieri, V., Paille, V., Di Filippo, M., Pendolino, V., Tozzi, A., Giampa, C., Fusco, F.R., Sgobio, C.*, et al.* (2011). Inhibition of phosphodiesterases rescues striatal long-term depression and reduces levodopa-induced dyskinesia. Brain *134*, 375-387.

Picconi, B., Centonze, D., Hakansson, K., Bernardi, G., Greengard, P., Fisone, G., Cenci, M.A., and Calabresi, P. (2003). Loss of bidirectional striatal synaptic plasticity in L-DOPA-induced dyskinesia. Nat Neurosci *6*, 501-506.

Picconi, B., Pisani, A., Centonze, D., Battaglia, G., Storto, M., Nicoletti, F., Bernardi, G., and Calabresi, P. (2002). Striatal metabotropic glutamate receptor function following experimental parkinsonism and chronic levodopa treatment. Brain *125*, 2635-2645.

Pierce, K.L., and Lefkowitz, R.J. (2001). Classical and new roles of beta-arrestins in the regulation of G-protein-coupled receptors. Nat Rev Neurosci *2*, 727-733.

Pike, N.B. (2005). Flushing out the role of GPR109A (HM74A) in the clinical efficacy of nicotinic acid. The Journal of clinical investigation *115*, 3400-3403.

Pin, J.P., Comps-Agrar, L., Maurel, D., Monnier, C., Rives, M.L., Trinquet, E., Kniazeff, J., Rondard, P., and Prezeau, L. (2009). G-protein-coupled receptor oligomers: two or more for what? Lessons from mGlu and GABAB receptors. J Physiol *587*, 5337-5344.

Pin, J.P., Joly, C., Heinemann, S.F., and Bockaert, J. (1994). Domains involved in the specificity of G protein activation in phospholipase C-coupled metabotropic glutamate receptors. EMBO J *13*, 342-348.

Pisani, A., Calabresi, P., Centonze, D., and Bernardi, G. (1997). Activation of group III metabotropic glutamate receptors depresses glutamatergic transmission at corticostriatal synapse. Neuropharmacology *36*, 845-851.

Pisani, A., Gubellini, P., Bonsi, P., Conquet, F., Picconi, B., Centonze, D., Bernardi, G., and Calabresi, P. (2001). Metabotropic glutamate receptor 5 mediates the potentiation of N-methyl-D-aspartate responses in medium spiny striatal neurons. Neuroscience *106*, 579-587.

Pollock, P.M., Cohen-Solal, K., Sood, R., Namkoong, J., Martino, J.J., Koganti, A., Zhu, H., Robbins, C., Makalowska, I., Shin, S.S.*, et al.* (2003). Melanoma mouse model implicates metabotropic glutamate signaling in melanocytic neoplasia. Nature genetics *34*, 108-112.

Rashid, A.J., So, C.H., Kong, M.M., Furtak, T., El-Ghundi, M., Cheng, R., O'Dowd, B.F., and George, S.R. (2007). D1-D2 dopamine receptor heterooligomers with unique pharmacology are coupled to rapid activation of Gq/11 in the striatum. Proc Natl Acad Sci U S A *104*, 654-659.

Ray, K., and Hauschild, B.C. (2000). Cys-140 is critical for metabotropic glutamate receptor-1 dimerization. J Biol Chem *275*, 34245-34251.

Reynolds, I.J. (2008). Novel chemical scaffolds that show activity via intracerebroventricularly injection in in vivo antiparkinsonian rodent models. Paper presented at: 6th International Meeting on Metabotropic Glutamate Receptors (Taormina, Sicily, Italy).

Rives, M.L., Vol, C., Fukazawa, Y., Tinel, N., Trinquet, E., Ayoub, M.A., Shigemoto, R., Pin, J.P., and Prezeau, L. (2009). Crosstalk between GABAB and mGlu1a receptors reveals new insight into GPCR signal integration. EMBO J *28*, 2195-2208.

Romano, C., Miller, J.K., Hyrc, K., Dikranian, S., Mennerick, S., Takeuchi, Y., Goldberg, M.P., and O'Malley, K.L. (2001). Covalent and noncovalent interactions mediate metabotropic glutamate receptor mGlu5 dimerization. Mol Pharmacol *59*, 46-53.

Romano, C., Yang, W.L., and O'Malley, K.L. (1996). Metabotropic glutamate receptor 5 is a disulfide-linked dimer. J Biol Chem *271*, 28612-28616.

Ronesi, J.A., Collins, K.A., Hays, S.A., Tsai, N.P., Guo, W., Birnbaum, S.G., Hu, J.H., Worley, P.F., Gibson, J.R., and Huber, K.M. (2012). Disrupted Homer scaffolds mediate abnormal mGluR5 function in a mouse model of fragile X syndrome. Nat Neurosci *15*, 431-440, S431.

Ronesi, J.A., and Huber, K.M. (2008). Homer interactions are necessary for metabotropic glutamate receptor-induced long-term depression and translational activation. J Neurosci *28*, 543-547.

Rong, R., Ahn, J.Y., Huang, H., Nagata, E., Kalman, D., Kapp, J.A., Tu, J., Worley, P.F., Snyder, S.H., and Ye, K. (2003). PI3 kinase enhancer-Homer complex couples mGluRI to PI3 kinase, preventing neuronal apoptosis. Nat Neurosci *6*, 1153-1161.

Rowe, B.A., Schaffhauser, H., Morales, S., Lubbers, L.S., Bonnefous, C., Kamenecka, T.M., McQuiston, J., and Daggett, L.P. (2008). Transposition of three amino acids transforms the human metabotropic glutamate receptor (mGluR)-3-positive allosteric modulation site to mGluR2, and additional characterization of the mGluR2-positive allosteric modulation site. J Pharmacol Exp Ther *326*, 240-251.

Sartorius, L.J., Nagappan, G., Lipska, B.K., Lu, B., Sei, Y., Ren-Patterson, R., Li, Z., Weinberger, D.R., and Harrison, P.J. (2006). Alternative splicing of human metabotropic glutamate receptor 3. J Neurochem *96*, 1139-1148.

Sayer, R.J. (1998). Group I metabotropic glutamate receptors mediate slow inhibition of calcium current in neocortical neurons. J Neurophysiol *80*, 1981-1988.

Schaffhauser, H., Rowe, B.A., Morales, S., Chavez-Noriega, L.E., Yin, R., Jachec, C., Rao, S.P., Bain, G., Pinkerton, A.B., Vernier, J.M.*, et al.* (2003). Pharmacological characterization and identification of amino acids involved in the positive modulation of metabotropic glutamate receptor subtype 2. Mol Pharmacol *64*, 798-810.

Schann, S., Mayer, S., Franchet, C., Frauli, M., Steinberg, E., Thomas, M., Baron, L., and Neuville, P. (2010). Chemical switch of a metabotropic glutamate receptor 2 silent allosteric modulator into dual metabotropic glutamate receptor 2/3 negative/positive allosteric modulators. J Med Chem *53*, 8775-8779.

Schmid, A.W., Fauvet, B., Moniatte, M., and Lashuel, H.A. (2013). Alpha-synuclein post-translational modifications as potential biomarkers for Parkinson's disease and other synucleinopathies. Molecular & cellular proteomics : MCP.

Schulz, H.L., Stohr, H., and Weber, B.H. (2002). Characterization of three novel isoforms of the metabotrobic glutamate receptor 7 (GRM7). Neurosci Lett *326*, 37-40.

Schweitzer, C., Kratzeisen, C., Adam, G., Lundstrom, K., Malherbe, P., Ohresser, S., Stadler, H., Wichmann, J., Woltering, T., and Mutel, V. (2000). Characterization of [(3)H]-LY354740 binding to rat mGlu2 and mGlu3 receptors expressed in CHO cells using semliki forest virus vectors. Neuropharmacology *39*, 1700-1706.

Seebahn, A., Dinkel, H., Mohrluder, J., Hartmann, R., Vogel, N., Becker, C.M., Sticht, H., and Enz, R. (2011). Structural characterization of intracellular C-terminal domains of group III metabotropic glutamate receptors. FEBS Lett *585*, 511-516.

Servitja, J.M., Masgrau, R., Sarri, E., and Picatoste, F. (1999). Group I metabotropic glutamate receptors mediate phospholipase D stimulation in rat cultured astrocytes. J Neurochem *72*, 1441-1447.

Shannon, K.M., Keshavarzian, A., Dodiya, H.B., Jakate, S., and Kordower, J.H. (2012). Is alpha-synuclein in the colon a biomarker for premotor Parkinson's disease? Evidence from 3 cases. Movement disorders : official journal of the Movement Disorder Society *27*, 716-719.

Sharma, S., Kedrowski, J., Rook, J.M., Smith, R.L., Jones, C.K., Rodriguez, A.L., Conn, P.J., and Lindsley, C.W. (2009). Discovery of molecular switches that modulate modes of metabotropic glutamate receptor subtype 5 (mGlu5) pharmacology in vitro and in vivo within a series of functionalized, regioisomeric 2- and 5-(phenylethynyl)pyrimidines. J Med Chem *52*, 4103-4106.

Sheffler, D.J., and Conn, P.J. (2008). Allosteric potentiators of metabotropic glutamate receptor subtype 1a differentially modulate independent signaling pathways in baby hamster kidney cells. Neuropharmacology *55*, 419-427.

Sheffler, D.J., Wenthur, C.J., Bruner, J.A., Carrington, S.J., Vinson, P.N., Gogi, K.K., Blobaum, A.L., Morrison, R.D., Vamos, M., Cosford, N.D*., et al.* (2012). Development of a novel, CNS-penetrant, metabotropic glutamate receptor 3 (mGlu3) NAM probe (ML289) derived from a closely related mGlu5 PAM. Bioorg Med Chem Lett *22*, 3921-3925.

Shigemoto, R., Nomura, S., Ohishi, H., Sugihara, H., Nakanishi, S., and Mizuno, N. (1993). Immunohistochemical localization of a metabotropic glutamate receptor, mGluR5, in the rat brain. Neurosci Lett *163*, 53-57.

Sorensen, S.D., and Conn, P.J. (2003). G protein-coupled receptor kinases regulate metabotropic glutamate receptor 5 function and expression. Neuropharmacology *44*, 699-706.

Staudinger, J., Zhou, J., Burgess, R., Elledge, S.J., and Olson, E.N. (1995). PICK1: a perinuclear binding protein and substrate for protein kinase C isolated by the yeast two-hybrid system. The Journal of cell biology *128*, 263-271.

Suh, Y.H., Park, J.Y., Park, S., Jou, I., Roche, P.A., and Roche, K.W. (2013). Regulation of metabotropic glutamate receptor 7 (mGluR7) internalization and surface expression by Ser/Thr protein phosphatase 1. J Biol Chem *288*, 17544-17551.

Suh, Y.H., Pelkey, K.A., Lavezzari, G., Roche, P.A., Huganir, R.L., McBain, C.J., and Roche, K.W. (2008). Corequirement of PICK1 binding and PKC phosphorylation for stable surface expression of the metabotropic glutamate receptor mGluR7. Neuron *58*, 736-748.

Suratman, S., Leach, K., Sexton, P., Felder, C., Loiacono, R., and Christopoulos, A. (2011). Impact of species variability and 'probe-dependence' on the detection and in vivo validation of allosteric modulation at the M4 muscarinic acetylcholine receptor. Br J Pharmacol *162*, 1659-1670.

Surmeier, D.J., and Sulzer, D. (2013). The pathology roadmap in Parkinson disease. Prion *7*, 85-91.

Suzuki, G., Tsukamoto, N., Fushiki, H., Kawagishi, A., Nakamura, M., Kurihara, H., Mitsuya, M., Ohkubo, M., and Ohta, H. (2007). In vitro pharmacological characterization of novel isoxazolopyridone derivatives as allosteric metabotropic glutamate receptor 7 antagonists. J Pharmacol Exp Ther *323*, 147-156.

Teixeira, A.L., Barbosa, I.G., Diniz, B.S., and Kummer, A. (2010). Circulating levels of brain-derived neurotrophic factor: correlation with mood, cognition and motor function. Biomarkers in medicine *4*, 871-887.

Thakkar, M.M. (2011). Histamine in the regulation of wakefulness. Sleep Med Rev *15*, 65-74.

Thomsen, C., Pekhletski, R., Haldeman, B., Gilbert, T.A., O'Hara, P., and Hampson, D.R. (1997). Cloning and characterization of a metabotropic glutamate receptor, mGluR4b. Neuropharmacology *36*, 21-30.

Thomsen, W., Frazer, J., and Unett, D. (2005). Functional assays for screening GPCR targets. Curr Opin Biotechnol *16*, 655-665.

Tsuchiya, D., Kunishima, N., Kamiya, N., Jingami, H., and Morikawa, K. (2002). Structural views of the ligand-binding cores of a metabotropic glutamate receptor complexed with an antagonist and both glutamate and Gd3+. Proc Natl Acad Sci U S A *99*, 2660-2665.

Tu, J.C., Xiao, B., Naisbitt, S., Yuan, J.P., Petralia, R.S., Brakeman, P., Doan, A., Aakalu, V.K., Lanahan, A.A., Sheng, M.*, et al.* (1999). Coupling of mGluR/Homer and PSD-95 complexes by the Shank family of postsynaptic density proteins. Neuron *23*, 583-592.

Urban, J.D., Clarke, W.P., von Zastrow, M., Nichols, D.E., Kobilka, B., Weinstein, H., Javitch, J.A., Roth, B.L., Christopoulos, A., Sexton, P.M.*, et al.* (2007). Functional selectivity and classical concepts of quantitative pharmacology. J Pharmacol Exp Ther *320*, 1-13.

Valant, C., Felder, C.C., Sexton, P.M., and Christopoulos, A. (2012). Probe dependence in the allosteric modulation of a G protein-coupled receptor: implications for detection and validation of allosteric ligand effects. Molecular pharmacology *81*, 41-52.

Valenti, O., Conn, P.J., and Marino, M.J. (2002). Distinct physiological roles of the Gq-coupled metabotropic glutamate receptors Co-expressed in the same neuronal populations. J Cell Physiol *191*, 125-137.

Valenti, O., Mannaioni, G., Seabrook, G.R., Conn, P.J., and Marino, M.J. (2005). Group III metabotropic glutamate-receptor-mediated modulation of excitatory transmission in rodent substantia nigra pars compacta dopamine neurons. J Pharmacol Exp Ther *313*, 1296-1304.

Valenti, O., Marino, M.J., Wittmann, M., Lis, E., DiLella, A.G., Kinney, G.G., and Conn, P.J. (2003). Group III metabotropic glutamate receptor-mediated modulation of the striatopallidal synapse. J Neurosci *23*, 7218-7226.

Valerio, A., Ferraboli, S., Paterlini, M., Spano, P., and Barlati, S. (2001). Identification of novel alternatively-spliced mRNA isoforms of metabotropic glutamate receptor 6 gene in rat and human retina. Gene *262*, 99-106.

Vanbervliet, B., Akdis, M., Vocanson, M., Rozieres, A., Benetiere, J., Rouzaire, P., Akdis, C.A., Nicolas, J.F., and Hennino, A. (2011). Histamine receptor H1 signaling on dendritic cells plays a key role in the IFN-lance in T-cell mediated skin inflammation. . J Allergy Clin Immunol *124*, 493-453.

Varney, M.A., Cosford, N.D., Jachec, C., Rao, S.P., Sacaan, A., Lin, F.F., Bleicher, L., Santori, E.M., Flor, P.J., Allgeier, H.*, et al.* (1999). SIB-1757 and SIB-1893: selective,

noncompetitive antagonists of metabotropic glutamate receptor type 5. J Pharmacol Exp Ther *290*, 170-181.

Varrone, A., and Halldin, C. (2012). New developments of dopaminergic imaging in Parkinson's disease. Q J Nucl Med Mol Imaging *56*, 68-82.

Walters, R.W., Shukla, A.K., Kovacs, J.J., Violin, J.D., DeWire, S.M., Lam, C.M., Chen, J.R., Muehlbauer, M.J., Whalen, E.J., and Lefkowitz, R.J. (2009). beta-Arrestin1 mediates nicotinic acid-induced flushing, but not its antilipolytic effect, in mice. The Journal of clinical investigation *119*, 1312-1321.

Wang, S.S., Denk, W., and Hausser, M. (2000). Coincidence detection in single dendritic spines mediated by calcium release. Nat Neurosci *3*, 1266-1273.

Watts, V.J., and Neve, K.A. (1996). Sensitization of endogenous and recombinant adenylate cyclase by activation of D2 dopamine receptors. Mol Pharmacol *50*, 966-976.

Wisler, J.W., DeWire, S.M., Whalen, E.J., Violin, J.D., Drake, M.T., Ahn, S., Shenoy, S.K., and Lefkowitz, R.J. (2007). A unique mechanism of beta-blocker action: carvedilol stimulates beta-arrestin signaling. Proc Natl Acad Sci U S A *104*, 16657-16662.

Wittmann, M., Marino, M.J., Bradley, S.R., and Conn, P.J. (2001). Activation of group III mGluRs inhibits GABAergic and glutamatergic transmission in the substantia nigra pars reticulata. J Neurophysiol *85*, 1960-1968.

Woltering, T.J., Adam, G., Wichmann, J., Goetschi, E., Kew, J.N., Knoflach, F., Mutel, V., and Gatti, S. (2008a). Synthesis and characterization of 8-ethynyl-1,3-dihydro-benzo[b][1,4]diazepin-2-one derivatives: part 2. New potent non-competitive metabotropic glutamate receptor 2/3 antagonists. Bioorg Med Chem Lett *18*, 1091-1095.

Woltering, T.J., Wichmann, J., Goetschi, E., Adam, G., Kew, J.N., Knoflach, F., Ballard, T.M., Huwyler, J., Mutel, V., and Gatti, S. (2008b). Synthesis and characterization of 1,3-dihydro-benzo[b][1,4]diazepin-2-one derivatives: Part 3. New potent non-competitive metabotropic glutamate receptor 2/3 antagonists. Bioorg Med Chem Lett *18*, 2725-2729.

Wood, M.R., Hopkins, C.R., Brogan, J.T., Conn, P.J., and Lindsley, C.W. (2011). "Molecular switches" on mGluR allosteric ligands that modulate modes of pharmacology. Biochemistry *50*, 2403-2410.

Yanagawa, M., Yamashita, T., and Shichida, Y. (2013). Glutamate acts as a partial inverse agonist to metabotropic glutamate receptor with a single amino acid mutation in the transmembrane domain. J Biol Chem *288*, 9593-9601.

Zeitz, C., Forster, U., Neidhardt, J., Feil, S., Kalin, S., Leifert, D., Flor, P.J., and Berger, W. (2007). Night blindness-associated mutations in the ligand-binding, cysteine-rich, and intracellular domains of the metabotropic glutamate receptor 6 abolish protein trafficking. Hum Mutat *28*, 771-780.

Zhang, C., and Marek, G.J. (2007). Group III metabotropic glutamate receptor agonists selectively suppress excitatory synaptic currents in the rat prefrontal cortex induced by 5-hydroxytryptamine2A receptor activation. J Pharmacol Exp Ther *320*, 437-447.

Zhang, C.S., Bertaso, F., Eulenburg, V., Lerner-Natoli, M., Herin, G.A., Bauer, L., Bockaert, J., Fagni, L., Betz, H., and Scheschonka, A. (2008). Knock-in mice lacking the PDZ-ligand motif of mGluR7a show impaired PKC-dependent autoinhibition of glutamate release, spatial working memory deficits, and increased susceptibility to pentylenetetrazol. J Neurosci *28*, 8604-8614.

Zhang, Y., Rodriguez, A.L., and Conn, P.J. (2005). Allosteric potentiators of metabotropic glutamate receptor subtype 5 have differential effects on different signaling pathways in cortical astrocytes. J Pharmacol Exp Ther *315*, 1212-1219.

Zhou, Y., Manka, J.T., Rodriguez, A.L., Weaver, C.D., Days, E.L., Vinson, P.N., Jadhav, S., Hermann, E.J., Jones, C.K., Conn, P.J.*, et al.* (2010). Discovery of N-Aryl Piperazines as Selective mGlu(5) Potentiators with Efficacy in a Rodent Model Predictive of Anti-Psychotic Activity. ACS Med Chem Lett *1*, 433-438.